The Dissertation Committee for Martin Luke Gran Certifies that this is the approved version of the following dissertation:

Metal-Polymer Nanoparticulate Systems for Externally-Controlled Delivery

Committee:

Nicholas A. Peppas, Supervisor

Donald R. Paul

Benny D. Freeman

Keith P. Johnston

Stanislav Emelianov

Metal-Polymer Nanoparticulate Systems for Externally-Controlled Delivery

by

Martin Luke Gran, B.S.

Dissertation

Presented to the Faculty of the Graduate School of

The University of Texas at Austin

in Partial Fulfillment

of the Requirements

for the Degree of

Doctor of Philosophy

The University of Texas at Austin

December 2010

Acknowledgements

First of all I would like to thank my family. My mother has always been there to help me through the difficult times and give me advice when needed. Without my mom's support and guidance I never could have made it near this far. She has always been a phone call away when I needed a few extra words of encouragement or I needed to talk through a difficult situation. I also could not have stayed sane the past four years without frequent phone calls with my dad to talk football. He and Lea have been a strong presence in my life to encourage me, keep me focused, and visits with them were always a refreshing break during my time in Austin. I'd also like to thank my brother Nick who I always enjoyed chatting with at odd hours while he was in Japan.

I would like to sincerely thank Dr. Nicholas A. Peppas for his guidance and support as my graduate advisor. He has been an invaluable resource for me during my graduate career at the University of Texas and I could not have accomplished what I have without him. He helped me through every step of this process and helped me to learn how to be a better student and researcher.

The various members of the Peppas lab at the University of Texas have been an endless supply of encouragement and helpfulness. Thank you to Adam, Bill, Brandon, Carolyn, Cody, Daniel, David, Don, Eileen, Justin, Maggie, Mary, Omar, Ruben, and Steve.

I would like to thank Maggie for her support over the last several years. Maggie has helped me with research in the lab including assisting me with the cell studies, but more importantly she has also been a constant source of support, understanding, and encouragement. She helped to keep me moving forward and has been there to lend a hand to me every step of the way.

I would like to acknowledge Dr. Stanislav Emelianov and his lab for helping me with the photoacoustic imaging studies. Jason Cook was quick to help me with these studies and none could have been done without him. Yun-Sheng Chen generously donated his time and energy to supply some of the gold nanorods used in these experiments.

I have had several wonderful undergraduate students who have helped me the past few years. Ekta Shah and Bobby Galindo both left their mark on this project. Danny Strinden contributed to this project in many ways during his time in the lab and his help was invaluable.

The entire crew who lived in the Treadwell House during my three years there helped shape my graduate school experience and it was always a place where I could relax and be myself. Sean, Tom, Mark, Peter and honorary member Bobby T all helped make my experience here in Austin a time that I will never forget. I also wouldn't have made it through without other countless graduate students who have shared this time with me at monthly mixers, BBQ trips, football tailgates, Austin music festivals, and all the other great times that made this experience so enjoyable.

Metal-Polymer Nanoparticulate Systems for Externally Controlled Delivery

Publication No._____

Martin Gran, Ph.D.

The University of Texas at Austin, 2010

Supervisor: Nicholas A. Peppas

Metal-polymer nanocomposites consisting of gold nanorods and temperature-responsive hydrogel nanoparticulates were investigated for use in externally-controlled drug delivery systems. Several different thermo-responsive hydrogels including poly(N-isopropyl acrylamide) (PNIPAAm) and poly(N-isopropryl acrylamide-co-acrylic acid) (P(NIPAAm-co-AA)) nanoparticles were synthesized for these nanocomposites using an aqueous dispersion polymerization method. In addition, nanoparticles of interpenetrating polymer networks (IPN) composed of poly(acrylamide) (PAAm) and poly(acrylic acid) (PAA) were synthesized using a water-in-oil emulsion polymerization. Temperature-responsive equilibrium swelling behavior of nanoparticles with varying crosslinking densities was characterized using dynamic light scattering. IPN systems

exhibited a positive swelling response upon heating while PNIPAAm and copolymer systems collapsed upon increase in temperature above the transition point. Nanoparticles were characterized using scanning electron microscopy (SEM) and transmission electron microscopy (TEM) which demonstrated shape and morphology of polymer particles.

Gold-polymer nanocomposites were formed by grafting gold nanorods to the surface of the polymer nanoparticles. Amine-functionalized gold nanorods were coupled to polymers using 1-ethyl-3-(3-dimethylaminopropyl)carbodiimide hydrochloride (EDC) and N-hydroxysulfosuccinimide (Sulfo-NHS) to activate carboxyl groups on the surface of the polymer nanoparticles. TEM confirmed successful formation of the metal-polymer nanocomposites.

Loading and release of a model therapeutic were done to assess the potential use of the polymer component of the nanocomposite for drug delivery. Fluorescein, a model for chemotherapeutics, was loaded into P(NIPAAm-co-AA) polymer nanoparticulates. Loading of the compound was shown to be a function of crosslinking density in the polymer network. Maximum loading was achieved using nanoparticles synthesized with a 10 mol% crosslinker feed ratio with entrapment efficiencies of 80.0 % and loading capacities of 12.0 %. Cytotoxicity studies were performed using a NIH/3T3 mouse fibroblast cell model. Cell viabilities in presence of P(NIPAAm-co-AA) nanoparticles were comparable to (not statistically different than) controls at

concentrations up to 4 mg/ml. Similarly, gold-polymer composite concentrations up to 0.5 mg/ml caused limited cell death.

Table of Contents

List of Tables xii

List of Figures xiii

List of Figures xiii

Chapter 1: Introduction 1

References 5

Chapter 2: BACKGROUND 6

2.1 Breast Cancer 7

2.2 Chemotherapy 11

2.3 Targeted Drug Delivery 14

2.4 Polymer Nanoparticles 17

2.4.1 Biodegradable Systems 18

2.4.2 Self-Assembled Systems 23

2.4.3 Nanogels 27

2.5 Gold Nanoparticles 35

2.6 Externally-Controlled Delivery 37

2.7 Photoacoustic Imaging 39

2.8 Conclusions 40

References 43

Chapter 3: OBJECTIVES 55

Chapter 4: Polymer Nanogel Synthesis and Characterization 57

4.1 Introduction 57

4.2 Materials and Methods 64

4.2.1 LCST Nanoparticle Synthesis 64

4.2.2 UCST Nanoparticle Synthesis 66

4.2.3 Nanoparticle Swelling Characterization by Dynamic Light Scattering 68
4.2.4 Polymer Nanoparticle Characterization 69
4.3 Results and Discussion 70
4.3.1 LCST Nanoparticle Synthesis 70
4.3.2 UCST Nanoparticle Synthesis 71
4.3.3 Polymer Nanoparticle Characterization by Dynamic Light Scattering 72
4.3.4 Polymer Nanoparticle Characterization by Electron Microscopy74
4.4 Conclusions..... 75
References..... 91
Chapter 5: Gold-Polymer Composite Nanoparticle Synthesis and Characterization94
5.1 Introduction..... 94
5.2 Materials and Methods..... 98
5.2.1 LCST Composite Nanoparticle Synthesis..... 98
5.2.2 UCST Composite Nanoparticle Synthesis..... 101
5.2.3 Composite Nanoparticle Characterization by Transmission Electron Microscopy..... 104
5.3 Results and Discussion 104
5.3.1 LCST Composite Nanoparticle Synthesis..... 104
5.3.2 UCST Composite Nanoparticle Synthesis..... 105
5.3.3 Composite Nanoparticle Characterization by Transmission Electron Microscopy..... 106
5.4 Conclusions..... 107
References..... 123
Chapter 6: Loading and Release Characteristics of a Model Therapeutic from Hydrogel Nanoparticles..... 125
6.1 Introduction..... 125
6.2 Materials and Methods..... 132
6.2.1 Hydrogel Nanoparticle Synthesis 132

6.2.2 Loading of Fluorescein into Hydrogel Nanoparticles 134
6.2.3 Release of Fluorescein from Hydrogel Nanoparticles 136
6.3 Results and Discussion 137
6.3.1 Hydrogel Nanoparticle Synthesis 137
6.3.2 Loading of Fluorescein into Hydrogel Nanoparticles 139
6.3.3 Release of Fluorescein from Hydrogel Nanoparticles 140
6.4 Conclusions 141
References 148

Chapter 7: Characterization of Externally Triggered Systems, Light Responsive Behavior, Cytocompatibility, and Medical Imaging 152
7.1 Introduction 152
7.2 Materials and Methods 155
7.2.1 Gold-Polymer Composite Synthesis 155
7.2.2 Light-responsive Swelling Behavior 157
7.2.3 Cytocompatibility 158
7.2.4 Photoacoustic Imaging 159
7.3 Results and Discussion 160
7.3.1 Gold-Polymer Composite Synthesis 160
7.3.2 Light-responsive Swelling Behavior 161
7.3.3 Cytocompatibility 162
7.3.4 Photoacoustic Imaging 162
7.4 Conclusions 163
References 169

Chapter 8: Conclusions 171

References 177

Vita 189

List of Tables

Table 6.1 Encapsulation efficiencies and loading capacities for fluorescein loaded into P(NIPAAm-co-AA) polymer nanoparticles of varying extents of crosslinking. 143

List of Figures

Figure 2.1 TEM micrograph of gold nanoshells formed from a gold shell on a silica core with strong NIR absorption. 41

Figure 1.2 TEM micrograph of gold nanorods having 4:1 aspect ratio leading to peak absorption at 808 nm. 42

Figure 4.1 Monomers used in the synthesis of polymer nanoparticles with UCST behavior (a) Acrylic acid (b) Acrylamide (c) Methylene bisacrylamide. 77

Figure 4.2 Monomers used in the synthesis of polymer nanoparticles with LCST behavior (a) Acrylic acid (b) Acrylamide (c) N-Isopropylacrylamide (d) Methylene bisacrylamide. 78

Figure 4.3 Hydrodynamic diameters of PNIPAAm hydrogel particles with varying amounts of SDS surfactant concentration. 79

Figure 4.4 Intensity based particle size distribution for PAAm/PAA IPN polymer nanoparticles 80

Figure 4.5 Equilibrium swelling behavior of IPN nanoparticles with varying molar extents of crosslinking based on intensity based hydrodynamic diameters from dynamic light scattering. 81

Figure 4.6 Equilibrium swelling behavior of PNIPAAm nanogels with varying molar extents of crosslinking based on intensity based hydrodynamic diameters from dynamic light scattering. 82

Figure 4.7 Equilibrium volume swelling ratios of PNIPAAm nanogels with varying molar extents of crosslinking based on intensity based hydrodynamic diameters from dynamic light scattering. 83

Figure 4.8 Equilibrium swelling behavior of PNIPAAm, 90/10 P(NIPAAm-co-AAm), and 90/10 P(NIPAAm-co-AA) nanogels with 10% molar extent of crosslinking based on intensity based hydrodynamic diameters from dynamic light scattering. 84
Figure 4.9 Equilibrium volume swelling ratios of PNIPAAm, 90/10 P(NIPAAm-co-AAm), and 90/10 P(NIPAAm-co-AA) nanogels with 10% molar extent of crosslinking based on intensity based hydrodynamic diameters from dynamic light scattering. 85
Figure 4.10 SEM micrograph of lyophilized PNIPAAm nanogels synthesized by dispersion polymerization. 86
Figure 4.11 TEM image of PNIPAAm nanogels synthesized via aqueous dispersion polymerization. 87
Figure 4.12 TEM Micrograph of P(NIPAAm-co-AA) nanogels synthesized via dispersion polymerization. 88
Figure 4.13 SEM Micrograph of lyophilized 50/50 PAAm/PAA IPN nanoparticles.89
Figure 4.13 TEM Micrograph of 50/50 PAAm/PAA IPN nanoparticles. 90
Figure 5.1 TEM micrograph of gold nanoshells formed from a gold coated silica particle with absorption centered around 800 nm..... 109
Figure 5.2 TEM micrograph of gold nanorods with 4:1 aspect ratio, 40 nm in length and 10 nm wide having absorption peak centered around 808 nm.110
Figure 5.2 Schematic of the proposed externally-controlled therapeutic system consisting of gold-nanorods grafted to a temperature sensitive polymer nanoparticle. 111

Figure 5.3 Schematic of the procedure for grafting of gold nanorods to polymer nanoparticles to form gold-polymer composites for externally-triggered systems. 112
Figure 5.5 FT-IR absorption spectrum of P(NIPAAm-co-AA) nanoparticles. 113
Figure 5.6 FT-IR absorption spectrum of 50/50 PAAm/PAA IPN nanoparticles. 114
Figure 5.7 TEM micrograph of gold-polymer composites formed during nucleation of LCST polymers in aqueous dispersion polymerization..... 115
Figure 5.8 TEM micrograph of a single gold-polymer composite formed during nucleation of LCST polymer via dispersion polymerization. 116
Figure 5.9 TEM image of gold-polymer composites formed during nucleation process in aqueous dispersion polymerization. 117
Figure 5.10 TEM micrograph of P(NIPAAm-co-AA) grafted with gold nanorods for externally-controlled systems. 118
Figure 5.11 TEM micrograph of gold-polymer composite with P(NIPAAm-co-AA) nanoparticles grafted with gold nanorods..... 119
Figure 5.12 Gold-polymer composite TEM micrograph og P(NIPAAm-co-AA) nanoparticles grafted with gold nanorods at high magnification. 120
Figure 5.13 TEM micrograph of IPN based gold-polymer composite formed by grafting gold nanorods to polymer nanoparticles. 121
Figure 5.4 TEM image of IPN nanoparticle grafted with gold nanorods for externally-controlled systems. 122
Figure 6.1 TEM micrograph of P(NIPAAm-co-AA) nanoparticles for use in fluorescein loading studies. 144
Figure 6.2 Entrapment efficiency of fluorescein loaded in P(NIPAAm-co-AA) hydrogel nanoparticles with varied extents of crosslinking..... 145

Figure 6.3 Loading Capacity of fluorescein in P(NIPAAm-co-AA) hydrogel nanoparticles with varied extents of crosslinking..... 146
Figure 6.4 Measurement of release of a model therapeutic, fluorescein, from nanogels at 37 °C over a 48 h period. Release is quantified as a percentage of total amount of fluorescein loaded in the particles.147
Figure 7.5 Swelling behavior of gold-polymer composites with alternating laser exposure. P(NIPAAm-co-AA) polymer nanoparticles grafted with gold nanorods were intermittently exposed to 808 nm CW laser. 165
Figure 7.2 Cell viability of 3T3 mouse fibroblasts as a percentage of control when incubated with varying concentrations of P(NIPAAm-co-AA) nanoparticles..... 166
Figure 7.3 Cell viability of 3T3 mouse fibroblasts as a percentage of control when incubated with varying concentrations of gold-polymer composite nanoparticles..... 167
Figure 7.4 Photoacoustic signal measured from gold-polymer composites. Signal measured from P(NIPAAm-co-AA) nanoparticles grafted with gold nanorods when exposed to 775 nm nanopulsed laser at 5 mJ/cm.168

Chapter 1: Introduction

In recent years, there has been interest in developing more efficient therapeutic systems that can provide highly effective therapy at a disease site while minimizing systemic effects. The goal is to improve the effectiveness of treatment while reducing any adverse effects associated with a therapeutic or drug, thereby improving overall patient quality of life. Targeted delivery systems involve the use of a carrier system that is capable of delivering a therapeutic in a preferential manner to a disease site. Externally controlled also sometimes referred to as remotely triggered delivery systems have the potential to go one step beyond standard targeted systems. In these types of systems, a therapeutic can be triggered to release at a specified time and location using some non-invasive external stimulus. Past work has shown that ultrasound, radio frequency pulses, magnetic fields, and light may be used to trigger delivery [1-6].

This thesis focuses on the development of nanoscale externally controlled therapeutic systems for the delivery of chemotherapeutics for breast cancer treatment. These systems will respond to exposure to a near infrared (NIR) light source to release an entrapped therapeutic. Light in the NIR range is of interest because of its ability to penetrate deeply through tissue compared to light in other wavelength ranges. Gold nanorods that are capable of adsorbing light in this region and converting it to heat will serve as a transducer to convert light to a drug release signal. The gold nanorods heat an adjacent thermally responsive polymer nanoparticle that undergoes a volume

swelling change in upon heating in an aqueous environment. This volume change leads to a subsequent release of the entrapped therapeutic. In this manner, a light signal can be externally applied to release the therapeutic at a desired time and location.

Cancer is a group of diseases that lead to uncontrolled, rapid growth of cells in the body typically leading to formation of a tumor often invading surrounding tissues and in some cases metastasizing, spreading to different areas of the body through blood or the lymphatic system. Overall, cancer is the fourth leading cause of death following cardiovascular disease, infectious diseases, and ischemic heart disease. Approximately 13% of all deaths worldwide each year are caused by various types of cancer [7, 8].

Breast cancer affects nearly 200,000 new women in the United States each year, leading to over 40,000 deaths per year. This disease is the second leading cause of cancer death and makes up 10% of all cancers among women in the United States. Chemotherapy is one of the primary treatments used among patients with breast cancer and important for both pre and postoperative therapies. Chemotherapeutic agents which are typically delivered systemically via either an oral or intravenous route most commonly work by disrupting cell growth in rapidly dividing cells. The systemic delivery of these agents leads to a number of adverse effects including nausea, vomiting, hair loss, cardiotoxicity, and immunosuppression [9, 10]. Limiting delivery of chemotherapeutics to the disease location may improve therapeutic efficacy while minimizing adverse health effects.

The drug carrier systems proposed in this thesis consist of temperature responsive polymer hydrogel nanoparticles that exhibit a swelling transition upon heating through a transition temperature range, with gold nanorods grafted to the polymer nanoparticles that are capable of absorbing light and transmitting heat to the polymer. The heating triggers a swelling response in the carrier and an associated release of a therapeutic. Nanoscale systems are of interest because they could be administered intravenously, localize at a disease site because of the enhanced permeability and retention (EPR) effect and have extended circulation half-lives.

Towards the development of these systems, temperature responsive nanogels were synthesized and their swelling behavior as a function of temperature was characterized. Chapter 3 describes emulsion and precipitation polymerization methods that were used to synthesize these materials. Dynamic light scattering measurements were used to measure the hydrodynamic diameter of the particles and quantify equilibrium swelling behavior. Properties of the materials such as incorporation of comonomers or extent of crosslinking were evaluated for their effect on temperature responsive behavior.

The addition of the gold nanorods to form gold-polymer composites is described in Chapter 4. Gold nanorods were grafted to the surface of polymer nanoparticles using a condensation reaction between amine-functionalized gold nanorods and carboxyl groups present in the polymer and characterized using transmission electron microscopy (TEM). Absorption spectra collected over the transition temperature range

indicated that as polymer nanoparticles collapsed the attached gold nanorods were drawn closer together causing plasmon coupling and an associated change in the absorbance spectrum.

The potential use as chemotherapeutic drug delivery systems was investigated using a model therapeutic, fluorescein, often as a model for cancer drugs such as doxorubicin. The model drug was loaded into polymer nanoparticles and results are quantified in Chapter 6. Release of the compound from the nanogels was also measured and characterized in Chapter 6.

In order to evaluate the potential of this system to be used *in vivo* as a therapeutic carrier and diagnostic tool, cellular toxicity and light-triggered swelling were investigated in Chapter 7. Cell viability studies demonstrate the potential biocompatibility of the nanoparticle systems. A swelling response was also shown to be induced in the gold-polymer composites in response to light. A photoacoustic signal was detected from the composite nanoparticles demonstrating the ability of the particles to act as a contrast agent in certain medical imaging techniques. The final chapter will discuss the conclusions that have been drawn from the results of this thesis work.

REFERENCES

1. Lentacker, I., Geers, B., Demeester, J., De Smedt, S.C., and Sanders, N.N., *Design and Evaluation of Doxorubicin-containing Microbubbles for Ultrasound-triggered Doxorubicin Delivery: Cytotoxicity and Mechanisms Involved.* Mol. Ther., 2010. **18**(1): p. 101-108.

2. *The Use of Ultrasound for Drug Delivery.* Echocardiography 2013 Jnl Cardiovascular Ultrasound & Allied Techniques, 2001. **18**(4): p. 323-328.

3. Zhang, J.L., Srivastava, R.S., and Misra, R.D.K., *Core-shell magnetite nanoparticles surface encapsulated with smart stimuli-responsive polymer: Synthesis, characterization, and LCST of viable drug-targeting delivery system.* Langmuir, 2007. **23**(11): p. 6342-6351.

4. Satarkar, N.S. and Hilt, J.Z., *Magnetic hydrogel nanocomposites for remote controlled pulsatile drug release.* J. Control. Release, 2008. **130**(3): p. 246-251.

5. Sershen, S.R., Halas, N.J., and West, J.L. *Pulsatile release of insulin via photothermally modulated drug delivery*. in *[Engineering in Medicine and Biology, 2002. 24th Annual Conference and the Annual Fall Meeting of the Biomedical Engineering Society] EMBS/BMES Conference, 2002. Proceedings of the Second Joint*. 2002.

6. Ferrara, K.W., *Driving delivery vehicles with ultrasound.* Adv. Drug Deliv. Rev., 2008. **60**(10): p. 1097-1102.

7. Jemal, A., Siegel, R., Ward, E., Hao, Y.P., et al., *Cancer statistics, 2008.* CA-Cancer J. Clin., 2008. **58**(2): p. 71-96.

8. Parkin, D.M., Bray, F., Ferlay, J., and Pisani, P., *Global cancer statistics, 2002.* CA-Cancer J. Clin., 2005. **55**(2): p. 74-108.

9. Abe, O., Abe, R., Enomoto, K., Kikuchi, K., et al., *Effects of chemotherapy and hormonal therapy for early breast cancer on recurrence and 15-year survival: an overview of the randomised trials.* Lancet, 2005. **365**(9472): p. 1687-1717.

10. Edwards, B.K., Brown, M.L., Wingo, P.A., Howe, H.L., et al., *Annual report to the Nation on the status of cancer, 1975-2002, featuring population-based trends in cancer treatment.* J. Natl. Cancer Inst., 2005. **97**(19): p. 1407-1427.

Chapter 2: BACKGROUND

In an effort to improve patient treatment and overall quality of life, recent work in biomaterials has sought to develop systems that can increase effective dosing while simultaneously decreasing adverse side effects that occur as a result of therapeutic administration.

Targeted drug delivery has been widely studied as a method of delivering a therapeutic to a localized disease site such as a tumor or a site of inflammation while minimizing the distribution of the drug to other parts of the body. The ability to concentrate therapeutic delivery at the disease site is advantageous over traditional systemic delivery because it may increase therapy at the disease site while decreasing the overall necessary dose and lessening the severity of adverse side effects.

Externally controlled or triggered delivery systems have been developed to specify both the time and location of therapeutic delivery. Externally controlled therapeutic systems are devices that can be triggered to release a therapeutic at a desired time and location, by external means. These systems release a therapeutic agent in response to triggering mechanisms such as ultrasound waves [1-3], light [4], magnetic field [5, 6], or other methods that can be used to transmit a signal to a delivery system *in vivo*. Metal nanoparticles can act as the signal receiver in light triggered systems because of their ability to convert light into heat. When coupled with a

temperature sensitive polymer, metal nanoparticles can trigger release of a drug as by causing a swelling transition in the polymer through heating.

Nanoscale devices are desirable for drug delivery systems because they more readily localize at tumor sites as a result of the enhanced permeability and retention (EPR) effect. Nanoparticles have improved circulation half-lives in the bloodstream and collect in tumor microvasculature with poor lymphatic drainage [7]. Nanoscale materials are essential for the development of injectable targeted and externally-triggered delivery systems.

This chapter discusses the motivation and methods behind the different strategies for targeted delivery for cancer treatment focusing on breast cancer. A short discussion of past work in polymer nanoparticles for drug delivery and background on the use of metal nanoparticles for biomedical applications will follow. Additionally, past successes in the area of externally controlled devices will be summarized. Use of gold nanoparticles as contrast agents in photoacoustic techniques for medical imaging will also be discussed. The conclusion of the chapter will summarize the motivation and aspects involved in the development of nanoscale externally-controlled systems.

2.1 Breast Cancer

Cancer is a group of diseases that lead to uncontrolled, rapid growth of cells in the body typically leading to formation of a tumor often invading surrounding tissues and in some cases metastasizing, spreading to different areas of the body through blood

or the lymphatic system. Overall, cancer is the fourth leading cause of death following cardiovascular disease, infectious diseases, and eschemic heart disease. Approximately 13% of all deaths worldwide each year are caused by various types of cancer [8-10].

Breast cancer is a type of cancer that originates in one of several areas in breast tissue. Most commonly the cancer begins in either the lobules which are glands for the production of milk or in the ducts that connect the lobules to the nipple, known as ductal carcinomas and lobular carcinomas respectively. Cancers that stay confined to these sites are known as *in situ* carcinomas, but most of the cancerous tumors that begin in the ducts or lobules will become invasive cancers that spread to the surrounding fatty, connective, or lymphatic tissue in the breast. In situ cancers are almost fully curable, while invasive cancers have varying negative effects depending on their extent of growth before diagnosis [11, 12].

The extent of the growth and spread of a breast cancer is typically quantified by classification into one of five different stages. Determination of the malignant stage is based on the TNM classification system: size of tumor (T), involvement of lymph nodes (N), and distant metastasis (M). Stage 0 is a pre-cancerous disease or marker such as an *in situ* carcinoma. Stage I is an early stage cancer referring to a small localized invasive tumor, typically less than 2 cm in diameter in the case of breast cancer. Cancers classified as Stage II are larger and more advanced. Breast cancers classified as Stage II are generally at least 2-5 cm in diameter and/or there is spread of cancerous cells to the lymph nodes. Stage III cancers are larger still and have in all cases spread to the lymph

nodes. Breast cancers at Stage III may have also spread to the skin on the breast or to the chest wall. Stage IV cancers are metastatic meaning cancerous cells have spread to other organs of the body. Stage I-III cancers are considered early stage cancers and potentially curable through treatment, while metastasized Stage IV cancer is typically incurable but may be treated [13].

Each year approximately 190,000 women in the United States are diagnosed with breast cancer. In 2006 40,820 women died from breast cancer in the United States making it the second leading cause of cancer death among women, making up over 10% of all cancer incidences among women in the United States [8, 9, 14]. Additionally, the disease affects a small number of men in the United States with approximately 1900 incidences per year causing over 400 deaths. Worldwide, breast cancer leads to over 500,000 deaths per year [10].

Primary methods of treatment of Stage I-III breast cancers include surgery, radiation therapy, and systemic therapies such as chemotherapy, biologic treatments, and hormone treatments. Most individuals who are diagnosed with an invasive breast cancer will have a surgery to remove the cancer from the breast accompanied by one or more of the other therapies to shrink the tumor, eliminate cancerous tissue following surgery, or to prevent recurrence[11-13].

Surgical removal of the cancerous tissue may consist of a lumpectomy, where only the tumor plus a small surrounding area of normal tissue is removed, or a

mastectomy which is removal of the entire breast. Frequently, lymph nodes are also removed during surgery to determine the extent of spread of the disease [12].

Radiation therapies used for breast cancer are typically applied using an external radiation source that is targeted at the affected breast to kill cancer cells. Radiation therapies may be used prior to surgery to reduce the size of the tumor or following surgery to eliminate remaining cancerous tissue. External radiation is almost always used for a period of 5-7 weeks following a lumpectomy [11].

Anti-cancer drugs are often delivered systemically through the oral delivery route or intravenous injection. When these drugs are administered prior to surgery, it is known as neoadjuvant therapy, with the goal typically being to shrink the tumor enough to allow for easier removal during lumpectomy. Adjuvant therapy consists of drugs adminstered following the removal of a tumor to eliminate cancer cells that may have migrated to the lymph nodes or other parts of the body [12].

Certain biologics administered systemically have been shown to minimize cancer growth. Monoclonal antibodies such as herceptin target the human epidermal growth factor receptor 2 (HER2). HER2 overexpression in breast cancers has been shown to be associated with faster growing, more aggressive tumors. The drugs can be used to minimize the HER2 effect [15]. Another monoclonal antibody, bevacizumab, blocks vascular endothelial growth factor A thereby minimizing growth of new blood vessels and slowing tumor growth [16].

Because hormones such as estrogen have been shown to promote breast cancer growth, drugs may be administered to control the production of estrogen or to block the effects of the hormone. Tamoxifen is commonly administered to minimize the effects of estrogen. Several other drugs known as aromatase inhibitors can be effective in minimizing the production of estrogen in postmenopausal women [17].

Chemotherapeutic drugs are a broad class of therapeutics that target fast-dividing cells, by either impairing cell division or causing actual cell death. Neoadjuvant treatments help to shrink the tumor prior to resection, while adjuvant treatments can treat remaining cancer cells and prevent resection. In later stage cancers that cannot be entirely removed or in the case of metastatic cancers chemotherapies are often applied to minimize further spread of the tumor with the goal of extending lifespan [17-19].

2.2 CHEMOTHERAPY

Anticancer drugs known as chemotherapeutics are administered systemically to around 75% of all cancer patients via either an oral or intravenous route. Chemotherapeutics may be used in all stages of breast cancer and delivered either preoperatively or postoperatively [18]. Preoperative or neoadjuvant delivery can help to shrink the tumor allowing for easier and more total lumpectomy while adjuvant therapy following operation is used to prevent recurrence and to eliminate cancer cells that may be in the lymph nodes or other parts of the body. For nearly all Stage 3 breast cancers and many Stage 2 invasive breast cancers, neoadjuvant therapy is the standard

treatment and has been shown to allow for increased removal of locally advanced tumors [20].

There are a number of different chemotherapeutic drugs that are administered to breast cancer patients, and frequently these drugs are administered together in combinations of 2-4 of the different types of drugs. The most common classes of chemotherapeutic drugs used to treat breast cancer are alkylating agents, antimetabolites, anthracyclines, and taxanes [18].

Alkylating agents such as cyclophosphamide work by effectively crosslinking DNA strands thereby preventing cell division and tumor growth. The alkylating agents alkylate guanine bases in DNA, and because of the fast dividing nature of cancer cells, they are susceptible to this modification. Side effects for cyclophosphamide tend to be less severe than for many other chemotherapeutics, but some side effects do commonly occur including nausea and vomiting, hair loss, diarrhea, and joint pain [17].

Antimetabolites used in chemotherapy typically mimic the structure of either purine or pyrimidine. The pyrimidine analog fluorouracil (5-FU) is the most common antimetabolite used to treat breast cancer. 5-FU blocks DNA replication by acting as a thymidylate synthase inhibitor preventing synthesis of pyridimine thymidine which is necessary for replication [21]. Antimetobolites affect all DNA replication and cell growth, most pronounced in any fast dividing cells. Because of their far reaching effects, they may have severe side effects such as bone marrow suppression, digestive tract inflammation, dermatitis, diarrhea, and hair loss. Additionally, individuals with a

condition known as dihydropyrimidine dehydrogenase deficiency (DPD deficiency) are unable to metabolize pyrimidine based drugs and for these patients 5-FU treatment can be lethal.

Anthracyclines are another class of drugs that inhibits the growth of cancer cells. Doxorubicin (adriamycin) is used most commonly in breast cancer chemotherapeutic regimens. Anthracylines, such as doxorubicin, are administered intravenously and inhibit replication by intercalating DNA. Doxorubicin is a very versatile drug used to treat a wide range of cancers including breast cancer. The positive effects of doxorubicin are accompanied by a number of adverse effects. Cardiotoxicity is a major concern for patients who are treated with antracyclines, and high doses can lead to a number of heart related conditions including heart arrhythmias, cardiomyopathy, heart failure, and the possibility of death. Other common side effects include nausea, vomiting, and total hair loss [19].

To reduce the side effects of doxorubicin, systems have been developed to enhance localization of the drug at the target cancer site and decrease systemic effects. Pegylated liposomal doxorubicin systems including Doxil and Caelyx have been shown to increase the therapeutic index of doxorubicin. Pegylation inhibits uptake by the reticulo-endothelial system (RES) increasing the half-life of circulation as well as increasing extravasation into the leaky vasculature of tumors. The liposomal systems have been shown to increase concentration of drug or radio tracers at tumor sites. Decreased cardiotoxicity has been observed in patients treated with pegylated

liposomal doxorubicin compared to free drug [22, 23]. A non-pegylated liposomal formulation, Myocet, has shown antitumor activity comparable to free doxorubicin while decreasing cardiotoxicity in treatment of metastatic breast cancer patients [24, 25]. Myocet has been approved for treatment of breast cancer in Europe and Canada, but it has not yet been approved by the FDA in the United States.

2.3 Targeted Drug Delivery

The targeting of drug delivery systems, most commonly micro- and nanoscale particles provides more efficient treatment and improves quality of life for patients by minimizing potential adverse effects. In a perfect targeted system, the entire drug payload of all carriers would be delivered at the preferential site. In this case, the dosage can be tailored to have the most significant effect at the disease site without causing systemic adverse affects. Externally-triggered devices seek to go a step beyond simple targeting as release of drug is only triggered at the site where treatment is desired at a specific point in time.

Nanoparticles are desirable in many targeted delivery systems because their properties allow them to circulate in the bloodstream for extended periods of time and they have a high level of accumulation at tumor sites. Delivery of anticancer drugs to tumor sites is the most commonly investigated use of targeted nanoparticles to date. Intravenously administered nanoparticles under the size of 200 nm have been shown to circulate much longer than systems larger than this size, because of their ability to

escape the body's natural defense mechanisms such as the RES [26]. These carriers are also the right size to take advantage of the enhanced permeability and retention (EPR) effect. Particles smaller than 400 nm have been shown to extravasate leaky tumor vasculature via the EPR effect, and those smaller than 200 nm may be even more effective [27].

While the EPR effect is an example of passive targeting, taking advantage of properties of the drug or carrier to localize at the target site, active targeting involves the incorporation of molecules in the delivery system that are intended to interact with the physiological target. Typically a targeting ligand is adhered to the surface of the nanoparticle or covalently attached. The addition of targeting ligands has been shown to improve the therapeutic effect of delivery systems both *in vitro* and *in vivo* [28, 29].

Folate receptor is a glycoprotein that has frequently been observed to have elevated expression in tumors while it is not present in most normal tissues making it a very attractive candidate for targeted anticancer delivery [30]. Nanoparticles functionalized with folate, the receptor target, have been shown to have higher therapeutic efficacies in the treatment of tumors than nontargeted nanoparticles in both *in vitro* and *in vivo* models [28].

Another common ligand used to target delivery systems to tumors is transferrin. The transferrin receptor (TfR) has been shown to be expressed at higher levels on cancer cells than on normal cells, so nanoparticle systems have been designed to target cancer cells by attaching transferrin to the delivery system [29]. Improvements in

delivery and associated cancer cell death have been observed using transferrin-functionalized systems [31]. Several studies have shown that the tumor accumulation is similar when comparing systems incorporating transferrin and their nontargeted counterparts [32]. The improved delivery has therefore been attributed to increased tumor cell internalization of the nontargeted nanoparticles.

Several systems have been developed to use monoclonal antibodies to target cancerous tumors. An anti-HER2 monoclonal antibody has been incorporated into doxorubicin loaded liposomes and shown to increase antitumor efficacy over control doxorubicin formulations [33]. Other studies have demonstrated that targeted liposomes with the anti-HER2 antibody were found at high concentrations in tumor cells while nontargeted liposomes where more commonly in the extracellular spaces. Additionally, targeted liposomes had a much greater preference for tumor cells over host cells while control systems showed no preference [34].

Another monoclonal antibody, 2C5, has been shown to increase efficacy when incorporated into liposomal doxorubicin systems. The targeted systems showed increased accumulation in lung cancer models when compared to nontargeted liposomal systems. The measured tumor reduction was also shown to be higher for the targeted systems compared to the control [35].

2.4 Polymer Nanoparticles

Particles that measure less than 0.1 μm in diameter are defined as nanoparticles. In practice, polymer particles smaller than 1 micron are commonly referred to as nanoparticles, and in this thesis they will be referred to as such. Polymer nanoparticles are of interest for applications in drug delivery because of their potential to target a variety of different specific locations in the body, elongate periods of dosage, protect sensitive therapeutics such as proteins, increase half-life circulation, and reduce systemic effects [36, 37]. Polymer nanoparticles with many different types of properties have been developed for use in drug delivery systems including biodegradable systems, hydrogel systems, and self-assembled systems such as micelles, liposomes, and polymersomes.

The use of polymer nanoparticles is particularly advantageous in drug delivery because of their inherent potential to avoid the RES and take advantage of the EPR effect [38, 39]. Microparticles or large nanoparticles are rapidly recognized by macrophages and cleared by the RES through the liver and spleen. Nanoparticles measuring less than 300 nm in diameter show increased avoidance of the RES particularly in particles that are less than 100 nm in diameter. This avoidance of the RES leads to a longer circulation half-life and ultimately greater localization at the delivery site. Because of the fast growth of tumors, the vasculature tends to be leaky and lymphatic drainage poor. Nanoparticles are preferentially extravasated and

concentrated at these tumor cites while small molecular weight drugs are not retained at such high concentrations.

Primarily, polymer nanoparticles are formed by one of two broad methods, either the dispersion of preformed polymers into nanoparticles, or monomer polymerization designed to directly polymerize into the final particle form. Additionally, block copolymers have been synthesized in order to assemble nanoscale polymersomes or micelles. These polymer nanoparticles along with various block copolymer assemblies have been extensively investigated for use as drug carriers [40, 41].

2.4.1 Biodegradable Systems

Biodegradable nanoparticle systems are of interest for the ability to combine desirable nanoscale properties with enhanced biocompatibility and controlled release. The most widely investigated biodegradable polymers for nanoparticle delivery are those based on the polyesters poly(lactic acid) (PLA), poly(glycolic acid) (PGA), and their copolymer poly(lactic acid-co-glycolic acid) (PLGA). By adjusting the ratio of lactic acid to glycolic acid in PLGA the rate of degradation can be controlled. Increased lactic acid content extends the degradation time of the polymer. The polymer degrades by hydrolysis to the monomers lactic acid and glycolic acid which can be metabolized by the body. Because the degradation time of PLGA can be easily tuned and the biocompatibility of the system has led to FDA approval for resorbable sutures, a large number of PLGA nanoparticle delivery systems have been developed.

Biodegradable polymer nanoparticles are formed most commonly using emulsion and solvent evaporation techniques, where the polymer is first dissolved in an organic phase that is subsequently dropped into a continuous aqueous phase and stirred until the solvent evaporates. Hydrophobic drugs can easily be incorporated into particles during this process by solvating the drug along with the polymer in the organic phase. These oil-in-water emulsions have been used to load a variety of hydrophobic drugs, such as anti-cancer therapeutics [42-44]. In addition to hydrophobic drugs, encapsulation of water-soluble drugs and biomolecules, including proteins and certain chemotherapeutics, has been achieved with water-in-oil-in-water double emulsion techniques [45-47].

Other synthesis techniques, such as nanoprecipitation and spray drying have also been used effectively to produce PLGA nanoparticles loaded with therapeutics [48]. In traditional spray-drying, the polymer is dissolved in a volatile solvent and the solution in sprayed into an apparatus where the particles are formed as the solvent evaporates [49]. Typically, this method yields particles at the upper limit of the nanoscale and in the microscale.

A modification of this method known as spray freezing into liquid (SFL) is also used to synthesize polymer micro and nanoparticles. In this case, a solution of the polymer is sprayed through an atomizing nozzle into liquid nitrogen over a solvent such as frozen ethanol [50]. Particles form upon contact with the liquid nitrogen and are collected in the ethanol after evaporation of the liquid nitrogen. Drugs have been

incorporated during particle formation by addition to polymer solution or formation of an oil-in-water emulsion prior to atomization [51, 52].

Recent studies have carefully evaluated the effects of PLGA nanoparticle properties on drug loading. For example, smaller nanodelivery systems have a smaller volume, and therefore, would be expected to have a smaller maximum loading capacity. In the majority of studies, the maximum loading capacity is not determined for a carrier. The achieved loading capacity of a delivery system is dependent on factors beyond volume alone. For example, drug loading and release from PLGA micro- and nanospheres have been shown to be inversely correlated with size. In a study that compared two sizes of PLGA particles, dexamethasone was first loaded into PLGA microspheres using a typical oil-in-water solvent evaporation method to produce 20 µm particles. Smaller 1 µm particles loaded with dexamethasone were produced via emulsion polymerization. The emulsion polymerization scheme for the smaller particles led to a dexamethasone encapsulation efficiency of 11.2% compared to 1% for the larger microparticles when incubating 100 mg of dexamethasone with 500 mg of polymer [53].

Drug delivery systems composed of polyanhydrides have been widely investigated because of their surface eroding degradation mechanism which can lead to near zero-order release profiles [54, 55]. In general, drugs have been successfully incorporated in polyanhydride disks such as the Gliadel® system or microparticles [56]. Double emulsion techniques including water-oil-water, or water-oil-oil have also been

used to synthesize biodegradable nanoparticles based on polyanhydrides for drug delivery [57]. However, there have been limited studies demonstrating loading and release from polyanhydride carriers on the nanoscale.

In one study, paclitaxel or 2-hydroxypropyl-β-cyclodextrin (HPCD)-complexed paclitaxel was encapsulated in polyanhydride nanoparticles composed of poly(methyl vinyl ether-co-maleic anhydride) during particle formation using a solvent displacement method which simultaneously allowed nanoparticle formation and loading. Up to a 167 μg/mg loading capacity was obtained for nanoparticles with an average diameter of 302 nm. The controlled release of HPCD-paclitaxel was then demonstrated in different simulated biological fluids. No release was observed from particles in simulated gastric fluid (pH 1.2) whereas there was complete release over a 24 hour period in simulated intestinal fluid (pH 7.5) [58].

Like synthetic biodegradable systems, nanodelivery systems composed of naturally occurring biodegradable polymers have been investigated for drug delivery. Some of the most widely studied are systems based on the biodegradable and biocompatible polysaccharide chitosan. The potential use of chitosan carriers has been demonstrated for a vast number of drugs and applications. For example, chitosan carriers have received considerable attention for delivery of nucleic acids due to chitosan's net positive charge. One of the contributing factors to chitosan's versatility is that a number of techniques have been developed to synthesize chitosan nanoparticles

including ionic gelation, precipitation, reverse micelle formation, self-assembly, and spray drying [59, 60].

In one study examining the use of chitosan for delivery of biomolecules, a model protein, bovine serum albumin (BSA), was loaded into chitosan nanoparticles prepared by two different methods using tripolyphosphate (TPP) as an ionic crosslinker. In the first method termed "incorporation", BSA was incorporated into the polymer matrix during particle formation by adding BSA to a chitosan solution before the addition of the TPP crosslinker at which point particles spontaneously formed during mixing. Using the "incubation" method, BSA was simply adsorbed to the surface of nanoparticles during incubation following particle coacervation. Encapsulation efficiencies up to 88% were obtained and BSA release was primarily shown to be a fast release over a 6 hour period [61]. In another study, chitosan nanoparticles crosslinked with TPP were loaded with methotrexate disodium (MTX) using a post-polymerization incubation method. Loading capacities up to 52% and loading efficiencies up to 78% were obtained when an MTX concentration of 1.26 mg/mL was incubated with a 0.16 wt% nanogel solution [62].

Chitosan nanoparticles have also been formulated to deliver anticancer drugs. For example, a water-in-oil microemulsion method was used to entrap a doxorubicin-dextran conjugate in chitosan nanoparticles having a hydrodynamic diameter of 100 nm. Entrapment efficiencies were measured between 60-65%. In a mouse model, treatment with the loaded nanoparticles led to faster and more complete tumor regression than free drug or empty nanoparticles [63].

Another natural biodegradable material used to synthesize nanoparticles for drug delivery applications is the anionic biopolymer alginate. Most often calcium chloride is added to a solution of alginate to induce ionic crosslinking, resulting in micro- and nanoparticle polymer networks. In one case, alginate gelation with calcium ions followed by coating with chitosan produced nanoparticles intended for oral insulin delivery applications. A maximum insulin encapsulation efficiency was measured at 92% with loading capacities up to 14.3% [64]. Isoniazid, rifampicin, and pyrazinamide were encapsulated in alginate particles using a cation gelation method in an effort to design aerosolized nanoparticles for treatment of tuberculosis. Calcium chloride was added to sodium alginate solution containing varying amounts of the three drugs to induce the gelation and encapsulation of the drug. Drug encapsulation efficiencies ranged from 70-90% in particles at the upper limit of so-called nanoparticles with an average size just around 1 μm [65].

2.4.2 Self-Assembled Systems

Self-assembled nanoparticles, including liposomes, micelles, and polymersomes, can be formed using various amphiphiles such as natural lipids or block copolymers. Liposomes are vesicles that consist of a spherical shaped lipid bilayer, or multilayers, containing an inner aqueous void space. Liposomal encapsulation is a versatile method to load therapeutics, because hydrophilic drugs and biomolecules can be loaded in the inner aqueous void, while hydrophobic molecules can be entrapped in the lipid bilayer.

Liposomal delivery of chemotherapeutics has been established as an effective method to increase efficacy and decrease toxicity over free drug, evidenced by the success of liposomal doxorubicin, Doxil®, which has been approved for human use in cancer treatment [66].

In addition to the lipid structures, synthetic block copolymers built with one hydrophilic block and one hydrophobic block have been shown to exhibit a variety of self-assembled structures including spherical or cylindrical micelles and vesicles with architectures that resemble liposomes known as polymersomes [67]. Micelles, nanoparticles with a hydrophobic core and hydrophilic outer layer, self-assembled from amphiphilic block copolymers in aqueous media, are frequently used to entrap hydrophobic drugs during micelle formation. During spontaneous micelle formation in an aqueous environment, hydrophobic drugs are localized in and around the hydrophobic core [68]. This loading method has been used to entrap a variety of therapeutics, particularly anticancer agents, in block copolymers of poloxamers, which consist of blocks of poly(ethylene oxide) (PEO) and poly(propylene oxide) (PPO), and NK105, which consists of blocks of PEG and a modified polyaspartate [41, 69, 70].

Using this method of drug loading, micelle nanoparticles have been used to entrap hydrophobic anticancer therapeutics. Biodegradable, cationic micelle nanoparticles were self-assembled using amphiphilic poly, P(MDS-co-CES). In this study, Herceptin®, which is a monoclonal antibody, was attached to the surface of the particles while paclitaxel was loaded into the micelles by dissolving the polymer and drug in DMF

and dialyzing against a sodium acetate/acetic acid buffer. This method let to encapsulation efficiencies of paclitaxel of 58.1% and a loading capacity of 14.3%. Release studies demonstrated the that the drug could be released from the nanoparticles over a 69 hour period [71].

While traditional micelle systems have been used primarily to incorporate hydrophobic drugs, adapted systems have been used to entrap more hydrophilic species such as biomolecules. For example, drug carrier systems called polyion complex (PIC) micelles have been synthesized from PEG block copolymers. The PIC micelles are formed using block copolymers consisting of a hydrophilic block and a polyionic block. In this case, electrostatic interactions between the ionic polymer and an oppositely charged species are a driving force for the formation of the micelles. Poly(ethylene glycol-grafted-chitosan), PEG-g-chitosan, block copolymers were used to entrap diammonium glycyrrhizinate (DG) in micelles assembled in acetate buffer after addition of TPP to induce chitosan aggregation. Loading efficiencies of DG over 96% have been obtained using these systems and the average diameter of micelles was between 20 and 30 nm. Release profiles varied based on the free ions in solution. In ionic solution, a burst release was observed, but there was limited release in DI water [72].

Polymer vesicles called polymersomes or polymerosomes have been used to entrap a variety of therapeutics and model drugs. For example, polymersomes with diameters around 100 nm were prepared from triblock copolymers, poly(caprolactone)-poly(ethylene glycol)-poly(caprolactone), PCL-PEG-PCL, using a double emulsion

method. Insulin was incorporated during self-assembly of 122 nm particles [73]. In another study, triblock copolymers, poly(ethylene oxide)-b-poly(acrylic acid)-b-poly(N-isopropylacrylamide) (PEO-PAA-PNIPAM), were synthesized via RAFT polymerization. The resulting polymers were water soluble at room temperature, but formed polymer vesicles with diameters between 170 and 250 nm above 32° C. These polymersomes were loaded with FITC-dextran during self-assembly at elevated temperatures and then crosslinked using cystamine via carbodiimide chemistry. The crosslinks were shown to degrade in the presence of dithiothreitol, and therefore, it was hypothesized that these systems are degradable *in vitro* and in vivo. Loading capacity of these nanoparticles was measured at levels exceeding 85% by weight [74].

Recently, there has been interest in creating systems that are hybrid particles combining properties of liposomes and synthetic polymer systems for nanodelivery applications. Cationic lipids have been combined with peptide-lipid amphiphiles and 1,2-distearoyl-*sn*-glycero-3-phosphoethanolamine-*N*-carboxy(polyethylene glycol) to design liposome nanoparticles targeted to the urokinase plasminogen activator receptor (uPAR) overexpressed on many tumors. The particles have an ABCD structure, an inner aqueous (A) layer of loaded anionic nucleic acids, a cationic lipid bilayer (B), a PEG layer for stealth characteristics (C), and a peptide sequence layer for targeting of uPAR (D). Loading efficiencies as high as 60% were achieved when 10 wt% docetaxel was added during the particle self-assembly process [75]. In another example, hybrid systems were formed through self-assembly to form nanoparticles with a lipid monolayer surrounding

a PLGA core loaded with a hydrophobic drug. This unique system relied on PEG-conjugated lecithin to form a hydrophilic outer shell of PEG as the lipid monolayer formed around the hydrophobic PLGA polymer. Drug loading of docetaxel into the PLGA core was accomplished during this self-assembly process by first dissolving polymer and drug in an organic solvent and then dripping this solution into an aqueous solution containing PEG-lecithin. This process led to the formation of the particles via self-assembly and the solvent was allowed to evaporate. Encapsulation efficiencies of 62% were obtained using this method when adding 10 wt% docetaxel to the organic polymer solution. Controlled release was observed over a 100 h period and shown to be a function of lipid coverage, where the release rate could be slowed by increasing the lipid to polymer ratio [76].

2.4.3 Nanogels

Upon injection into the bloodstream, nanoscale systems have the ability to circulate for extended periods of time and to be taken up by cells. Their dimensional properties such as high surface area and rapid response to external stimuli make them attractive candidates for *in vivo* systems [77]. In particular, nanoscale hydrogel systems, known as nanogels, are of interest for use as "intelligent" drug carriers. These intelligent materials respond to external stimuli such as pH, temperature, and ionic strength by imbibing water and swelling under certain of these conditions.

Hydrogels are crosslinked polymers that are hydrophilic but insoluble in aqueous environments. Under specific conditions, the polymer networks imbibe water to swell. Hydrogel carriers have been designed to exhibit stimuli-sensitive behavior, where degree of swelling is affected by some external stimulus such as pH, temperature, ionic strength, or electric field [78, 79]. Because of this swelling behavior in response to their environment, stimuli-sensitive polymers are known as “intelligent” or “smart” polymer systems.

Intelligent hydrogel carriers have been used to encapsulate various therapeutic molecules and subsequently release them following a change in one of these external conditions. Release from these systems has been triggered by both swelling and shrinking of hydrogel carriers [4, 80]. In the first case, a therapeutic molecule is encapsulated in a carrier in its collapsed state where the drug is protected and small mesh size limits diffusion in or out of the polymer matrix [81]. If the polymer encounters an environment that triggers swelling, the mesh size increases, and there is an increase in the rate of diffusion, so that the therapeutic is released into the surrounding environment. In the latter case, a polymer is synthesized so that in its swollen state the properties are such that the polymer can encapsulate and protect a molecule of interest. Upon deswelling or shrinking there is a fast release as some of the encapsulated material is squeezed out of the polymer matrix [82]. As this cycle is repeated, a pulsatile release of the therapeutic may be observed.

Temperature-responsive polymers can exhibit one of two different types of temperature behaviors in aqueous solutions and will separately be examined in this work. Both types of these systems, those that exhibit upper critical solution temperature (UCST) and those that fall into the class of lower critical solution temperature (LCST) behavior will be synthesized and investigated here. Hydrogels with UCST behavior have characteristics such that at lower temperatures some polymer-polymer interactions lead to a less swollen state. Upon heating through the UCST these interactions are weakened, so that the polymer effectively becomes miscible with the aqueous phase, but because the polymer is crosslinked the systems imbibes water and swells.

Certain types of interpenetrating polymer networks, IPNs, such as those based on acrylamide (AAm) and acrylic acid (AA) demonstrate this type of behavior with transition temperatures near 40 °C [83]. IPNs consist of two separately crosslinked polymer networks that are physically entangled with the first network, but not covalently attached. The PAA network and the PAAm network undergo hydrogen bonding at low temperatures, which breaks down above the UCST and electrostatic and steric interactions cause the polymer to swell.

Polymers demonstrating LCST behavior, most commonly poly(N-isopropylacrylamide), PNIPAAm, and related copolymers, have also been investigated for use as temperature sensitive drug carriers. The presence of separate hydrophilic and hydrophobic groups in the polymer chain generally leads to this behavior. At low

temperatures, hydrogen bonding interactions between water and the hydrophilic groups lead to a swollen state, but an increase in temperature beyond the transition temperature leads to a weakening of the water-polymer hydrogen bonding and a strengthening of hydrophobic polymer-polymer interactions [84]. LCST drug carriers have been developed that expel encapsulated therapeutics upon heating above transition temperatures at therapeutically relevant temperatures by what is known as a "squeezing out" method upon collapse of the polymer system [4].

While most biodegradable or self-assembled nanoparticle systems are formed from previously synthesized polymers, hydrogel nanoparticles are most commonly synthesized using heterogeneous polymerization techniques. Because the hydrogel nanoparticles are formed during polymerization, incorporating a therapeutic at this stage requires exposing the drug to polymerization conditions that could potentially damage or modify the drug. However, the porous characteristics of nanogel matrices allows for drug loading following polymerization by partitioning methods, which eliminates the need to subject the drug to harsh polymerization conditions. In most situations, the drug is loaded into the nanogel by incubating the nanoparticles with the drug in aqueous conditions such that the particles are in their most swollen state. After a period of time to allow the therapeutic to diffuse into the polymer matrix, a condition (most commonly pH or temperature) is altered, leading to a particle size transition to a more collapsed state with a smaller mesh size, physically entrapping the therapeutic in the polymer matrix.

Hydrogel nanoparticles, or nanogels have been synthesized using several techniques including dispersion and emulsion polymerization as well as step and flash imprint lithography [78, 85, 86]. These nano-scale hydrogels show rapid response rates, swelling quickly with small changes in stimuli. Synthetic nanogels have stimuli-sensitive properties similar to their bulk hydrogel counterparts, exhibiting volume phase transitions in response to pH, temperature, electric field, or other environmental stimuli [87].

Several heterogeneous polymerization techniques have been used to synthesize monomers directly into the desired polymer hydrogel nanoparticles. Two commonly used techniques are emulsion and dispersion polymerizations, and both are used to synthesize the various temperature-sensitive polymers in the proposed therapeutic systems. Oil-in-water emulsions are commonly used to synthesize hydrophobic polymers from similarly hydrophobic monomers. Polymerization occurs in micelles that are formed with the addition of surfactant as monomers diffuse from large droplets into micelles and react with initiator [88]. Similarly, water-in-oil emulsions have been used to synthesize polymers from more water soluble molecules. Previous work in this group featured the use of consecutive water-in-oil microemulsion polymerizations to synthesize IPN nanoparticles, and this technique has been adapted for use in this thesis. Monomer and crosslinker are dissolved in an aqueous phase and emulsified into a cyclohexane oil phase with surfactant. Initiator is added to start the polymerization in the aqueous micelles [89].

Dispersion polymerization has been used in free radical polymerizations where the growing polymer is much less soluble in a particular solvent than the monomer. Monomer and initiator are dissolved in a solvent in a homogenous mixture often with the inclusion of some molecule to act as a steric stabilizer for particle formation. As polymerization begins, growing macroradicals precipitate, and form stabilized particles. Continued polymerization occurs as the particles are slightly swollen in the polymerization medium [90]. An aqueous dispersion polymerization has been used to synthesize temperature-sensitive hydrogel polymers with LCST behavior. Nanoparticles of PNIPAAm and related copolymers have been synthesized by reaction of monomers in aqueous medium at elevated temperature with or without steric stabilizer molecules such as sodium dodecyl sulfate (SDS) [91]. The reaction is performed at a temperature well above the LCST of the resultant polymer. Since the temperature is above the LCST, the polymer is immiscible in the aqueous environment and particle nucleation occurs.

The hydrophilic nature of hydrogel systems makes them an ideal candidate for the loading and delivery of water soluble therapeutics such as protein or nucleic acid biomacromolecules. Several nanogel systems have been investigated for the delivery of insulin to the small intestine. In addition to their ability to entrap the water soluble insulin, some of these systems have advantageous pH-sensitive properties allowing them to protect insulin in the acidic environment of the stomach and release it in the more neutral pH of the small intestine [92, 93].

Polybasic nanoparticles consisting of cationic pH responsive hydrogels with PEG grafts, have been synthesized by a UV-initiated free radical emulsion polymerization was used to synthesize poly[2-(diethylamino) ethyl methacrylate] surface grafted with PEG (PDGP) nanogels. Insulin as a model drug was added to a solution of these nanogels and the pH was adjusted to 6.5 to swell the nanoparticles. After a loading period the pH was raised quickly to 7.4 to collapse the particles and entrap the loaded protein. The loaded nanogels were dialyzed against water for 5 days to remove any excess protein not loaded. Encapsulation efficiencies were measured up to 92% for insulin in PDGP particles with low crosslinking densities when equal weights of particles and protein were added to the loading solution [94].

Controlled drug loading and release has also been shown in several studies using hydrogels based on the temperature-sensitive polymer poly(N-isopropylacrylamide) (PNIPAAm). PNIPAAm exhibits a negative swelling transition at 34 °C, which makes it an attractive system from a physiological standpoint for applications in drug delivery. For example, poly(NIPAAm) and poly(NIPAAm-co-AA) nanoparticles were loaded with 5-fluorouracil and release was shown to be a function of pH and temperature [95].

Nanogels of poly(vinyl alcohol), PVA, and poly(vinyl pyrrolidone), PVP have also been investigated for drug delivery applications. For example, composite systems of PVA-crosslinked PVP nanogels were used to entrap ferromagnetic particles as well as bleomycin A5 hydrochloride. Nanogels were prepared using a water-in-oil emulsion polymerization initiated by gamma ray irradiation. For this emulsion polymerization,

the aqueous phase contained the PVA, PVP, and the ferromagnetic particles. The resulting nanogels entrapped the ferromagnetic particles and were then used to load bleomycin A5 hydrochloride. Dry nanoparticles were allowed to swell in an aqueous solution containing the drug, sonicated, and then placed on a shaker plate for 12 h of storage until no apparent liquid was visible. Encapsulation efficiency was not reported, because it was assumed that all of the drug had been immobilized, but *in vitro* release occurred over a minimum period of 8 hours [96].

While most hydrogel nanodelivery systems have been used to entrap hydrophilic molecules, recent work on modified hydrogels has demonstrated the potential to load hydrophobic drugs as well. In order to do so, the hydrophobicity of the nanogels has been increased through the incorporation of amphiphiles into the hydrogel matrix. An acrylated PEG-PPG-PEG triblock copolymer with both hydrophobic and hydrophilic groups was used to synthesize crosslinked nanoparticles via an inverse microemulsion using a PEG crosslinker. Properties of the emulsion could be altered to control for particle sizes ranging from 50 to 500 nm. These nanogels were then loaded with doxorubicin to determine their ability to carry hydrophobic drugs. Doxorubicin, solubilized in chloroform with triethylamine, was added to an aqueous solution of nanoparticles and the chloroform was allowed to evaporate overnight. The results indicated that the formation of nanogels from amphiphilic macromers was a successful strategy for loading hydrophobic drugs in a hydrogel with up to 9.8% loading capacity of doxorubicin [97].

2.5 GOLD NANOPARTICLES

Metal nanoparticles are of interest for biomedical applications because of their optical properties, specifically the scattering and absorption of light over a wide range of wavelengths. Gold and silver nanoparticles in particular have been used to absorb light in regions spanning the visible and near-infrared (NIR) [98]. These characteristics have been investigated for applications in medical imaging, drug delivery, and biosensing [99-101]. Metal particles capable of absorbing light in the NIR region are of interest for the applications discussed in this thesis, because light in this region is physiologically transmissive and not harmful to tissue [102]. Gold or silver nanoshells and gold nanorods have been demonstrated to absorb high amounts of light in this region and have been widely investigated for *in vivo* applications.

Nanoshells consist of a thin metal shell around a dielectric core. Commonly the core is silica and the surrounding metal shell is gold. These gold nanoshells can be tuned to have peak absorbance at wavelengths of light ranging from 700-1100 nm. By changing the ratio of the thickness of the gold shell to the diameter of the silica core the optical resonance varies from across wavelenths of the visible and NIR regions [103]. For example, a gold nanoshell with a 60 nm diameter silica core and a 20 nm thick gold shell has a maximum optical resonance near 725 nm while the same silica core with a 5nm gold shell displays peak resonance around 1025 nm [104]. By carefully controlling the size of the silica core and the growth of gold shell, particles can be formed with peak extinction in the NIR region where tissue transmissivity is highest. Figure 2.1 shows a

TEM micrograph of gold nanoshells of roughly 80 nm in total diameter that exhibit peak extinction around 800 nm in the desirable NIR region.

Many metal nanoparticles, particularly silver and gold, display strong absorption in the visible spectrum, typically ranging from yellow to reddish-brown [105]. By altering the size and in particular the shape of these nanoscale particles, absorption can be observed in nearly any part of the visible spectrum and into the infrared spectrum. Synthesis of structures ranging from nanospheres and nanowires to nanoprisms and nanoplates are reported in the literature exhibiting a variety of different visual appearances and absorbance spectra [106]. Gold nanorods are nanoscale spherocapped cylindrical particles. The nanorods show varying absorption spectra determined by the aspect ratio of the rods, which can be described using Mie theory. Small changes in aspect ratio have dramatic effects on the optical properties of the particles, for example changing the aspect ratio of a gold nanorod over a range of approximately 3:1 to 7:1 causes a red-shift from maximum absorption at 750 nm to 980nm [107]. Nanorods with aspect ratios near 4:1 such as those with a length of 40 nm and a width of 10 nm as shown in Figure 2.2 absorb strongly in the NIR region.

An effect known as localized surface Plasmon resonance occurs when two metallic nanoparticles are in close proximity to each other, typically within about 2.5 times the diameter of one of the particles [108]. When the particles are exposed to light there is a collective oscillation of electrons. The extinction behavior becomes a function of not only the size and shape of the nanoparticle but also the distance between

adjacent particles and their orientation to each other. For example, as 50 nm gold nanorods are moved closer together at distances less than 100 nm, the extinction spectrum becomes more red-shifted and the peak broadens.

2.6 Externally-Controlled Delivery

Externally-controlled or externally-triggered delivery systems are those in which some source external to the body can be used to create a signal to induce release a therapeutic at a desired time and location. The external source in most cases is a form of electromagnetic radiation or an acoustic signal. The signal must be able to penetrate through tissue to reach the delivery system. Typically the signal will either induce heating in the delivery vehicle or interact mechanically with the system to trigger release. These remotely controlled systems can have the same benefits as targeted systems in that they can improve therapeutic index locally while reducing systemic effects. In some cases, externally controlled systems have been functionalized with targeting ligands to further improve efficacy.

Externally applied electric fields, ultrasound, and mechanical forces have also been used to trigger a swelling transition and subsequent drug release [2, 5, 109]. For example ultrasound microbubbles have been developed for use as externally triggered delivery and imaging systems [110]. A focused ultrasound pulse can be used to disrupt the microbubbles and locally deliver a drug or contrast agent.

The swelling characteristics of temperature responsive hydrogels can be combined with a means to heat them via an external signal to trigger drug delivery. Heating can be triggered by several types of signals including light and magnetic fields. A magnetic field has been used to induce heating in a PNIPAAm hydrogel film system loaded with superparamagnetic iron oxide particles which triggers a negative swelling and release of a model drug [5].

Other systems have been developed to control the release of a therapeteutic using light. In one case, gold nanoshells have been incorporated into poly(N-isoproplyacrylamide-co-acrylamide), P(NIPAAm-co-AAm), films or disks. Upon exposure to certain wavelengths of light, gold nanoshells heat the polymer and trigger a negative swelling transition. This behavior has been used to externally control the opening and closing of a microvalve and to trigger pulsatile release of insulin from a polymer loaded film [82, 111].

Previous work in this laboratory has focused on developing a nanoscale system that incorporates light as the trigger to produce a temperature change, swelling transition, and subsequent drug release from UCST nanogel particles. In the IPN systems that have been developed, complexation of the two networks occurs at low temperatures because of hydrogen bonding. As the polymer is heated, hydrogen bonding begins to break down and a positive swelling transition is observed around 38-42 °C [89]. A synthetic procedure has been developed for temperature-sensitive IPNs composed of interpenetrating networks of poly(acrylic acid), PAA, and poly(acrylamide),

PAAm [112]. The inverse-microemulsion produces particles between 100 nm and 1 µm in diameter, and there is potential to incorporate gold particles in the polymer matrix when added to the aqueous phase of the water-in-oil emulsion leading to a light-triggered release system.

2.7 PHOTOACOUSTIC IMAGING

A contrast agent that absorbs nanopulsed light undergoes thermoelastic expansion in response to the pulsed laser light. A temperature rise associated with the excitation from the nanopulsed light leads to thermal expansion. This pulsed expansion produces ultrasonic waves that are detected by the transducer. The detected acoustic signal can be used to reconstruct an image of the area of interest. A number of materials have been used as contrast agents for photoacoustic imaging.

Single-walled carbon nanotubes have been used as a contrast agent to image tumors [113]. The targeted carbon nanotubes were administered intravenously to mice with tumors and a photoacoustic signal was observed at the tumor that was 8 times stronger than the signal from nontargeted carbon nanotubes.

Metal nanoparticles have been used as a contrast agent to induce an acoustic signal. Gold nanoparticles, nanoshells, nanocages, and nanorods have all been used as contrast agents to create a photoacoustic signal when irradiated with short pulses of light [114-118]. Silver nanosystems have also been used as a contrast agent for

photoacoustic imaging [119]. In another system gold coated ferromagnetic cobalt nanoparticles were shown to be an effective contrast agent [120].

2.8 Conclusions

Because of the adverse health effects associated with systemic delivery of therapeutic agents such as anticancer drugs there is great interest in developing systems that can deliver a therapeutic locally to a disease site. In the case of chemotherapy, the use of nanoscale drug delivery systems is of interest because of their ability to passively target tumors, and in some cases actively target following functionalization of these particulate systems with targeting ligands. Externally-triggered systems can go one step further by precisely controlling the time and place that a drug is released. There is a great need for improved systems that can better maximize therapy while minimizing adverse systemic effects.

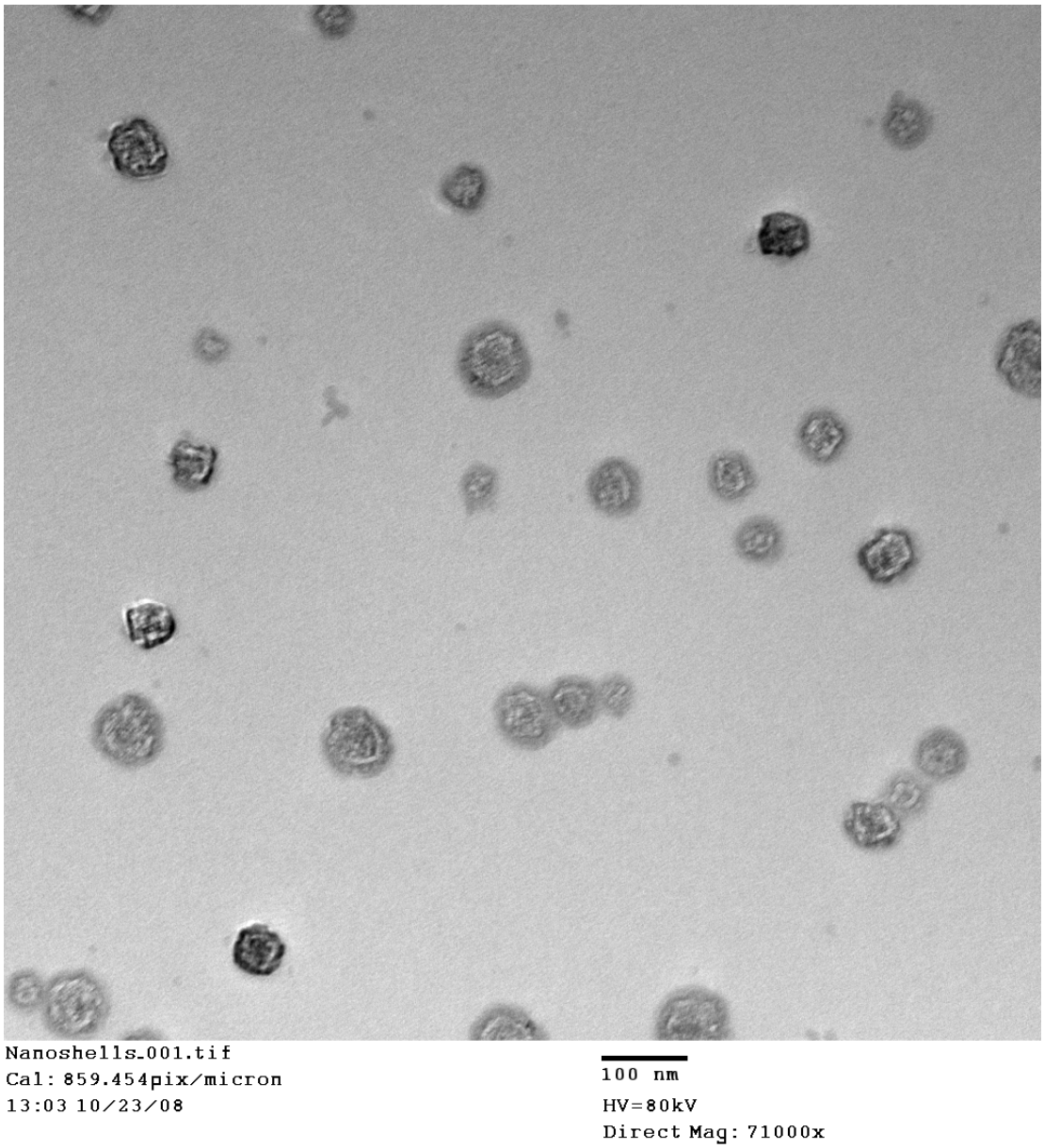

Figure 2.1 TEM micrograph of gold nanoshells formed from a gold shell on a silica core with strong NIR absorption.

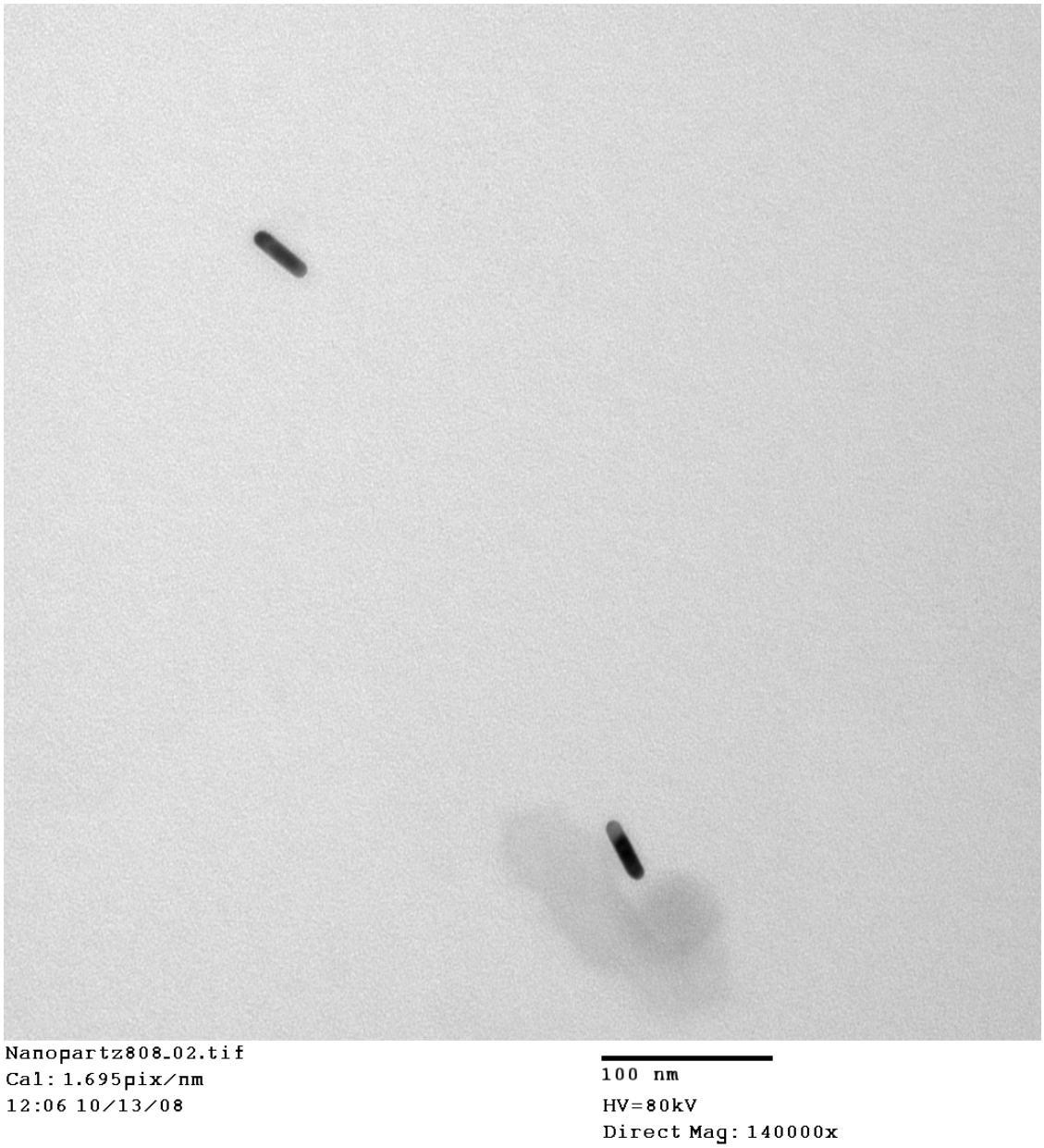

Figure 1.2 TEM micrograph of gold nanorods having 4:1 aspect ratio leading to peak absorption at 808 nm.

REFERENCES

1. Lentacker, I., Geers, B., Demeester, J., De Smedt, S.C., and Sanders, N.N., *Design and Evaluation of Doxorubicin-containing Microbubbles for Ultrasound-triggered Doxorubicin Delivery: Cytotoxicity and Mechanisms Involved.* Mol. Ther., 2010. **18**(1): p. 101-108.

2. *The Use of Ultrasound for Drug Delivery.* Echocardiography 2013 Jnl Cardiovascular Ultrasound & Allied Techniques, 2001. **18**(4): p. 323-328.

3. Ferrara, K.W., *Driving delivery vehicles with ultrasound.* Adv. Drug Deliv. Rev., 2008. **60**(10): p. 1097-1102.

4. S. R. Sershen, S.L.W., N. J. Halas, J. L. West,, *Temperature-sensitive polymer-nanoshell composites for photothermally modulated drug delivery.* J. Biomed. Mater. Res., 2000. **51**(3): p. 293-298.

5. Satarkar, N.S. and Hilt, J.Z., *Magnetic hydrogel nanocomposites for remote controlled pulsatile drug release.* J. Control. Release, 2008. **130**(3): p. 246-251.

6. Zhang, J.L., Srivastava, R.S., and Misra, R.D.K., *Core-shell magnetite nanoparticles surface encapsulated with smart stimuli-responsive polymer: Synthesis, characterization, and LCST of viable drug-targeting delivery system.* Langmuir, 2007. **23**(11): p. 6342-6351.

7. Byrne, J.D., Betancourt, T., and Brannon-Peppas, L., *Active targeting schemes for nanoparticle systems in cancer therapeutics.* Adv. Drug Deliver. Rev., 2008. **60**(15): p. 1615-1626.

8. Jemal, A., Siegel, R., Ward, E., Hao, Y.P., et al., *Cancer statistics, 2008.* CA-Cancer J. Clin., 2008. **58**(2): p. 71-96.

9. Edwards, B.K., Brown, M.L., Wingo, P.A., Howe, H.L., et al., *Annual report to the Nation on the status of cancer, 1975-2002, featuring population-based trends in cancer treatment.* J. Natl. Cancer I., 2005. **97**(19): p. 1407-1427.

10. Parkin, D.M., Bray, F., Ferlay, J., and Pisani, P., *Global cancer statistics, 2002.* CA-Cancer J. Clin., 2005. **55**(2): p. 74-108.

11. Services, C.D.o.H., Council, C.S.C.A., and California, M.B.o., *Breast cancer treatment: summary of effective methods, risks, advantages, disadvantages*. 1991: Printed and distributed by the Medical Board of California.

12. Fowble, B., *Breast cancer treatment: a comprehensive guide to management*. 1991: Mosby-Year Book.

13. McPhee, S., Tierney, L., and Papadakis, M., *Current medical diagnosis & treatment 2007*. 2006: McGraw-Hill Medical.

14. Moulder, S. and Hortobagyi, G.N., *Advances in the Treatment of Breast Cancer.* Clin. Pharmacol. Ther., 2007. **83**(1): p. 26-36.

15. Romond, E.H., Perez, E.A., Bryant, J., Suman, V.J., et al., *Trastuzumab plus adjuvant chemotherapy for operable HER2-positive breast cancer.* N. Engl. J. Med., 2005. **353**(16): p. 1673-1684.

16. Miller, K., Wang, M.L., Gralow, J., Dickler, M., et al., *Paclitaxel plus bevacizumab versus paclitaxel alone for metastatic breast cancer.* N. Engl. J. Med., 2007. **357**(26): p. 2666-2676.

17. Abe, O., Abe, R., Enomoto, K., Kikuchi, K., et al., *Effects of chemotherapy and hormonal therapy for early breast cancer on recurrence and 15-year survival: an overview of the randomised trials.* Lancet, 2005. **365**(9472): p. 1687-1717.

18. Abe, O., Abe, R., Enomoto, K., Kikuchi, K., et al., *Polychemotherapy for early breast cancer: an overview of the randomised trials.* Lancet, 1998. **352**(9132): p. 930-942.

19. Eifel, P., Axelson, J.A., Costa, J., Crowley, J., et al., *National Institutes of Health Consensus Development Conference statement: Adjuvant therapy for breast cancer, November 1-3, 2000.* J. Natl. Cancer I., 2001. **93**(13): p. 979-989.

20. Buzdar, A.U., *Preoperative chemotherapy treatment of breast cancer—A review.* Cancer, 2007. **110**(11): p. 2394-2407.

21. Longley, D.B., Harkin, D.P., and Johnston, P.G., *5-Fluorouracil: mechanisms of action and clinical strategies.* Nat. Rev. Cancer, 2003. **3**(5): p. 330-338.

22. Gabizon, A., Shmeeda, H., and Barenholz, Y., *Pharmacokinetics of pegylated liposomal doxorubicin - Review of animal and human studies.* Clin. Pharmacokinet., 2003. **42**(5): p. 419-436.

23. Cattel, L., Ceruti, M., and Dosio, F., *From conventional to stealth liposomes a new frontier in cancer chemotherapy.* Tumori, 2003. **89**(3): p. 237-249.

24. Harris, L., Batist, G., Belt, R., Rovira, D., et al., *Liposome-encapsulated doxorubicin compared with conventional doxorubicin in a randomized multicenter trial as first-line therapy of metastatic breast carcinoma.* Cancer, 2002. **94**(1): p. 25-36.

25. Kim, H.S. and Wainer, I.W., *Simultaneous analysis of liposomal doxorubicin and doxorubicin using capillary electrophoresis and laser induced fluorescence.* J. Pharm. Biomed. Anal., 2010. **52**(3): p. 372-376.

26. Owens III, D.E. and Peppas, N.A., *Opsonization, biodistribution, and pharmacokinetics of polymeric nanoparticles.* Int. J. Pharm., 2006. **307**(1): p. 93-102.

27. Peer, D., Karp, J.M., Hong, S., Farokhzad, O.C., et al., *Nanocarriers as an emerging platform for cancer therapy.* Nat. Nanotechnol., 2007. **2**(12): p. 751-760.

28. Wang, X., Li, J., Wang, Y., Cho, K.J., et al., *HFT-T, a Targeting Nanoparticle, Enhances Specific Delivery of Paclitaxel to Folate Receptor-Positive Tumors.* ACS Nano, 2009. **3**(10): p. 3165-3174.

29. Daniels, T.R., Delgado, T., Rodriguez, J.A., Helguera, G., and Penichet, M.L., *The transferrin receptor part I: Biology and targeting with cytotoxic antibodies for the treatment of cancer.* Clin. Immunol., 2006. **121**(2): p. 144-158.

30. Sudimack, J. and Lee, R.J., *Targeted drug delivery via the folate receptor.* Adv. Drug Deliver. Rev., 2000. **41**(2): p. 147-162.

31. Sahoo, S.K. and Labhasetwar, V., *Enhanced Antiproliferative Activity of Transferrin-Conjugated Paclitaxel-Loaded Nanoparticles Is Mediated via Sustained Intracellular Drug Retention.* Mol. Pharm., 2005. **2**(5): p. 373-383.

32. Bartlett, D.W., Su, H., Hildebrandt, I.J., Weber, W.A., and Davis, M.E., *Impact of tumor-specific targeting on the biodistribution and efficacy of siRNA*

nanoparticles measured by multimodality in vivo imaging. P. Natl. Acad. Sci. U.S.A., 2007. **104**(39): p. 15549-15554.

33. Shmeeda, H., Tzernach, D., Mak, L., and Gabizon, A., *Her2-targeted pegylated liposomal doxorubicin: Retention of target-specific binding and cytotoxicity after in vivo passage.* J. Control. Release, 2009. **136**(2): p. 155-160.

34. Lee, A.L.Z., Wang, Y., Cheng, H.Y., Pervaiz, S., and Yang, Y.Y., *The co-delivery of paclitaxel and Herceptin using cationic micellar nanoparticles.* Biomaterials, 2009. **30**(5): p. 919-927.

35. El Bayoumil, T. and Torchilin, V.P., *Tumor-Targeted Nanomedicines: Enhanced Antitumor Efficacy In vivo of Doxorubicin-Loaded, Long-Circulating Liposomes Modified with Cancer-Specific Monoclonal Antibody.* Clin. Cancer Res., 2009. **15**(6): p. 1973-1980.

36. Hans, M.L. and Lowman, A.M., *Biodegradable nanoparticles for drug delivery and targeting.* Curr. Opin. Solid St. M., 2002. **6**(4): p. 319-327.

37. Singh, R. and Lillard, J.W., *Nanoparticle-based targeted drug delivery.* Exp. Mol. Pathol., 2009. **86**(3): p. 215-223.

38. Brannon-Peppas, L. and Blanchette, J.O., *Nanoparticle and targeted systems for cancer therapy.* Adv. Drug Deliver. Rev., 2004. **56**(11): p. 1649-1659.

39. Maeda, H., Wu, J., Sawa, T., Matsumura, Y., and Hori, K., *Tumor vascular permeability and the EPR effect in macromolecular therapeutics: a review.* J. Control. Release, 2000. **65**(1-2): p. 271-284.

40. Vauthier, C. and Bouchemal, K., *Methods for the Preparation and Manufacture of Polymeric Nanoparticles.* Pharm. Res., 2009. **26**(5): p. 1025-1058.

41. Kataoka, K., Harada, A., and Nagasaki, Y., *Block copolymer micelles for drug delivery: design, characterization and biological significance.* Adv. Drug Deliver. Rev., 2001. **47**(1): p. 113-131.

42. Govender, T., Stolnik, S., Garnett, M.C., Illum, L., and Davis, S.S., *PLGA nanoparticles prepared by nanoprecipitation: drug loading and release studies of a water soluble drug.* J. Control. Release, 1999. **57**(2): p. 171-185.

43. Mu, L. and Feng, S.S., *A novel controlled release formulation for the anticancer drug paclitaxel (Taxol®): PLGA nanoparticles containing vitamin E TPGS.* J. Control. Release, 2003. **86**(1): p. 33-48.

44. Fonseca, C., Simões, S., and Gaspar, R., *Paclitaxel-loaded PLGA nanoparticles: preparation, physicochemical characterization and in vitro anti-tumoral activity.* J. Control. Release, 2002. **83**(2): p. 273-286.

45. Bilati, U., Allemann, E., and Doelker, E., *Poly(D,L-lactide-co-glycolide) protein-loaded nanoparticles prepared by the double emulsion method-processing and formulation issues for enhanced entrapment efficiency.* J. Microencapsul., 2005. **22**(2): p. 205-214.

46. Li, Y.P., Pei, Y.Y., Zhang, X.Y., Gu, Z.H., et al., *PEGylated PLGA nanoparticles as protein carriers: synthesis, preparation and biodistribution in rats.* J. Control. Release, 2001. **71**(2): p. 203-211.

47. Avgoustakis, K., Beletsi, A., Panagi, Z., Klepetsanis, P., et al., *PLGA-mPEG nanoparticles of cisplatin: in vitro nanoparticle degradation, in vitro drug release and in vivo drug residence in blood properties.* J. Control. Release, 2002. **79**(1-3): p. 123-135.

48. Astete, C.E. and Sabliov, C.M., *Synthesis and characterization of PLGA nanoparticles.* J. Biomater. Sci.-Polym. Ed., 2006. **17**(3): p. 247-289.

49. Raffin Pohlmann, A., Weiss, V., Mertins, O., Pesce da Silveira, N., and Stanisçuaski Guterres, S., *Spray-dried indomethacin-loaded polyester nanocapsules and nanospheres: development, stability evaluation and nanostructure models.* Eur. J. Pharm. Sci., 2002. **16**(4-5): p. 305-312.

50. Rogers, T.L., Hu, J., Yu, Z., Johnston, K.P., and Williams, R.O., *A novel particle engineering technology: spray-freezing into liquid.* Int. J. Pharm., 2002. **242**(1-2): p. 93-100.

51. Hu, J., Johnston, K.P., and Williams, R.O., *Spray freezing into liquid (SFL) particle engineering technology to enhance dissolution of poorly water soluble drugs: organic solvent versus organic/aqueous co-solvent systems.* Eur. J. Pharm. Sci., 2003. **20**(3): p. 295-303.

52. Rogers, T.L., Overhoff, K.A., Shah, P., Santiago, P., et al., *Micronized powders of a poorly water soluble drug produced by a spray-freezing into liquid-emulsion process.* Eur. J. Pharm. Biopharm., 2003. **55**(2): p. 161-172.

53. Dawes, G.J., Fratila-Apachitei, L.E., Mulia, K., Apachitei, I., et al., *Size effect of PLGA spheres on drug loading efficiency and release profiles.* Journal of Materials Science: Materials in Medicine, 2009. **20**(5): p. 1089-1094.

54. Tabata, Y., Gutta, S., and Langer, R., *Controlled Delivery Systems for Proteins Using Polyanhydride Microspheres.* Pharm. Res., 1993. **10**(4): p. 487-496.

55. Lopac, S.K., Torres, M.P., Wilson-Welder, J.H., Wannemuehler, M.J., and Narasimhan, B., *Effect of polymer chemistry and fabrication method on protein release and stability from polyanhydride microspheres.* Journal of Biomed. Mater. Res. Part B: Applied Biomaterials, 2009. **91**(2): p. 938-947.

56. Langer, R., *Polymer Implants For Drug Delivery In The Brain.* J. Control. Release, 1991. **16**(1-2): p. 53-59.

57. Determan, A.S., Graham, J.R., Pfeiffer, K.A., and Narasimhan, B., *The role of microsphere fabrication methods on the stability and release kinetics of ovalbumin encapsulated in polyanhydride microspheres.* J. Microencapsul., 2006. **23**(8): p. 832-843.

58. Agüeros, M., Ruiz-Gatón, L., Vauthier, C., Bouchemal, K., et al., *Combined hydroxypropyl-[beta]-cyclodextrin and poly(anhydride) nanoparticles improve the oral permeability of paclitaxel.* Eur. J. Pharm. Sci., 2009. **38**(4): p. 405-413.

59. Agnihotri, S.A., Mallikarjuna, N.N., and Aminabhavi, T.M., *Recent advances on chitosan-based micro- and nanoparticles in drug delivery.* J. Control. Release, 2004. **100**(1): p. 5-28.

60. Berger, J., Reist, M., Mayer, J.M., Felt, O., et al., *Structure and interactions in covalently and ionically crosslinked chitosan hydrogels for biomedical applications.* Eur. J. Pharm. Biopharm., 2004. **57**(1): p. 19-34.

61. Gan, Q. and Wang, T., *Chitosan nanoparticle as protein delivery carrier--Systematic examination of fabrication conditions for efficient loading and release.* Colloid. Surface. B, 2007. **59**(1): p. 24-34.

62. Zhang, H., Mardyani, S., Chan, W.C., and Kumacheva, E., *Design of biocompatible chitosan microgels for targeted pH-mediated intracellular release of cancer therapeutics.* Biomacromolecules, 2006. **7**(5): p. 1568-1572.

63. Mitra, S., Gaur, U., Ghosh, P.C., and Maitra, A.N., *Tumour targeted delivery of encapsulated dextran-doxorubicin conjugate using chitosan nanoparticles as carrier.* J. Control. Release, 2001. **74**(1-3): p. 317-323.

64. Sarmento, B., Ribeiro, A.J., Veiga, F., Ferreira, D.C., and Neufeld, R.J., *Insulin-Loaded Nanoparticles are Prepared by Alginate Ionotropic Pre-Gelation Followed by Chitosan Polyelectrolyte Complexation.* J. Nanosci. Nanotechnol. **7**: p. 2833-2841.

65. Zahoor, A., Sharma, S., and Khuller, G.K., *Inhalable alginate nanoparticles as antitubercular drug carriers against experimental tuberculosis.* International J. Antimicrob. Ag., 2005. **26**(4): p. 298-303.

66. Malam, Y., Loizidou, M., and Seifalian, A.M., *Liposomes and nanoparticles: nanosized vehicles for drug delivery in cancer.* Trends Pharmacol. Sci., 2009. **30**(11): p. 592-599.

67. Discher, D.E., Ortiz, V., Srinivas, G., Klein, M.L., et al., *Emerging applications of polymersomes in delivery: From molecular dynamics to shrinkage of tumors.* Prog. Polym. Sci., 2007. **32**(8-9): p. 838-857.

68. Torchilin, V.P., *Micellar Nanocarriers: Pharmaceutical Perspectives.* Pharm. Res., 2007. **24**(1): p. 1-16.

69. Kabanov, A.V., Batrakova, E.V., and Alakhov, V.Y., *Pluronic® block copolymers as novel polymer therapeutics for drug and gene delivery.* J. Control. Release, 2002. **82**(2-3): p. 189-212.

70. Hamaguchi, T., Matsumura, Y., Suzuki, M., Shimizu, K., et al., *NK105, a paclitaxel-incorporating micellar nanoparticle formulation, can extend in vivo antitumour activity and reduce the neurotoxicity of paclitaxel.* Brit. J. Cancer, 2005. **92**(7): p. 1240-1246.

71. Lee, A.L., Wang, Y., Cheng, H.Y., Pervaiz, S., and Yang, Y.Y., *The co-delivery of paclitaxel and Herceptin using cationic micellar nanoparticles.* Biomaterials, 2009. **30**(5): p. 919-927.

72. Yang, K.W., Li, X.R., Yang, Z.L., Li, P.Z., et al., *Novel polyion complex micelles for liver-targeted delivery of diammonium glycyrrhizinate: in vitro and in vivo characterization.* J. Biomed. Mater. Res. A, 2009. **88**(1): p. 140-148.

73. Rastogi, R., Anand, S., and Koul, V., *Flexible polymerosomes-An alternative vehicle for topical delivery.* Colloid. Surf. B, 2009. **72**(1): p. 161-166.

74. Xu, H., Meng, F., and Zhong, Z., *Reversibly crosslinked temperature-responsive nano-sized polymersomes: synthesis and triggered drug release.* J. Mater. Chem., 2009. **19**(24): p. 4183-4190.

75. Wang, M., Lowik, D.W., Miller, A.D., and Thanou, M., *Targeting the Urokinase Plasminogen Activator Receptor with Synthetic Self-Assembly Nanoparticles.* Bioconjugate Chem., 2009. **20**(1): p. 32-40.

76. Chan, J.M., Zhang, L., Yuet, K.P., Liao, G., et al., *PLGA-lecithin-PEG core-shell nanoparticles for controlled drug delivery.* Biomaterials, 2009. **30**(8): p. 1627-1634.

77. Brigger, I., Dubernet, C., and Couvreur, P., *Nanoparticles in cancer therapy and diagnosis.* Adv. Drug Deliver. Rev., 2002. **54**(5): p. 631-651.

78. Ganta, S., Devalapally, H., Shahiwala, A., and Amiji, M., *A review of stimuli-responsive nanocarriers for drug and gene delivery.* J. Control. Release, 2008. **126**(3): p. 187-204.

79. Qiu, Y. and Park, K., *Environment-sensitive hydrogels for drug delivery.* Adv. Drug Deliver. Rev., 2001. **53**(3): p. 321-339.

80. Peppas, N.A., Bures, P., Leobandung, W., and Ichikawa, H., *Hydrogels in pharmaceutical formulations.* Eur. J. Pharm. Biopharm., 2000. **50**(1): p. 27-46.

81. Peppas, N.A. and Klier, J., *Controlled release by using poly(methacrylic acid-g-ethylene glycol) hydrogels.* J. Control. Release, 1991. **16**(1-2): p. 203-214.

82. Sershen, S.R., Halas, N.J., and West, J.L. *Pulsatile release of insulin via photothermally modulated drug delivery*. in *[Engineering in Medicine and Biology, 2002. 24th Annual Conference and the Annual Fall Meeting of the Biomedical Engineering Society] EMBS/BMES Conference, 2002. Proceedings of the Second Joint*. 2002.

83. Okano, T., *MOLECULAR DESIGN OF TEMPERATURE-RESPONSIVE POLYMERS AS INTELLIGENT MATERIALS.* Adv. Polym. Sci., 1993. **110**: p. 179-197.

84. Pelton, R., *Temperature-sensitive aqueous microgels.* Adv. Colloid Interface Sci., 2000. **85**(1): p. 1-33.

85. Chia-Fen Lee, C.-C.L., Wen-Yen Chiu,, *Thermosensitive and control release behavior of poly (N-isopropylacrylamide-co-acrylic acid) latex particles.* J. Polym. Sci. Polym. Chem., 2008. **46**(17): p. 5734-5741.

86. Glangchai, L.C., Caldorera-Moore, M., Shi, L., and Roy, K., *Nanoimprint lithography based fabrication of shape-specific, enzymatically-triggered smart nanoparticles.* J. Control. Release, 2008. **125**(3): p. 263-272.

87. Raemdonck, K., Demeester, J., and De Smedt, S., *Advanced nanogel engineering for drug delivery.* Soft Matter, 2009. **5**(4): p. 707-715.

88. K. Landfester, *The Generation of Nanoparticles in Miniemulsions.* Adv. Mater., 2001. **13**(10): p. 765-768.

89. Owens, D.E., Jian, Y., Fang, J.E., Slaughter, B.V., et al., *Thermally Responsive Swelling Properties of Polyacrylamide/Poly(acrylic acid) Interpenetrating Polymer Network Nanoparticles.* Macromolecules, 2007. **40**(20): p. 7306-7310.

90. Murray, M.J. and Snowden, M.J., *The preparation, characterisation and applications of colloidal microgels.* Adv. Colloid Interface Sci., 1995. **54**: p. 73-91.

91. Andersson, M. and Maunu, S.L., *Structural studies of Poly(N-isopropylacrylamide) microgels: Effect of SDS surfactant concentration in the microgel synthesis.* J. Polym. Sci. Pol. Phys., 2006. **44**(23): p. 3305-3314.

92. Yamagata, T., Morishita, M., Kavimandan, N.J., Nakamura, K., et al., *Characterization of insulin protection properties of complexation hydrogels in gastric and intestinal enzyme fluids.* J. Control. Release, 2006. **112**(3): p. 343-349.

93. Morishita, M., Goto, T., Nakamura, K., Lowman, A.M., et al., *Novel oral insulin delivery systems based on complexation polymer hydrogels: Single and multiple administration studies in type 1 and 2 diabetic rats.* J. Control. Release, 2006. **110**(3): p. 587-594.

94. Fisher, O.Z. and Peppas, N.A., *Polybasic Nanomatrices Prepared by UV-Initiated Photopolymerization.* Macromolecules, 2009. **42**(9): p. 3391-3398.

95. Chen, H., Gu, Y., Hu, Y., and Qian, Z., *Characterization of pH- and Temperature-sensitive Hydrogel Nanoparticles for Controlled Drug Release.* PDA J. Pharm. Sci. Tech., 2007. **61**(4): p. 303-313.

96. Guowei, D., Adriane, K., Chen, X., Jie, C., and Yinfeng, L., *PVP magnetic nanospheres: Biocompatibility, in vitro and in vivo bleomycin release.* Int. J. Pharm., 2007. **328**(1): p. 78-85.

97. Missirlis, D., Kawamura, R., Tirelli, N., and Hubbell, J.A., *Doxorubicin encapsulation and diffusional release from stable, polymeric, hydrogel nanoparticles.* Eur. J. Pharm. Sci., 2006. **29**(2): p. 120-129.

98. Sun, Y. and Xia, Y., *Shape-Controlled Synthesis of Gold and Silver Nanoparticles.* Science, 2002. **298**(5601): p. 2176-2179.

99. Lee, K.S. and El-Sayed, M.A., *Gold and silver nanoparticles in sensing and imaging: Sensitivity of plasmon response to size, shape, and metal composition.* J. Phys. Chem. B, 2006. **110**(39): p. 19220-19225.

100. Zhu, S.L., Du, C.L., and Fu, Y.Q., *Fabrication and characterization of rhombic silver nanoparticles for biosensing.* Opt. Mater., 2009. **31**(6): p. 769-774.

101. Ren, L. and Chow, G.M., *Synthesis of NIR-sensitive Au-Au2S nanocolloids for drug delivery.* Mat. Sci. Eng. C., 2003. **23**: p. 113-116.

102. Strangman, G., Boas, D.A., and Sutton, J.P., *Non-invasive neuroimaging using near-infrared light.* Biol.l Psychiat., 2002. **52**(7): p. 679-693.

103. West, J.L. and Halas, N.J., *Engineered nanomaterials for biophotonics applications: Improving sensing, imaging, and therapeutics.* Annu. Rev. Biomed. Eng., 2003. **5**: p. 285-292.

104. Loo, C., Lin, A., Hirsch, L., Lee, M.H., et al., *Nanoshell-enabled photonics-based imaging and therapy of cancer.* Technol. Cancer Res. T., 2004. **3**(1): p. 33-40.

105. Vorobyova, S.A., Lesnikovich, A.I., and Sobal, N.S., *Preparation of silver nanoparticles by interphase reduction.* Colloid. Surface. A, 1999. **152**(3): p. 375-379.

106. Zhang, J.Z. and Noguez, C., *Plasmonic Optical Properties and Applications of Metal Nanostructures.* Plasmonics, 2008. **3**(4): p. 127-150.

107. Pérez-Juste, J., Pastoriza-Santos, I., Liz-Marzán, L.M., and Mulvaney, P., *Gold nanorods: Synthesis, characterization and applications.* Coordin. Chem. Rev., 2005. **249**(17-18): p. 1870-1901.

108. Funston, A.M., Novo, C., Davis, T.J., and Mulvaney, P., *Plasmon Coupling of Gold Nanorods at Short Distances and in Different Geometries.* Nano Lett., 2009. **9**(4): p. 1651-1658.

109. Langer, R., *New methods of drug delivery.* Science, 1990. **249**(4976): p. 1527-1533.

110. Ferrara, K., Pollard, R., and Borden, M., *Ultrasound microbubble contrast agents: fundamentals and application to gene and drug delivery.* Annu. Rev. Biomed. Eng., 2007. **9**: p. 415-47.

111. Sershen, S.R., Mensing, G.A., Ng, M., Halas, N.J., et al., *Independent optical control of microfluidic valves formed from optomechanically responsive nanocomposite hydrogels.* Adv. Mater., 2005. **17**(11): p. 1366-+.

112. Bouillot, P. and Vincent, B., *A comparison of the swelling behaviour of copolymer and interpenetrating network microgel particles.* Colloid Polym. Sci., 2000. **278**(1): p. 74-79.

113. De La Zerda, A., Zavaleta, C., Keren, S., Vaithilingam, S., et al., *Carbon nanotubes as photoacoustic molecular imaging agents in living mice.* Nat. Nanotechnol., 2008. **3**(9): p. 557-562.

114. Li, P.-C., Wei, C.-W., Liao, C.-K., Chen, C.-D., et al. *Multiple targeting in photoacoustic imaging using bioconjugated gold nanorods*. 2006: SPIE.

115. Eghtedari, M., Oraevsky, A., Copland, J.A., Kotov, N.A., et al., *High Sensitivity of In Vivo Detection of Gold Nanorods Using a Laser Optoacoustic Imaging System.* Nano Lett., 2007. **7**(7): p. 1914-1918.

116. Mallidi, S., Larson, T., Tam, J., Joshi, P.P., et al., *Multiwavelength Photoacoustic Imaging and Plasmon Resonance Coupling of Gold Nanoparticles for Selective Detection of Cancer.* Nano Lett., 2009. **9**(8): p. 2825-2831.

117. Joshi, P.P., Yun-Sheng, C., Seungsoo, K., Shah, J., et al. *Molecular therapeutic agents for noninvasive photoacoustic image-guided photothermal therapy*. in *Engineering in Medicine and Biology Society, 2009. EMBC 2009. Annual International Conference of the IEEE*. 2009.

118. Yang, X., Skrabalak, S.E., Li, Z.-Y., Xia, Y., and Wang, L.V., *Photoacoustic Tomography of a Rat Cerebral Cortex in vivo with Au Nanocages as an Optical Contrast Agent.* Nano Lett., 2007. **7**(12): p. 3798-3802.

119. Homan, K., Shah, J., Gomez, S., Gensler, H., et al., *Silver nanosystems for photoacoustic imaging and image-guided therapy.* J. Biomed. Opt.. **15**(2): p. 021316-9.

120. Bouchard, L.-S., Anwar, M.S., Liu, G.L., Hann, B., et al., *Picomolar sensitivity MRI and photoacoustic imaging of cobalt nanoparticles.* P. Natl. Acad. Sci. U.S.A., 2009. **106**(11): p. 4085-4089.

Chapter 3: OBJECTIVES

Delivery systems that can more carefully direct a therapeutic to a site of interest have several advantages over systemic delivery of a therapeutic. Targeted delivery systems can be used to localize the release of a drug or other therapeutic compound at a disease site while minimizing or eliminating distribution of the drug to other parts of the body. The development of externally-controlled therapeutic systems seeks to take this type of therapy a step further by precisely controlling when and where a therapeutic is delivered.

The overall goal of this research was to develop systems that are capable of carrying a therapeutic and releasing it in response to a near-infrared (NIR) light trigger. Because NIR light penetrates safely through tissue, a disease site of interest such as a cancerous tumor could be exposed to the light causing nanoparticle carriers to release a drug at that location.

The light-triggered drug delivery systems are composed of metal-polymer composites. The nano-scale composites consist of gold nanorods covalently attached to or entrapped in a polymer network. The gold nanorods are capable of absorbing NIR light and converting it to heat which is transmitted to temperature responsive polymer nanoparticles. The polymer nanoparticles undergo a size transition upon heating which could be used to trigger the release of the entrapped therapeutic. The specific aims of this research are listed here:

(1) Synthesis, optimization, and characterization of equilibrium swelling behavior of temperature responsive hydrogel nanoparticles.

(2) Formulation and characterization of gold-polymer composites using gold nanorods and temperature responsive hydrogel nanoparticles

(3) Evaluation of the ability of the nanoparticle systems to entrap and release a model therapeutic

(4) Investigation of the cytocompatibility of composite nanoparticle systems.

(5) Investigation of the light-triggered properties of the system and the potential use as a contrast agent in medical imaging techniques.

Each of these specific aims will be addressed in the chapters that follow. Polymer nanoparticle development described in Specific Aim #1 was discussed in Chapter 4. Gold-polymer composite formulation indicated in Specific Aim #2 was covered in Chapter 5. Specific Aim #2 and the investigation of loading and release properties will be detailed in Chapter 6. Chapter 7 will cover all of the studies that indicate the potential use of these therapeutic systems in vivo as describe in Specific Aims #4 and 5. Chapter 8 will conclude the discussions of the specific aims with an overview of the results from this work.

Chapter 4: Polymer Nanogel Synthesis and Characterization

4.1 Introduction

Current standards of practice for chemotherapy are to administer drugs either orally or intravenously depending on the combination of therapeutics that is being administered. Because these types of molecules generally work by interfering with growth or killing fast dividing cells, they can have significant adverse effects systemically on healthy cells in addition to the targeted disease cells. Common chemotherapeutics that are used for breast cancer have a variety of potential adverse side effects. Systemic chemotherapy is used for cancer treatment because of its benefits in overall reduction of tumor size, potential elimination of cancer cells that can not be surgically removed, and reduction of recurrence rates. Because of the severity of many of the adverse effects associated with this important type of therapy, there is significant interest in developing more efficient delivery systems for chemotherapeutics.

In order for a chemotherapeutic delivery system to be an improvement over traditional systemic delivery, it must be able to deliver a drug preferentially to cancer cells over healthy tissue. Ideally, such a system would carry its entire therapeutic payload to the disease site and release it in such a location that the drug (or particle and drug) would only be uptaken by the cancer cells. In this case a chemotherapeutic drug can be delivered at its maximum therapeutic concentration at the disease site that may

otherwise reach systemic toxicity levels leading to serious adverse effects if the same dose was administered systemically.

Several strategies have been pursued to develop chemotherapeutic delivery systems. In order to more efficiently localize delivery at a cancerous disease site, most modified chemotherapies that are currently available enhance delivery by taking advantage of the enhanced permeability and retention (EPR) effect. Because of the fast growth of tumors, the vasculature tends to be leaky and lymphatic drainage poor. Large molecular weight materials such as polymers or nanoparticles are preferentially extravasated and concentrated at tumor cites while small molecular weight drugs are retained at significantly lower concentrations [1-3].

In order to increase the molecular weight of chemotherapeutic drugs and take advantage of the EPR effect, chemotherapeutic prodrugs have been formulated by conjugating a therapeutic to a polymer or other high molecular weight compounds such as proteins or lipids. Several polymer drug complexes have been synthesized using important chemotherapeutics including paclitaxel and doxorubicin and have shown positive results in clinical trials [4]. These polymer drug complexes have additional benefits in cancer treatment because they can increase the solubility of hydrophobic chemotherapy molecules, and the polymer-drug linker can be made to degrade in response to enzymes present at the cancer site.

Because paclitaxel is poorly soluble in aqueous media it must be administered in a mixture of polyethoxylated castor oil (Cremophor) and ethanol and a typical

administration period takes at minimum 3 hours. These solvents are known to contribute to toxicity of the treatments [5]. Alternative methods have been used to improve the solubility of the drug through conjugation. Paclitaxel conjugated to poly(l-glutamic acid) is highly soluble in water and has shown improved anti-tumor results in *in vitro* and animal models [6]. In Phase I and II clinical trials, results were positive, and measured adverse effects were greatly reduced compared to traditional paclitaxel administration.

Additionally, delivery vehicles such as polymer nanoparticles, micelles, and liposomes have been developed to take advantage of the EPR effect and deliver a chemotherapeutic to a delivery site [2]. Particles smaller than 400 nm have been shown to extravasate leaky tumor vasculature via the EPR effect, and those smaller than 200 nm may be even more effective [7]. The Doxil © system made by Johnson and Johnson is a pegylated liposome formulation of doxorubicin which has been approved for clinical use in the United States, and Myocet is another liposomal formulation that has been approved for use in Europe and Canada for treatment of breast cancer [8]. A nanoparticle composed of the protein albumin has been used to encapsulate paclitaxel and has been approved by the FDA for treatment of metastatic breast cancer [9].

Nanoparticle systems that incorporate externally-controlled behavior have the potential to go a step beyond the benefits of standard nanoparticle based treatments for breast cancer. As the nanoparticles accumulate at the tumor site due to the EPR effect, they can be triggered to release the entire drug payload at the target site using

an external trigger such as a magnetic field, light, or radio frequency pulse. Externally applied electric fields, ultrasound, and mechanical forces have also been used to trigger a swelling transition and subsequent drug release [10, 11]. In other work, so called ultrasound microbubbles have been developed for use as externally triggered delivery and imaging systems [12, 13]. A focused ultrasound pulse can be used to disrupt the microbubbles and locally deliver a drug or contrast agent.

Past work in this group has focused on using stimuli-responsive hydrogel materials for a number of applications in biomaterials and drug delivery. This thesis work seeks to combine absorption properties of metal nanoparticles with temperature responsive hydrogels to create systems that are capable of undergoing volume changes in response to light exposure. Certain types of metal nanoparticles including gold or silver nanoshells and gold nanorods can be tuned to absorb light in the near-infrared (NIR) region which is of interest for biomedical applications because of the ability of light in this region to penetrate through tissue [14-18].

Metal nanoparticles can convert absorbed light to heat when coupled to an adjacent stimuli-responsive hydrogel. Heat transmitted from the metal triggers a swelling response and an associated release of an entrapped therapeutic.

Gold nanoshells have been entrapped in temperature responsive P(NIPAAm-co-AAm) hydrogel films [11, 19]. These films have been shown to deswell upon exposure to NIR light, and when loaded with insulin, a light trigger can be used to induce a pulsatile release of insulin from the gels. Using a similar concept, a magnetic field has

been used to induce heating in a PNIPAAm hydrogel film system loaded with superparamagnetic iron oxide particles which triggers a deswelling and release of a model drug [11].

Two classes of temperature responsive polymer hydrogel nanoparticles have been synthesized and investigated in this thesis to produce systems that will have the positive effects associated with nanoparticle delivery while serving as the stimuli-responsive basis for externally-triggered delivery systems. Crosslinked polymers that exhibit lower critical solution temperature (LCST) behavior are more swollen at lower temperatures, and deswell or shrink upon heating through a transition temperature region. The class of materials that have upper critical solution temperature (UCST) behavior behave in an opposite manner where they are in a more collapsed state at lower temperatures and swell above the transition temperature. In either case, LCST or UCST, the temperature-responsive behavior can be utilized to trigger the release of a drug from the hydrogel carriers [20].

Polymers demonstrating LCST behavior, most commonly poly(N-isopropylacrylamide), PNIPAAm, and related copolymers, have been investigated for use as temperature sensitive drug carriers. The presence of separate hydrophilic and hydrophobic groups in the polymer chain leads to this behavior. At low temperatures, hydrogen bonding interactions between water and the hydrophilic groups lead to a swollen state, but an increase in temperature beyond the transition temperature leads

to weakening of the water-polymer hydrogen bonding and a strengthening of hydrophobic polymer-polymer interactions [21].

To trigger release of an entrapped therapeutic, a polymer is designed so that in its swollen state the properties are such that the polymer can encapsulate and protect a molecule of interest in its swollen state. Upon deswelling or shrinking, there is a fast release as some of the encapsulated material is squeezed out of the polymer matrix [11, 19]. As this cycle is repeated, a pulsatile release of the therapeutic may be observed. LCST carriers have been developed that expel encapsulated therapeutics upon heating above transition temperatures at therapeutically relevant temperature, by what is known as a deswelling method upon collapse of the system.

Dispersion polymerization has been used in free radical polymerizations where the growing polymer is much less soluble in a particular solvent than the monomer. These methods can be applied to synthesis of certain LCST polymer nanoparticles. Monomer and initiator are dissolved in a solvent in a homogenous mixture often with the inclusion of some molecule to act as a steric stabilizer for particle formation. As polymerization begins, growing macroradicals precipitate, and form stabilized particles. Continued polymerization occurs as the particles are slightly swollen in the polymerization medium [22]. An aqueous dispersion polymerization has been used to synthesize temperature-sensitive hydrogel polymers with LCST behavior. PNIPAAm based nanoparticle systems have been synthesized using aqueous dispersion polymerizations and can be formulated using a stabilizing molecule such as sodium

dodecyl sulfate (SDS) or no surfactant at all [21, 23]. The reaction is performed at a temperature well above the LCST of the resultant polymer. Since the temperature is above the LCST, the polymer is immiscible in the aqueous environment and particle nucleation occurs.

Hydrogels with UCST behavior have characteristics such that at lower temperatures some polymer-polymer interactions lead to a less swollen state. Upon heating through the UCST, these interactions are weakened so that the polymer effectively becomes miscible with the aqueous phase, but because the polymer is crosslinked the systems imbibes water and swells. Certain types of interpenetrating polymer networks, IPNs, such as those based on acrylamide (AAm) and acrylic acid (AA) demonstrate this type of behavior with transition temperatures near 40 °C [24]. IPNs consist of two separately crosslinked polymer networks that are physically entangled with the first network, but not covalently attached. The PAA network and the PAAm network undergo hydrogen bonding at low temperatures, which breaks down above the UCST and electrostatic and steric interactions cause the polymer to swell. If a therapeutic molecule is encapsulated in a carrier in its collapsed state where the drug is protected and small mesh size limits diffusion in or out of the polymer matrix [25]. If the polymer encounters an environment that triggers swelling, the mesh size increases, and there is an increase in the rate of diffusion so that the therapeutic is released into the surrounding environment.

In PAA/PAAm based IPN systems hydrogen bonding begins to break down and a positive swelling transition is observed around 38-42 °C [24]. A synthetic procedure has been developed for temperature-sensitive IPNs composed of interpenetrating networks of poly(acrylic acid), PAA, and poly(acrylamide), PAAm [26]. The inverse-microemulsion produces particles between 100 nm and 1 micron in diameter. This method involves two consecutive water-in-oil microemulsion polymerizations. The acrylamide monomer and crosslinker are dissolved in an aqueous phase and emulsified into a cyclohexane oil phase with surfactant. Initiator is then added to start polymerization in the aqueous micelles and synthesize polyacrylamide microparticles or nanoparticles [26]. Following termination of the first reaction acrylic acid and crosslinker are added in a second aqueous phase and initiated to synthesize the PAA interpenetrating network that is not covalently attached to the PAAm network.

4.2 Materials and Methods

4.2.1 LCST Nanoparticle Synthesis

Acrylic acid (AA, inhibited with 200 ppm hydroquinone monomethyl ether), N-Isopropylacrylamide (NIPAAm), and sodium dodecyl sulfate (SDS) were obtained from Sigma Aldrich (Milwaukee, WI), acrylamide (AAm) and ammonium persulfate (APS) were obtained from Fisher Scientific (Hampton, NH). Acrylic acid was purified using vacuum distillation. All other materials were used as received.

Nanogels demonstrating LCST behavior were synthesized using an aqueous free radical dispersion polymerization. Polymers were synthesized with various monomer feed ratios. Crosslinked PNIPAAM nanoparticles were synthesized along with several copolymers. Copolymers were synthesized that incorporated hydrophilic comonomers, either AAm or AA. The AAm or AA were be added in molar ratios up to 10 % of total monomer. Crosslinking molar feed ratios were also varied from 1 to 10 %.

To synthesize LCST polymers monomer, crosslinker, N,N'-Methylene bisacrylamide, and a stabilizer, sodium dodecyl sulfate (SDS) are added to a 100 ml aqueous phase in a 250 ml round bottomed flask at a total monomer concentration of 5.5 g/L and a typical stabilizer concentration of 0.3 g/L. Monomers are pictured in Figure 4.1. The monomers and stabilizer were first dissolved in the aqueous medium. Next, the aqueous reaction solution was purged with nitrogen to remove oxygen from the reaction flask. A 70 °C oil bath was prepared and the purged reaction flask was submerged in the oil bath. An aqueous solution of the free radical initiator, APS, was injected into the reaction flask to initiate reaction. The reaction was allowed to proceed for at least two hours. After completion, the reaction flask was opened to the air and removed from the heat source.

The resulting nanoparticle suspension was dialyzed against DI water for 10 days using a 12-14,000 MWCO dialysis tubing (Spectrum Laboratories, Rancho Domingo, CA) . Dialysis water was changed twice daily. Particle solutions were then frozen in a -80° C

freezer and lyophilized until dry. Dry particle solutions were resuspended in the appropriate medium or used dry as necessary for further analysis.

4.2.2 UCST Nanoparticle Synthesis

Acrylic acid (AA, inhibited with 200 ppm hydroquinone monomethyl ether), N,N'-methylenebisacrylamide (MBAAm), polyethylene glycol laurylether (Brij 30), cyclohexane, and sodium bis(2-ethylhexyl) sulfosuccinate (AOT) were obtained from Sigma Aldrich (Milwaukee, WI), acrylamide (AAm) and lauroyl peroxide were obtained from Fisher Scientific (Hampton, NH). Acrylic acid was purified using vacuum distillation. All other materials were used as received.

Procedures developed previously within the lab were used to synthesize temperature-responsive nanogels exhibiting UCST behavior [26]. The particles composed of acrylamide (AAm) and acrylic acid (AA) were synthesized using a two-step inverse (water-in-oil) microemulsion free radical polymerization. The inverse emulsion solution consisted of a cyclohexane continuous phase, surfactants, and an aqueous phase split into two separate mixtures one for each of the two reactions, containing monomer, initiator, and water. The only difference in these two aqueous solutions was that one contains only AAm monomer and the other only AA monomer.

A typical polymerization medium consisted of 81% cyclohexane oil phase, 13% surfactants, and 6% total aqueous phase by weight. The surfactant mixture was a 50:50 weight percent mixture of Brij 30 and AOT. The aqueous phase typically consisted of

approximately 80% water and 5% initiator by weight with the remaining balance consisting of monomer and crosslinker, N,N'-Methylene bisacrylamide (MBAAm), in the desired synthesis ratio. Figure 4.2 displays the monomers used in the polymerization.

The surfactant was dissolved first in cyclohexane. AAm monomer along with MBAAm crosslinker was dissolved in the separate water phase. The first premixed aqueous phase containing AAm monomer was added to the cyclohexane and the mixture of the two phases along with surfactant was homogenized at 24,000 RPM for 5 minutes. The reaction flask was then purged with nitrogen for 30 minutes to remove oxygen from the system which acts as a free radical scavenger.

An oil bath was prepared at 60 °C . The reaction was initiated following the purge by immersion in the oil bath to heat to 60 °C. After reaction for 2 hours, the reaction was terminated by removal from the heat source and exposure to the atmosphere. The second aqueous monomer phase was then prepared. The second aqueous phase, consisting of AA and additional initiator and crosslinker, is added to the reaction flask and again homogenized, purged, and reacted for 2 hours at 60 °C to form a second crosslinked polymer network that is physically entangled with the first network, but not covalently attached.

After synthesis the cyclohexane solvent was removed using rotary evaporation under vacuum at 40 °C. Five successive ethanol wash cycles were used to wash the polymer. One wash cycle consisted of suspension of approximately 0.5 g of nanoparticles in 25 ml of ethanol and centrifugation at 3200 rcf. Ethanol supernatant

was then removed and particles resuspended in ethanol for the next wash. After ethanol washing the particles were suspended in DI water and dialyzed for 10 days using a 12-14,000 MWCO dialysis tubing with dialysis water being changed twice daily. Particle solutions were then frozen in a -80° C freezer and lyophilized until dry. Dry particle solutions were resuspended in the appropriate medium or used dry as necessary for further analyses.

4.2.3 Nanoparticle Swelling Characterization by Dynamic Light Scattering

Dynamic light scattering was used to quantify the swelling behavior of nanogels in response to pH or temperature. The hydrodynamic diameter of the particles in solution was determined using a dynamic light scattering (DLS, ZetaPlus, Brookhaven, Holtsville, NY) instrument operating at a 90˚ scattering angle with a 635 nm 35 mW diode laser source.

Freeze-dried LCST nanoparticle samples were resuspended in PBS buffer for temperature responsive swelling measurements at a pH of 7.4. The concentration of the particle solution was adjusted as necessary to achieve a photon count rate of approximately 300,000 counts per second. Hydrodynamic diameter was measured over a temperature range from 10 °C to 50 °C in increments of 2 °C or 5 °C.

The copolymers of NIPAAm and AAm were characterized for their temperature sensitive behavior at molar feed ratios ranging from 95/5 to 80/20 NIPAAM:AAm. Copolymers composed of NIPAAm and AA were synthesized and examined at similar

compositions. Polymers with crosslinking ratios ranging from 1-10 % molar feed ratio were also characterized for their temperature sensitive swelling behavior.

To measure the swelling behavior or PAAm/PAA IPN systems freeze-dried particles were suspended in a DMGA buffer solution and adjusted to a pH of 3.5 using NaOH. Concentration of the particle solution was adjusted as necessary to achieve a photon count rate of 300,000 counts per second. Hydrodynamic diameter was measured over a temperature range from 10 °C to 50 °C.

4.2.4 Polymer Nanoparticle Characterization

Electron microscopy was performed to analyze particle size, morphology, and polydispersity. Both transmission electron microscopy (TEM) and scanning electron microscopy (SEM) techniques were used.

Freeze-dried particles were imaged with a LEO 1530 scanning electron microscopy (Carl Zeiss AG; Oberkochen, Germany). Microgels were placed onto double sided conductive tape attached to an aluminum SEM stage (Ted Pella, Inc.; Redding, CA) and sputter coated with gold.

TEM samples were prepared by placing 5 µl of aqueous particle suspension on a formvar coated copper TEM grid (Electron Microscopy Sciences, Hatfield, PA). After one minute, the grid was blotted dry using filter paper. Particles were imaged using a FEI Tecnai Transmission Electron Microscope (FEI; Hillsboro, OR) operating at 80 kV equipped with a top mount AMT Advantage HR 1kX1k digital camera.

4.3 Results and Discussion

4.3.1 LCST Nanoparticle Synthesis

Several types of LCST nanoparticle systems were synthesized by varying parameters of the polymerization to find optimized systems. These nanocarrier systems must be able to entrap a drug in a swollen state and limit diffusion of the drug out of the system, have a swelling transition around 40 °C, and quickly deswell upon heating to release a drug. They also should have a size of less than 300 nm in their most swollen state to take advantage of the EPR effect and to limit clearance by the reticuloendothelial system. The amount of stabilizing molecule, SDS, in the solution was varied as well as the amount of crosslinker in the polymerization.

Nanoparticles composed of 10% mol crosslinked PNIPAAm that were synthesized with varying amounts of SDS demonstrate that there is a relationship between the amount of SDS in the dispersion and the resulting size of the nanoparticles. Figure 4.3 shows that as the amount of SDS in the dispersion is decreased there is a decrease in average particle size as measured by dynamic light scattering in PBS.

The copolymers P(NIPAAm-co-AAm) and P(NIPAAm-co-AA) were successfully synthesized as nanoparticles using the aqueous dispersion polymerization. Synthesis of these copolymers at an SDS concentration of 0.3 g/L produced spherical nanoparticles with hydrodynamic diameters in the desired range.

Crosslinking ratio is an important parameter when considering a LCST hydrogel based drug delivery system. The crosslinking ratio affects the mesh size of the polymer which must be small enough to entrap and protect the therapeutic at 37 °C, but such that there is release when the polymer shrinks and squeezes out the drug. Dispersion polymerization was used to successfully synthesize LCST polymer nanoparticles with molar extents of crosslinking between 1 and 10%. Crosslinking ratio also affects the size of the nanoparticle and swelling behavior which is discussed in detail in section 4.3.3. More highly crosslinked polymers have more tightly bound networks and a smaller relative mesh size which has important implications for therapeutic loading which are described in detail in Chapter 6.

4.3.2 UCST Nanoparticle Synthesis

IPN nanoparticle systems with UCST behavior were synthesized by varying parameters of the polymerization to find optimized systems. These nanocarrier systems must be able to entrap a drug in the collapsed state and limit diffusion of the drug out of the system, have a swelling transition around 40 °C, and quickly swell upon heating above the transition temperature to release a drug. They also should have a size of less than 300 nm in their most swollen state to take advantage of the EPR effect and to limit clearance by the RES. Previous work demonstrated that the surfactant phase wt % could be increased to decrease particle size. A surfactant weight ratio of 15% leads to particles below the 300 nm size threshold. Figure 4.4 shows a typical size distribution of

50/50 PAAm/PAA IPN nanoparticles synthesized under these conditions. Swelling behavior was characterized for the IPN systems using DLS at crosslinking molar feed ratios between 1 and 10% as shown in Figure 4.5.

Crosslinking ratio is also an important parameter when considering a UCST hydrogel delivery system. The crosslinking ratio affects the mesh size of the polymer which must be small enough to entrap and protect the therapeutic at 37 °C, but such that there is release due to diffusion when the polymer swells above the transition temperature. Water-in-oil microemulsion polymerization was used to successfully synthesize IPN nanoparticles with molar extents of crosslinking of 1%, 5%, and 10%. Crosslinking ratio also affects the size of the nanoparticle and swelling behavior which is discussed in detail in Section 4.3.3. As with LCST systems a more highly crosslinked network leads to a smaller mesh size which is necessary to entrap smaller molecular weight molecules.

4.3.3 Polymer Nanoparticle Characterization by Dynamic Light Scattering

In order for LCST hydrogel nanocarriers to be of use in externally-controlled drug delivery systems, they must have a negative swelling transition that occurs just above body temperature, approximately 40 °C. Optimized systems should have the largest swelling differential possible between the 37 °C body temperature and a temperature of 42 °C where healthy cell death may begin. Addition of the more hydrophilic monomers AAm or AA led to an increase in the swelling transition temperature or LCST. Several

synthesis parameters were examined to compose an optimized temperature-responsive nanoparticle system, including monomer feed composition and crosslinker feed ratio. Dynamic light scattering results that demonstrate swelling behavior have been used to determine the LCST swelling transition and volume swelling ratios of the various systems.

Crosslinked homopolymers of PNIPAAm synthesized at different crosslinking ratios displayed unique swelling behavior. As seen in Figure 4.6 as the molar fraction of crosslinking agent in the feed was increased there was an accompanying decrease in total volume swelling ratio observed when considering the maximum swelling volume compared to the minimum swelling volume. Less crosslinker in the feed leads to a looser network structure that will swell to a larger size than the tight network structure that results from a feed with a higher ratio of crosslinker. When the particles are in the most collapsed state it is clear that crosslinking ratio does not have a great effect on particle size. Volume swelling ratio based plots are shown in Figure 4.7. As the particles collapse to the point where the chains are so close together the amount of crosslinking does not play a significant role.

The hydrophilic monomers AAm and AA were added along with NIPAAm to synthesize copolymer nanoparticles that will exhibit LCST behavior with higher LCST transition temperatures. As shown in Figure 4.8 the addition of 10% molar ratio of either AAm or AA to the feed shifts the transition temperature higher than when compared to the homopolymer at 10% extent of crosslinker. Similar swelling curves

based on volume swelling ratio are produced in Figure 4.9. Copolymers with a 90/10 ratio have a temperature based swelling transition that takes place in a region which is of interest for the applications described in this thesis. Particles can be loaded in their most swollen state at temperatures below physiological, will be slightly collapsed to entrap a drug at 37 °C, and will further decrease in size upon heating above this temperature.

IPN nanoparticles demonstrating UCST behavior were synthesized with various crosslinking ratios. As the percent of crosslinker in the feed is reduced the volume swelling ratio increases. A high amount of crosslinker in the feed leads to a tightly bound network structure and an associated decrease in ability to swell as much as a more lightly crosslinked, loose structure.

4.3.4 Polymer Nanoparticle Characterization by Electron Microscopy

Scanning electron microscopy was used to confirm the spherical shape of nanoparticles and to examine morphology. All PNIPAAm based materials displayed a spherical shape with a low polydispersity and smooth surfaces. An SEM micrograph of representative PNIPAAm nanoparticles in Figure 4.10.

Transmission electron microscopy was used as a means to further confirm the spherical nature of the nanoparticles. TEM samples were prepared by depositing nanoparticles on a TEM grid directly from aqueous suspensions. Microscopy images confirm the results from SEM of spherical nanoparticles and appear to be even less

polydisperse when they have not been dried by lyophilization as the SEM procedure required. A TEM image of PNIPAAm particles is shown in Figure 4.11 and P(NIPAAm-co-AA) in figure 4.12.

UCST nanoparticles were also imaged using electron microscopy techniques. IPN nanoparticles are spherical with smooth morphologies and an SEM micrograph is shown in Figures 4.12. IPN nanoparticles are shown in a representative TEM micrograph labeled as Figure 4.13.

4.4 CONCLUSIONS

Several types of temperature responsive nanogels were synthesized for use in drug delivery systems. Particles exhibiting LCST behavior including PNIPAAm, P(NIPAAm-co-AAm), and P(NIPAAm-co-AA) were synthesized using an aqueous dispersion polymerization. Copolymers with varying monomer ratios were examined for their ability to tune the LCST of the systems and the ability to increase the temperature of this transition by addition of a more hydrophilic monomer was confirmed. IPN nanoparticles exhibiting UCST behavior composed of equimolar networks of PAA and PAAm were formulated with a water in oil microemulsion polymerization. The effect of surfactant concentration and crosslinking ratio on size and swelling behavior of the nanoparticles was analyzed. Polymer size, shape, and morphology were verified using microscopy techniques including SEM and TEM. The characterizations can be used to gain insight into the potential of these systems as nanoscale drug carriers, where the

determination of size and swelling behavior can be used to select the appropriate particles for delivery of a specified therapeutic.

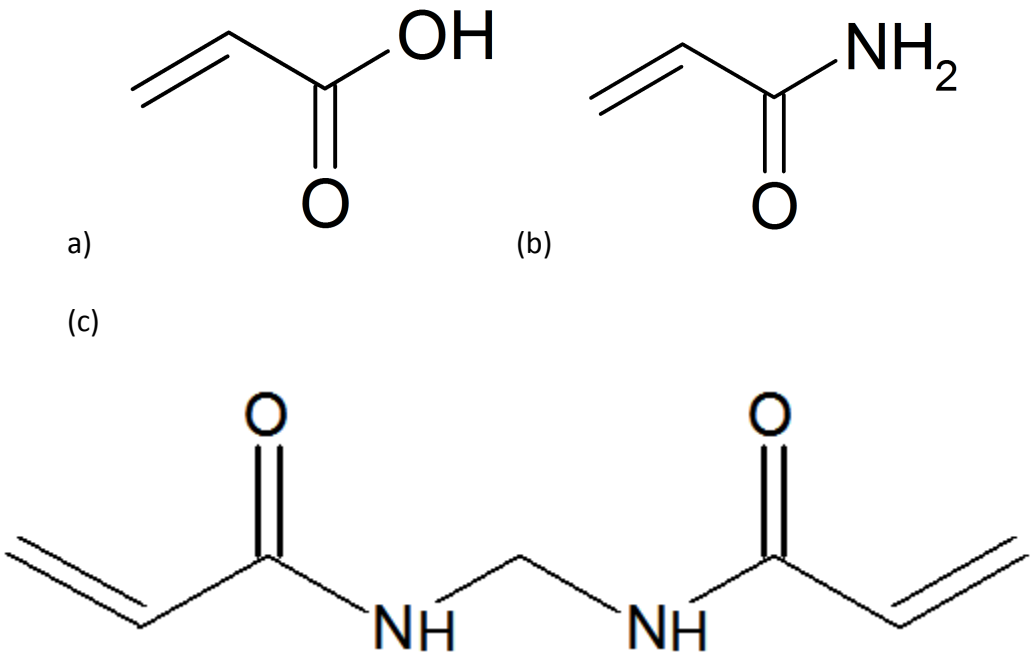

Figure 4.1 Monomers used in the synthesis of polymer nanoparticles with UCST behavior (a) Acrylic acid (b) Acrylamide (c) Methylene bisacrylamide.

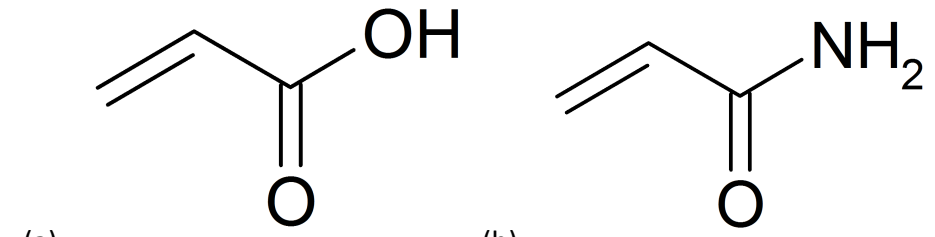

(a)

(b)

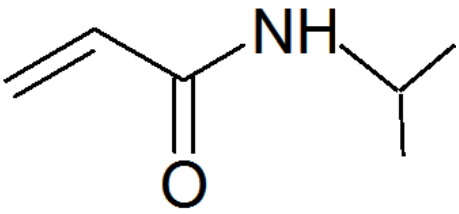

(c)

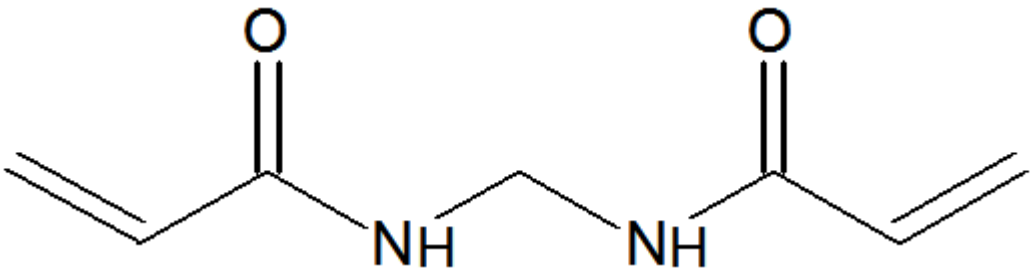

(d)

Figure 4.2 Monomers used in the synthesis of polymer nanoparticles with LCST behavior (a) Acrylic acid (b) Acrylamide (c) N-Isopropylacrylamide (d) Methylene bisacrylamide.

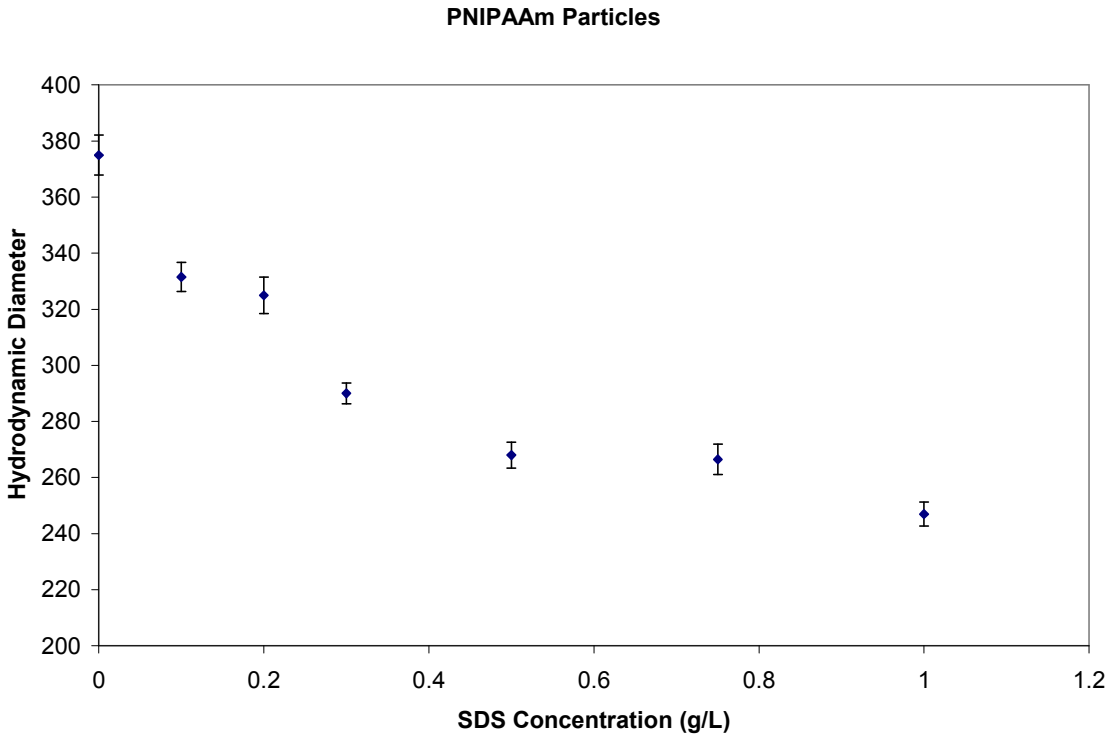

Figure 4.3 Hydrodynamic diameters of PNIPAAm hydrogel particles with varying amounts of SDS surfactant concentration.

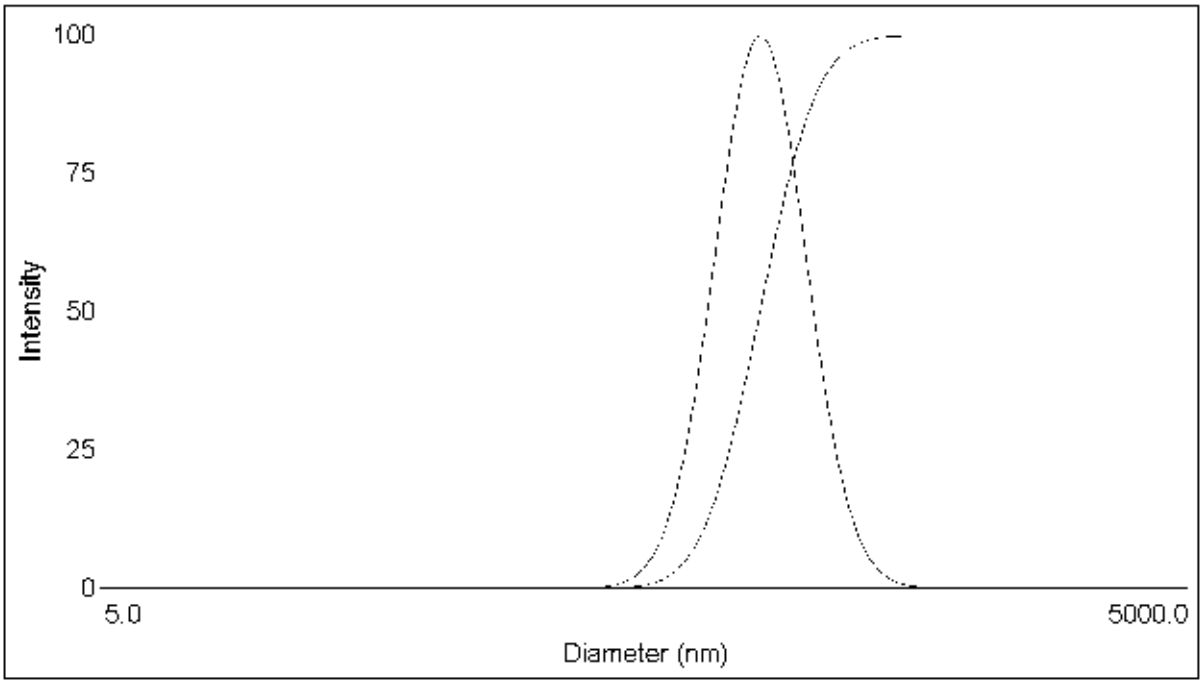

Figure 4.4 Intensity based particle size distribution for PAAm/PAA IPN polymer nanoparticles

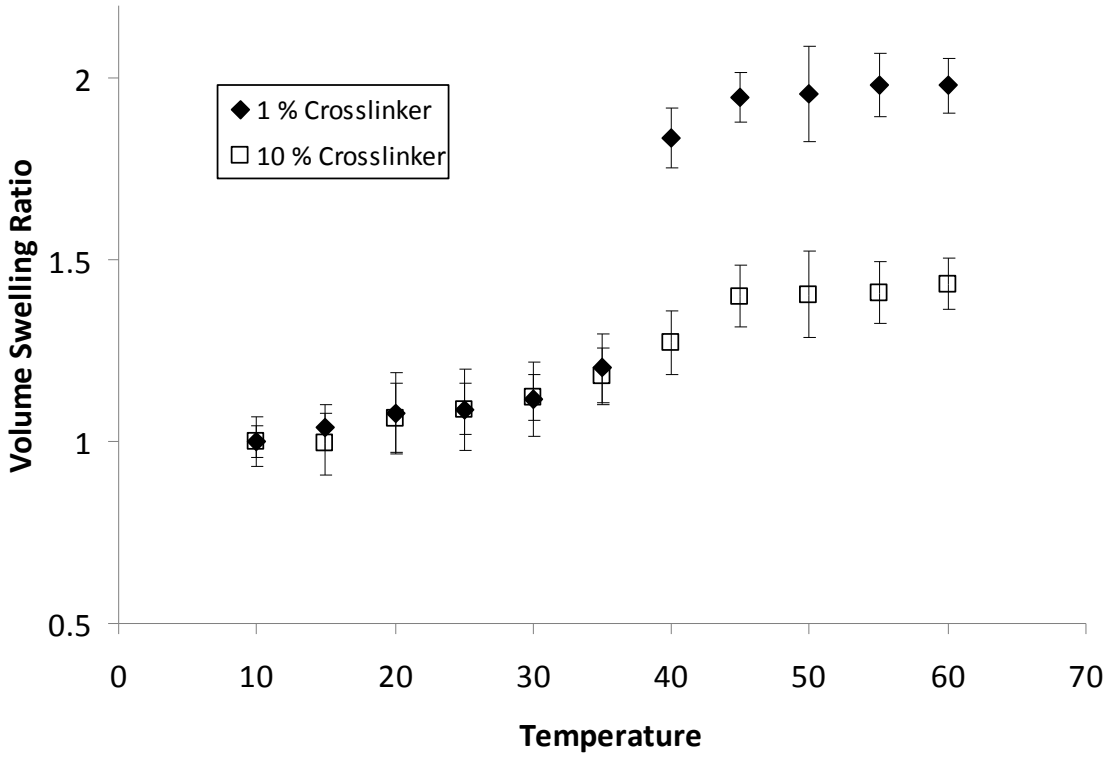

Figure 4.5 Equilibrium swelling behavior of IPN nanoparticles with varying molar extents of crosslinking based on intensity based hydrodynamic diameters from dynamic light scattering.

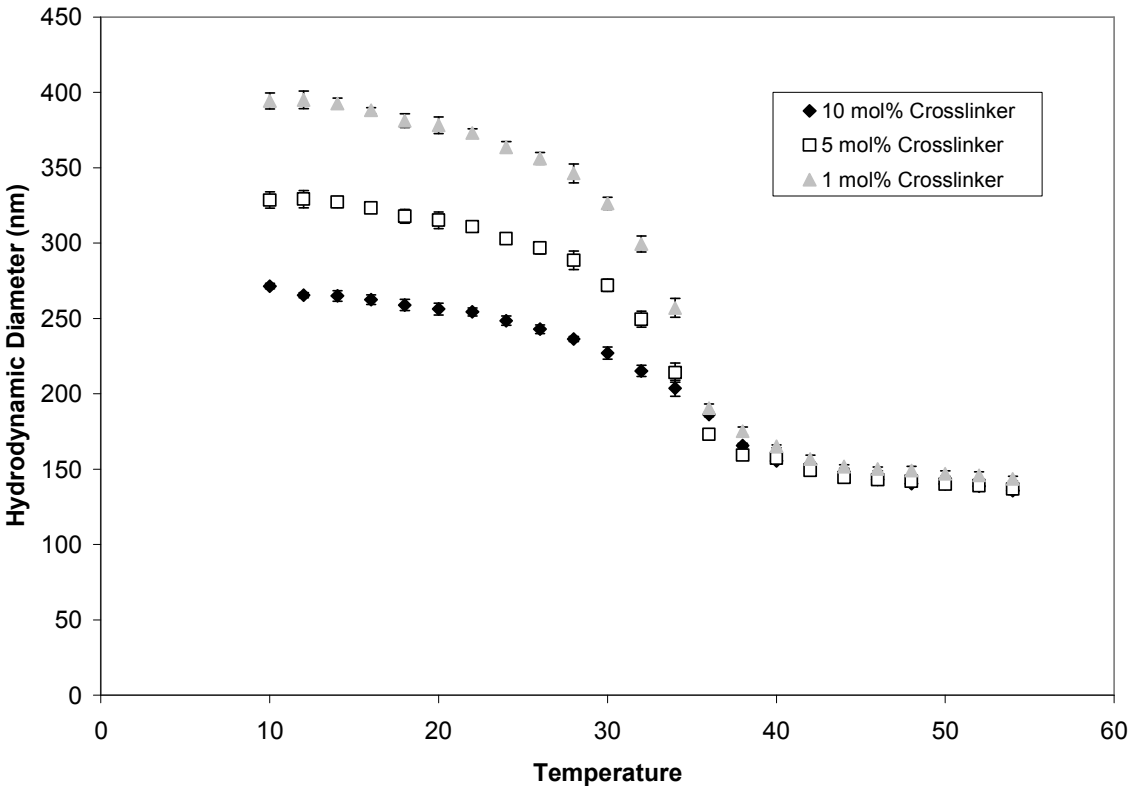

Figure 4.6 Equilibrium swelling behavior of PNIPAAm nanogels with varying molar extents of crosslinking based on intensity based hydrodynamic diameters from dynamic light scattering.

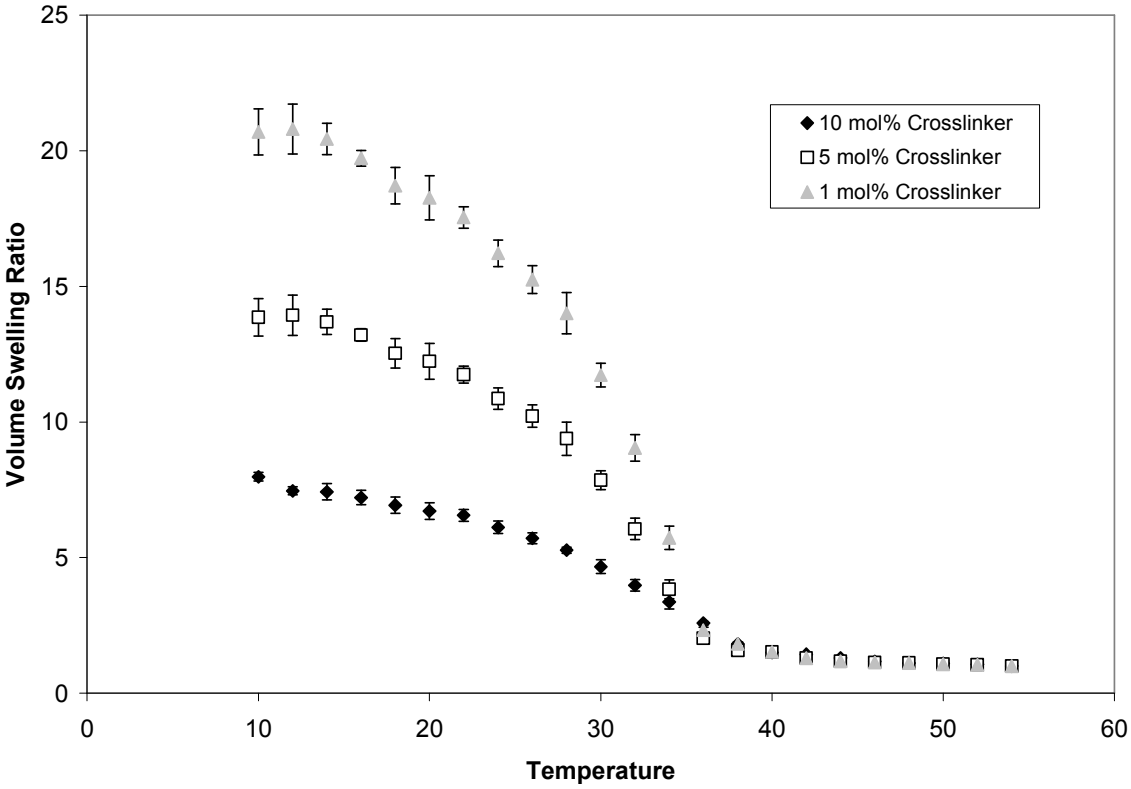

Figure 4.7 Equilibrium volume swelling ratios of PNIPAAm nanogels with varying molar extents of crosslinking based on intensity based hydrodynamic diameters from dynamic light scattering.

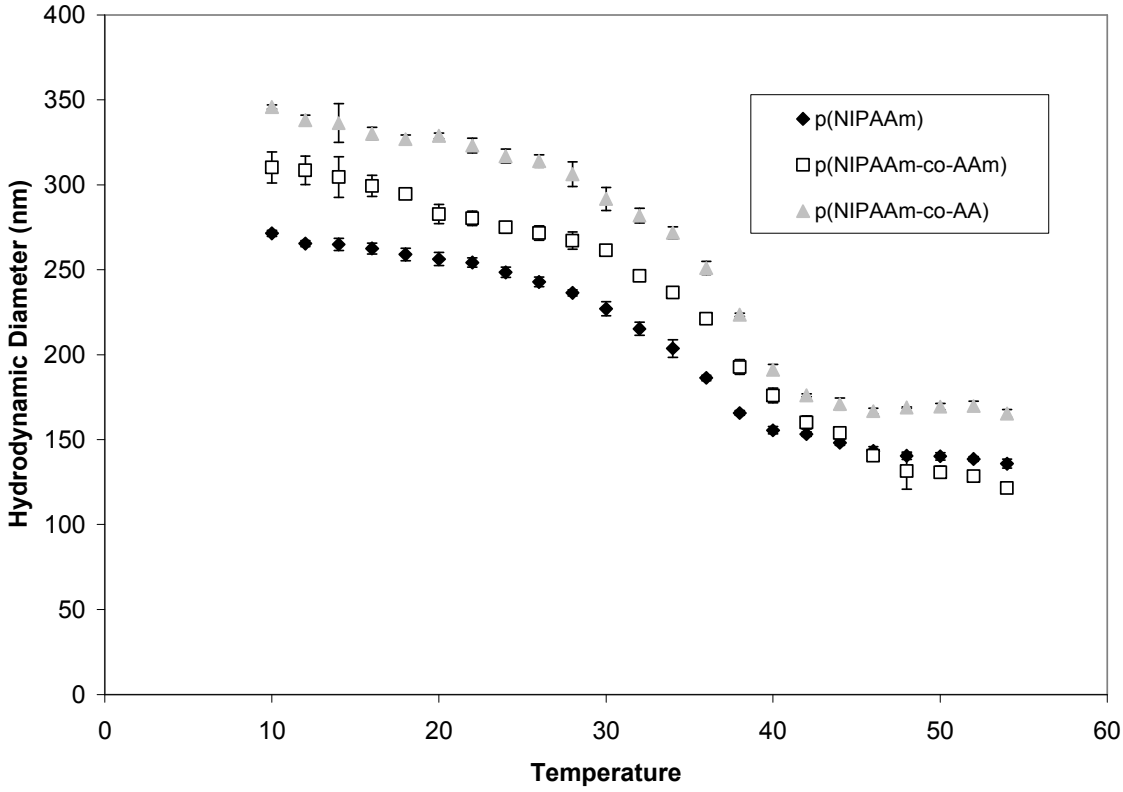

Figure 4.8 Equilibrium swelling behavior of PNIPAAm, 90/10 P(NIPAAm-co-AAm), and 90/10 P(NIPAAm-co-AA) nanogels with 10% molar extent of crosslinking based on intensity based hydrodynamic diameters from dynamic light scattering.

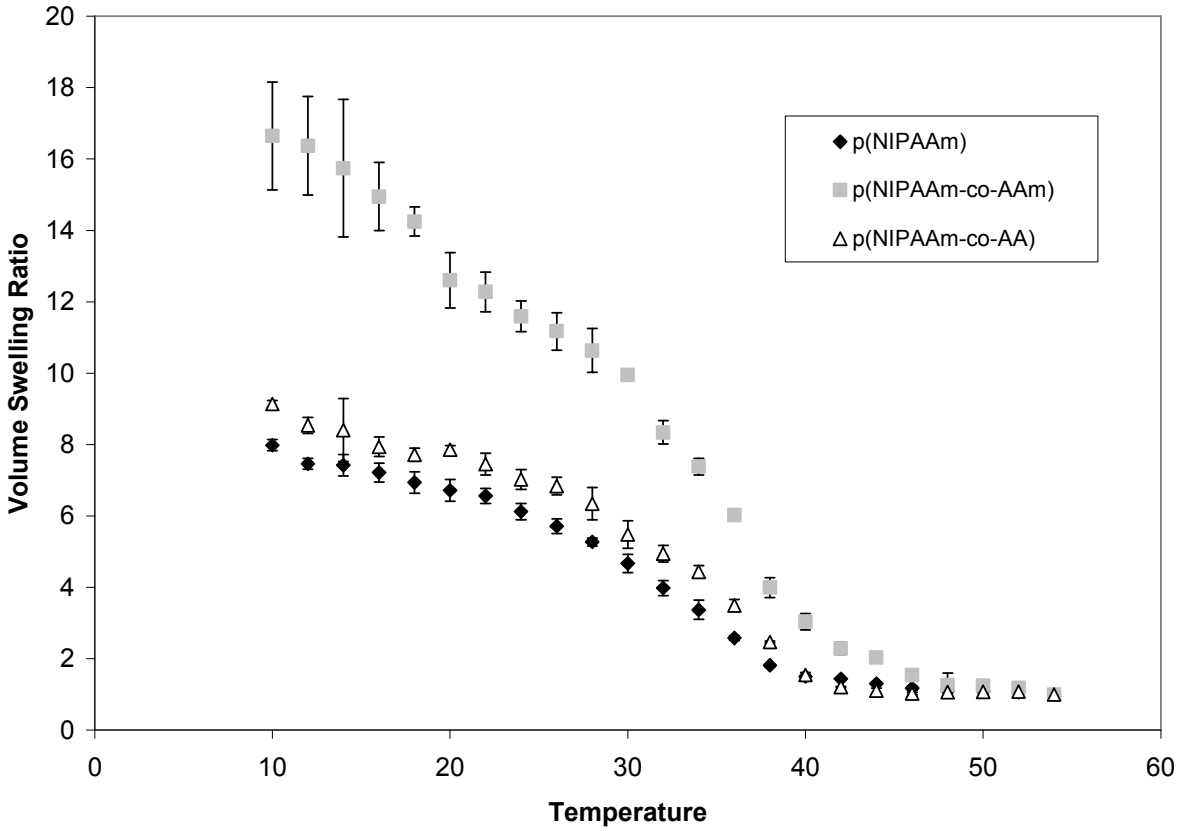

Figure 4.9 Equilibrium volume swelling ratios of PNIPAAm, 90/10 P(NIPAAm-co-AAm), and 90/10 P(NIPAAm-co-AA) nanogels with 10% molar extent of crosslinking based on intensity based hydrodynamic diameters from dynamic light scattering.

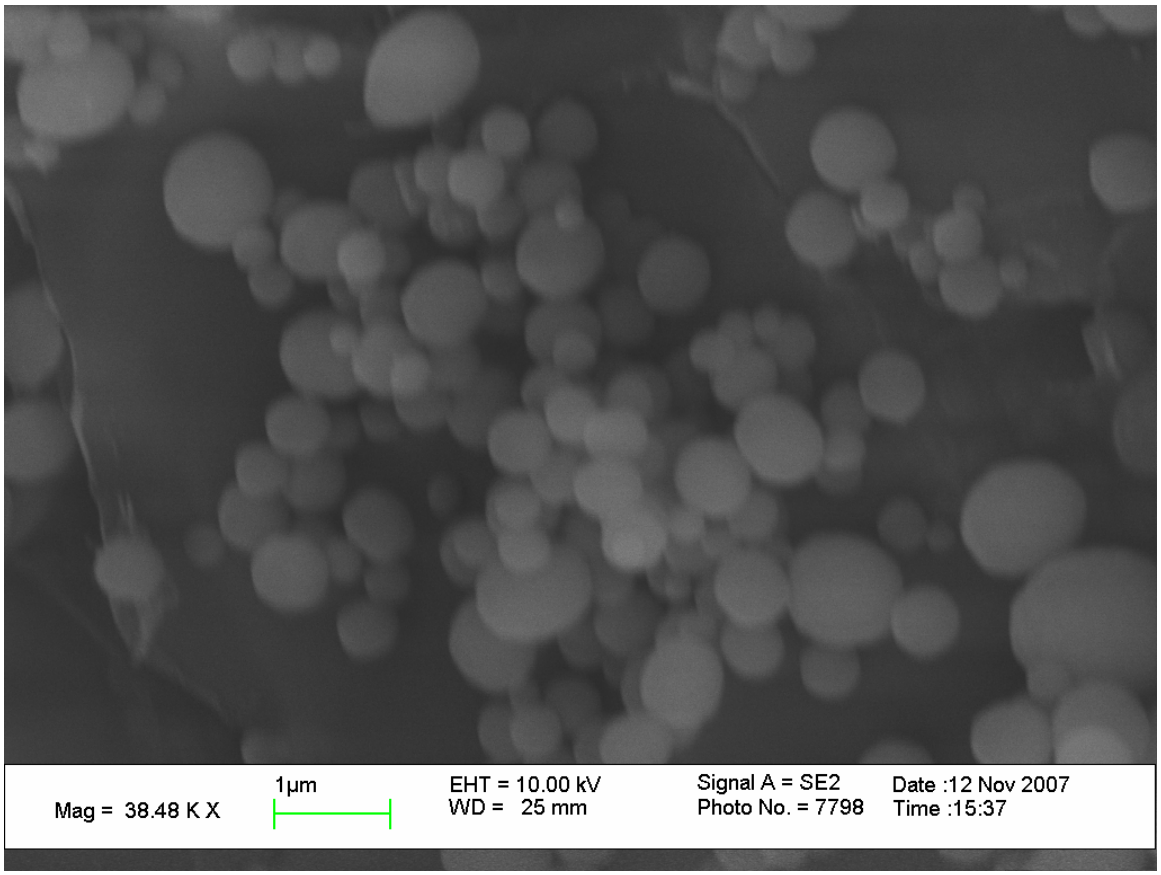

Figure 4.10 SEM micrograph of lyophilized PNIPAAm nanogels synthesized by dispersion polymerization.

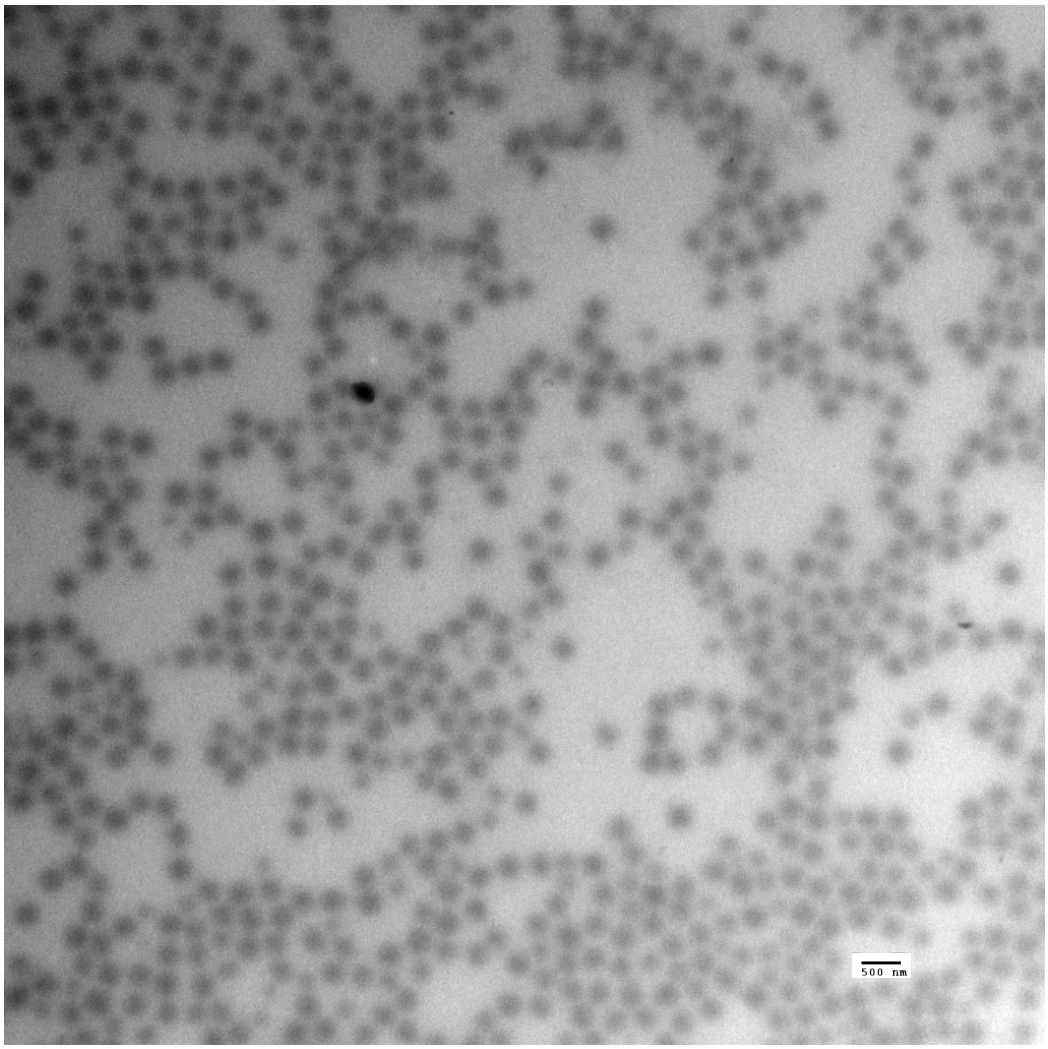

Figure 4.11 TEM image of PNIPAAm nanogels synthesized via aqueous dispersion polymerization.

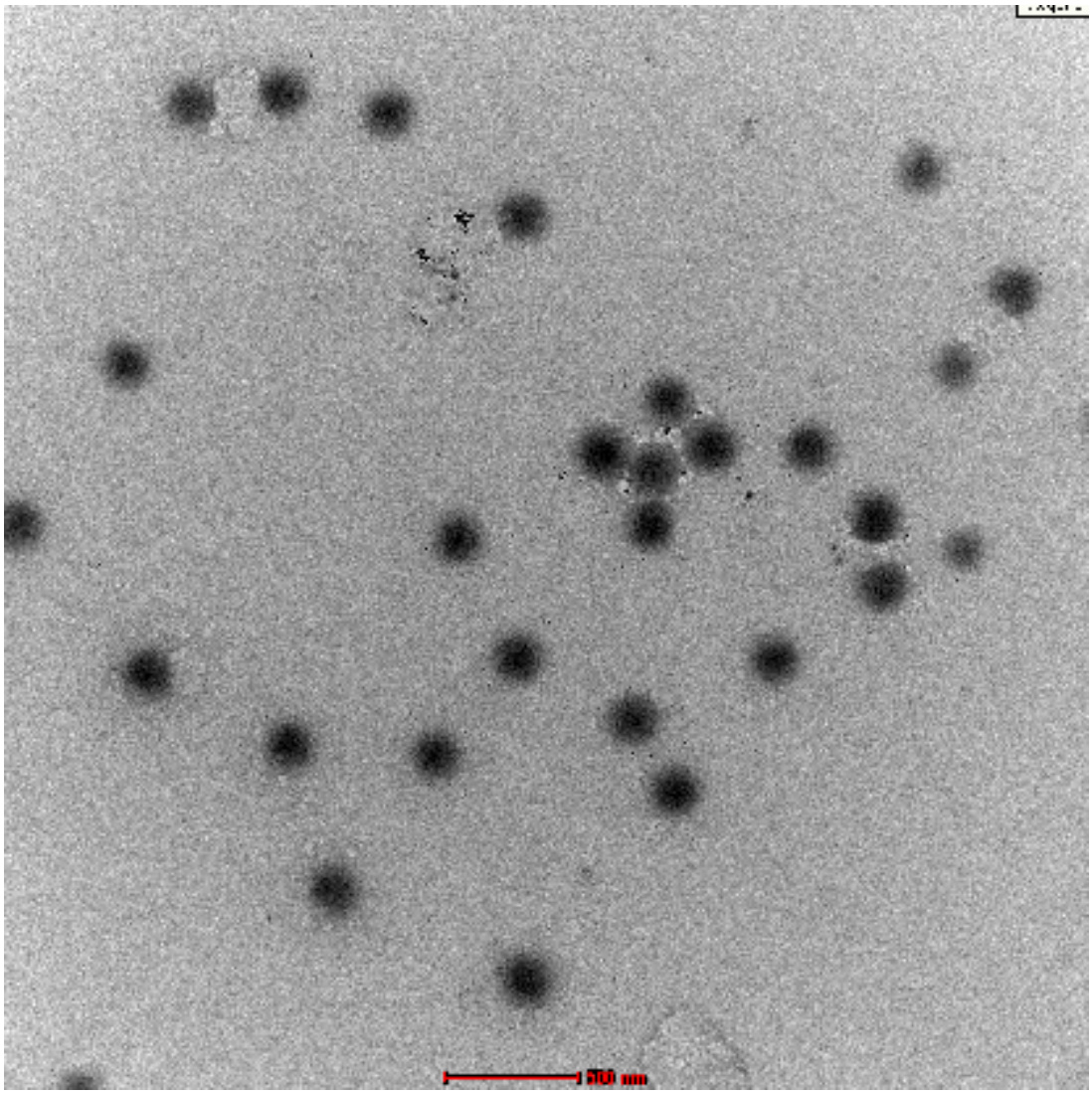

Figure 4.12 TEM Micrograph of P(NIPAAm-co-AA) nanogels synthesized via dispersion polymerization.

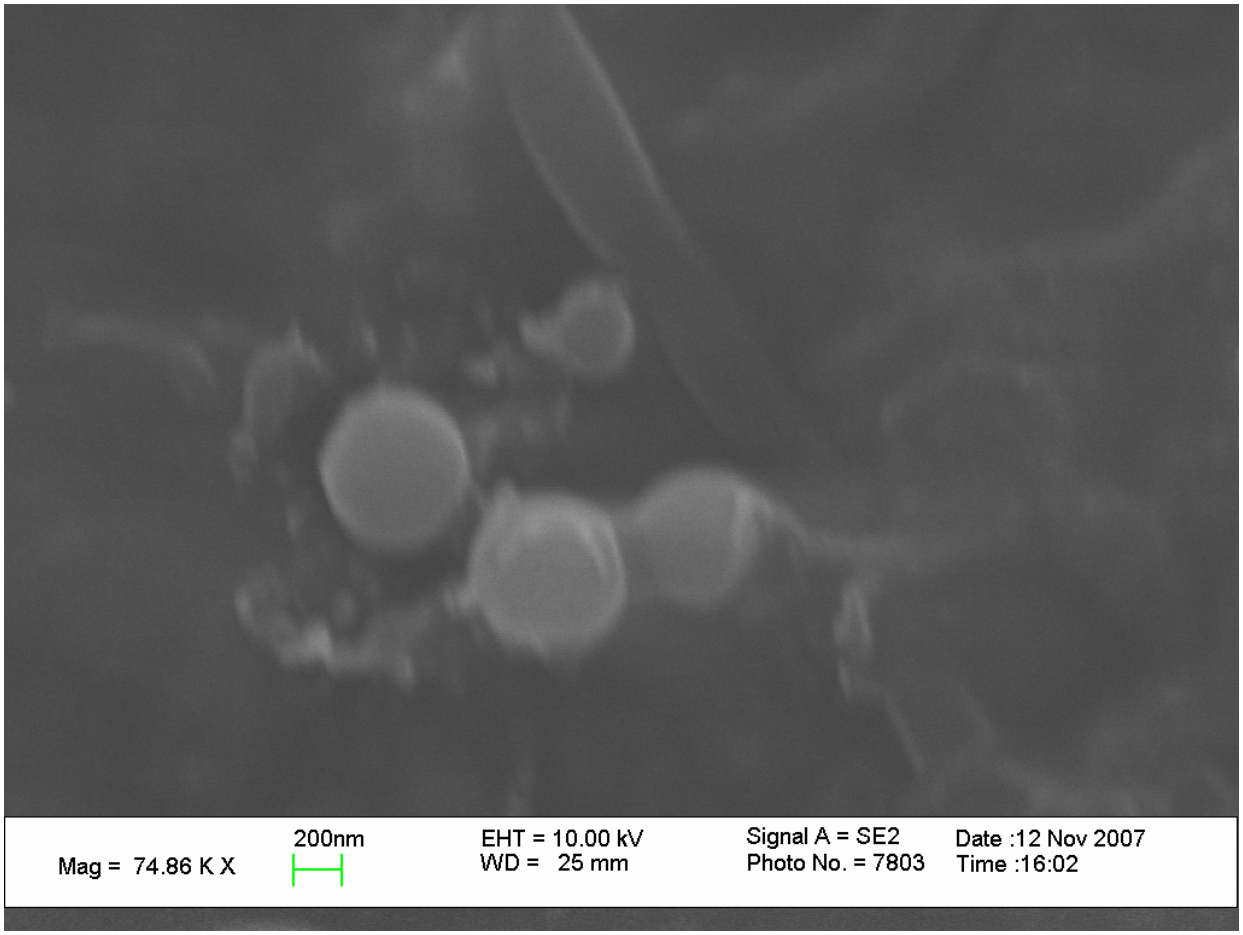

Figure 4.13 SEM Micrograph of lyophilized 50/50 PAAm/PAA IPN nanoparticles.

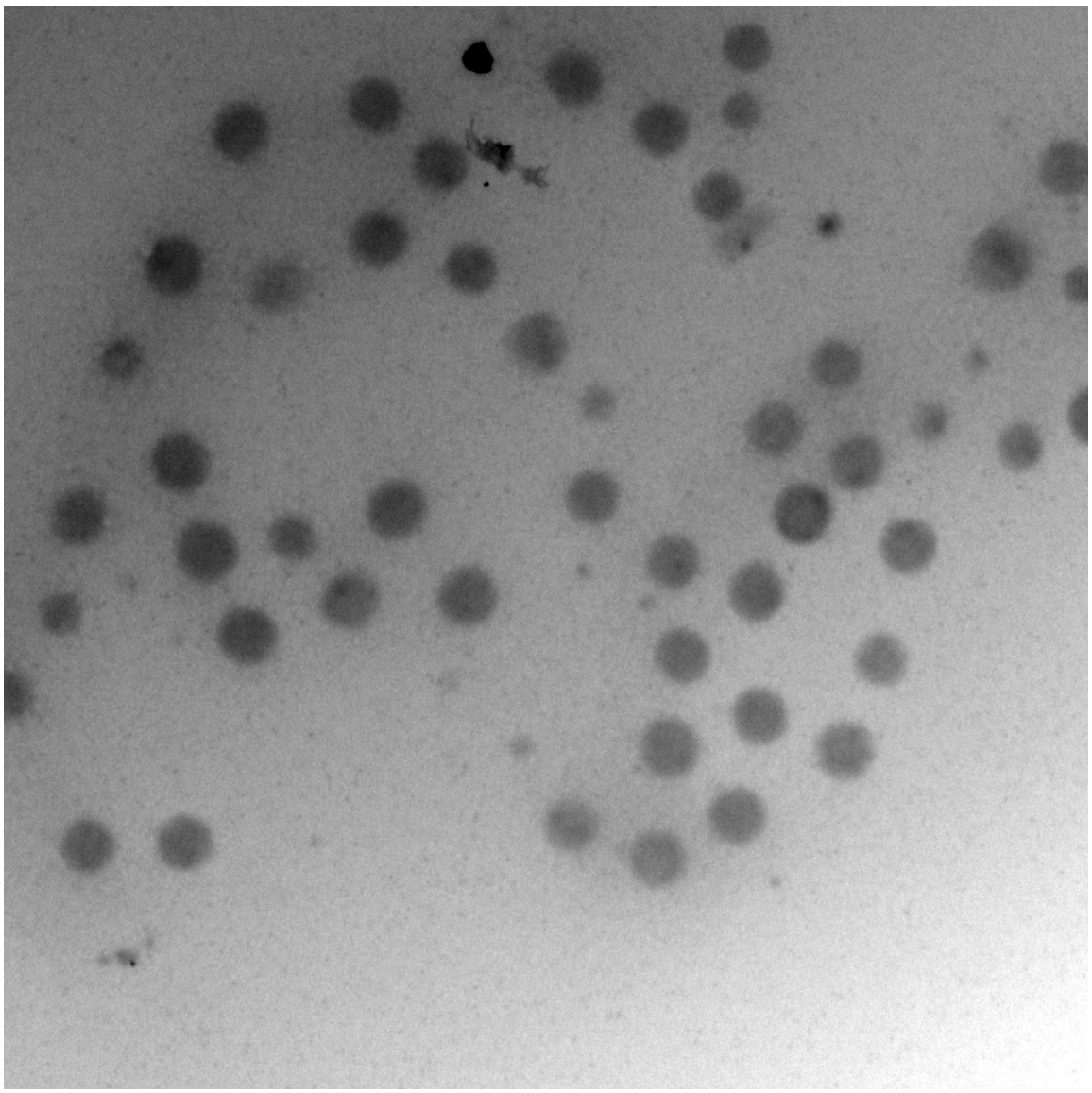

Figure 4.13 TEM Micrograph of 50/50 PAAm/PAA IPN nanoparticles.

REFERENCES

1. Brannon-Peppas, L. and Blanchette, J.O., *Nanoparticle and targeted systems for cancer therapy.* Adv. Drug Deliv. Rev., 2004. **56**(11): p. 1649-1659.

2. Maeda, H., Wu, J., Sawa, T., Matsumura, Y., and Hori, K., *Tumor vascular permeability and the EPR effect in macromolecular therapeutics: a review.* J. Control. Release, 2000. **65**(1-2): p. 271-284.

3. Fang, J., Nakamura, H., and Maeda, H., *The EPR effect: Unique features of tumor blood vessels for drug delivery, factors involved, and limitations and augmentation of the effect.* Adv. Drug Deliv. Rev., 2010. **doi: 10.1016/j.addr.2010.04.009**.

4. Vicent, M.J. and Duncan, R., *Polymer conjugates: nanosized medicines for treating cancer.* Trends Biotechnol., 2006. **24**(1): p. 39-47.

5. Fonseca, C., Simoes, S., and Gaspar, R., *Paclitaxel-loaded PLGA nanoparticles: preparation, physicochemical characterization and in vitro anti-tumoral activity.* J. Control. Release, 2002. **83**(2): p. 273-286.

6. Li, C. and Wallace, S., *Polymer-drug conjugates: Recent development in clinical oncology.* Adv. Drug Deliv. Rev., 2008. **60**(8): p. 886-898.

7. Peer, D., Karp, J.M., Hong, S., Farokhzad, O.C., et al., *Nanocarriers as an emerging platform for cancer therapy.* Nat. Nanotechnol., 2007. **2**(12): p. 751-760.

8. Wang, Y., Wei, X., Zhang, C., Zhang, F., and Liang, W., *Nanoparticle delivery strategies to target doxorubicin to tumor cells and reduce side effects.* Therapeutic Delivery, 2010. **1**(2): p. 273-287.

9. Iglesias, J., *nab-Paclitaxel (Abraxane(R)): an albumin-bound cytotoxic exploiting natural delivery mechanisms into tumors.* Breast Cancer Res., 2009. **11**(Suppl 1): p. S21.

10. Satarkar, N.S. and Hilt, J.Z., *Magnetic hydrogel nanocomposites for remote controlled pulsatile drug release.* J. Control. Release, 2008. **130**(3): p. 246-251.

11. Sershen, S.R., Halas, N.J., and West, J.L. *Pulsatile release of insulin via photothermally modulated drug delivery*. in *[Engineering in Medicine and*

Biology, 2002. 24th Annual Conference and the Annual Fall Meeting of the Biomedical Engineering Society] EMBS/BMES Conference, 2002. Proceedings of the Second Joint. 2002.

12. Lentacker, I., Geers, B., Demeester, J., De Smedt, S.C., and Sanders, N.N., *Design and Evaluation of Doxorubicin-containing Microbubbles for Ultrasound-triggered Doxorubicin Delivery: Cytotoxicity and Mechanisms Involved.* Mol. Ther., 2010. **18**(1): p. 101-108.

13. Ferrara, K., Pollard, R., and Borden, M., *Ultrasound microbubble contrast agents: fundamentals and application to gene and drug delivery.* Annu. Rev. Biomed. Eng., 2007. **9**: p. 415-47.

14. Ferrari, M., Desai, T., Bhatia, S., Hirsch, L.R., et al., *Diagnostic and Therapeutic Applications of Metal Nanoshells*, in *BioMEMS and Biomedical Nanotechnology*. 2007, Springer US. p. 157-169.

15. O'Neal, D.P., Hirsch, L.R., Halas, N.J., Payne, J.D., and West, J.L., *Photo-thermal tumor ablation in mice using near infrared-absorbing nanoparticles.* Cancer Lett., 2004. **209**(2): p. 171-176.

16. Loo, C., Lin, A., Hirsch, L., Lee, M.H., et al., *Nanoshell-enabled photonics-based imaging and therapy of cancer.* Technol. Cancer Res. T., 2004. **3**(1): p. 33-40.

17. Pérez-Juste, J., Pastoriza-Santos, I., Liz-Marzán, L.M., and Mulvaney, P., *Gold nanorods: Synthesis, characterization and applications.* Coordin. Chem. Rev., 2005. **249**(17-18): p. 1870-1901.

18. Lee, K.S. and El-Sayed, M.A., *Gold and silver nanoparticles in sensing and imaging: Sensitivity of plasmon response to size, shape, and metal composition.* J. Phys. Chem. B, 2006. **110**(39): p. 19220-19225.

19. Sershen, S.R., Westcott, S.L., Halas, N.J., and West, J.L., *Temperature-sensitive polymer-nanoshell composites for photothermally modulated drug delivery.* J. Biomed. Mater. Res., 2000. **51**(3): p. 293-298.

20. Peppas, N.A., Bures, P., Leobandung, W., and Ichikawa, H., *Hydrogels in pharmaceutical formulations.* Eur. J. Pharm. Biopharm., 2000. **50**(1): p. 27-46.

21. Pelton, R., *Temperature-sensitive aqueous microgels.* Adv. Colloid Interfac., 2000. **85**(1): p. 1-33.

22. Murray, M.J. and Snowden, M.J., *The preparation, characterisation and applications of colloidal microgels.* Adv. Colloid Interfac., 1995. **54**: p. 73-91.

23. Andersson, M. and Maunu, S.L., *Structural studies of Poly(N-isopropylacrylamide) microgels: Effect of SDS surfactant concentration in the microgel synthesis.* J. Polym. Sci. Pt. B-Polym. Phys., 2006. **44**(23): p. 3305-3314.

24. Okano, T., *MOLECULAR DESIGN OF TEMPERATURE-RESPONSIVE POLYMERS AS INTELLIGENT MATERIALS.* Adv. Polym. Sci., 1993. **110**: p. 179-197.

25. Peppas, N.A. and Klier, J., *Controlled release by using poly(methacrylic acid-g-ethylene glycol) hydrogels.* J. Control. Release, 1991. **16**(1-2): p. 203-214.

26. Owens, D.E., Jian, Y., Fang, J.E., Slaughter, B.V., et al., *Thermally Responsive Swelling Properties of Polyacrylamide/Poly(acrylic acid) Interpenetrating Polymer Network Nanoparticles.* Macromolecules, 2007. **40**(20): p. 7306-7310.

Chapter 5: Gold-Polymer Composite Nanoparticle Synthesis and Characterization

5.1 Introduction

In order to develop the externally-controlled light-responsive nanoparticle systems, a component must be introduced into the system that will lead to the heating of the polymer layer which triggers the swelling response and associated drug release. The heating element must meet several criteria. First, it must be on the nanoscale so that the entire particle systems are at most 400 nm in diameter. Second, the component must be able to heat in response to exposure to light in the near infrared (NIR) region. Light with wavelengths in the NIR region is of interest because there is a minimum in the absorption characteristics of the main absorbers is tissue in this region including water and hemoglobin. Several types of metal based nanoparticles are of interest because they are capable of absorbing light in this region and converting it to heat.

Nanoshells consist of a thin metal shell around a dielectric core. Commonly the core is silica and the surrounding metal shell is gold. These gold nanoshells can be tuned to have peak absorbance at wavelengths of light ranging from 700-1100 nm. By changing the ratio of the thickness of the gold shell to the diameter of the silica core, the optical resonance varies from across parts of the visible and near infrared regions

[1]. For example a nanoshell with a 60 nm diameter silica core and a 20 nm thick gold shell has a maximum optical resonance near 725 nm while the same silica core with a 5 nm gold shell displays peak resonance around 1025 nm [2]. By carefully controlling the size of the silica core and the growth of gold shell, particles can be formed with peak extinction in the NIR region where tissue transmittance is highest. Figure 5.1 shows a TEM micrograph of gold nanoshells of roughly 80 nm in total diameter that exhibit peak extinction around 800 nm in the desirable near-infrared region.

Many metal nanoparticles, particularly silver and gold, display strong absorption in the visible spectrum, typically ranging from yellow to reddish-brown [3]. By altering the size and in particular the shape of these nanoscale particles, absorption can be observed in nearly any part of the visible spectrum and wavelengths into the infrared spectrum. Synthesis of structures ranging from nanospheres and nanowires to nanoprisms and nanoplates are reported in the literature exhibiting a variety of different visual appearances and absorbance spectra [4].

Gold nanorods are nanoscale spherically capped cylindrical particles. The nanorods show varying absorption spectra determined by the aspect ratio of the rods which can be described using Mie theory. Small changes in aspect ratio have dramatic effects on the optical properties of the particles, for example changing the aspect ratio of a gold nanorod over a range of approximately 3:1 to 7:1 causes a red-shift from maximum absorption at 750 nm to 980 nm [5]. Nanorods with aspect ratios near 4:1

such as those with a length of 40 nm and a width of 10 nm as shown in Figure 5.2 absorb strongly in the NIR region.

Gold nanorods were selected for use in the composite systems developed in this thesis. The smaller size of the gold nanorods with peak absorption at 800 nm (approximately 40 nm in length) will allow them to be incorporated into composite systems that will have total diameters below 400 nm in their drug entrapping states. Nanoshells that have the required properties would be closer to 100 nm in diameter making composite delivery systems considerably more bulky. Gold nanorods also have been shown to have higher absorption values and associated heating when compared to similar nanoshells.

A composite nanoparticle system is of interest in order to couple the gold nanorod heating element to the temperature sensitive polymer hydrogel carrier. Metal-polymer composites have been formed for a variety of applications in past work. Much of this work has focused on entrapping metal nanoparticles within larger polymer matrices. Systems that incorporate both metal and polymers have been synthesized through direct polymerization, assembly of polymers around nanoscale metals, or attachment of metals to functional polymers [6].

Past work has been done in the development of temperature based externally controlled systems. In one case where light was used an external trigger, gold nanoshells have been incorporated into poly(N-isoproplyacrylamide-co-acrylamide), P(NIPAAm-co-AAm), films or disks. Upon exposure to certain wavelengths of light, gold

nanoshells heat the polymer and trigger a negative swelling transition. This behavior has been used to externally control the opening and closing of a microvalve and to trigger pulsatile release of insulin from a polymer loaded film [7, 8].

In this thesis, gold nanorods have been grafted to polymer nanoparticles using a peptide bond so that they will heat the adjacent polymer hydrogel network. A schematic of the particle system is shown in Figure 5.3. The amide bond covalently attaching the nanorods to the particles is formed by coupling an amine and a carboxyl group. Gold nanorods have been functionalized with a poly(ethylene glycol) (PEG) linking molecule with a primary amine group termination. All of the temperature responsive polymer nanoparticles used for composite synthesis included acrylic acid in the polymerization so that there were free carboxyl groups on the surface of the hydrogel for grafting of the gold nanorods. Carboxyl groups can be activated for this type of condensation reaction by the inclusion of one or more catalysts to act as leaving groups during the reaction. Water soluble carboxyl activating agents, 1-ethyl-3-(3-dimethylaminopropyl) carbodiimide (EDC) and *N*-Hydroxysulfosuccinimide (sulfo-NHS) were used here to graft the gold nanorods to the surface of the polymer nanoparticles. The mechanism for the peptide coupling reaction using EDC is shown in Figure 5.4.

An effect known as localized surface plasmon resonance occurs when two metallic nanoparticles are in close proximity to each other, typically within about 2.5 the diameter of one of the particles [9]. When the particles are exposed to light, there is a collective oscillation of electrons. The extinction behavior becomes a function of not

only the size and shape of the nanoparticle but also the distance between adjacent particles and their orientation to each other. For example, as 50 nm gold nanorods are moved closer together at distances less than 100 nm the extinction spectrum becomes more red-shifted and the peak broadens. As the composite gold-polymer nanoparticles go towards the more collapsed structure and the gold nanoparticles are drawn closer together these plasmon coupling effects are likely to occur.

5.2 Materials and Methods

5.2.1 LCST Composite Nanoparticle Synthesis

Acrylic acid (AA, inhibited with 200 ppm hydroquinone monomethyl ether), N-Isopropylacrylamide (NIPAAm), and sodium dodecyl sulfate (SDS) were obtained from Sigma Aldrich (Milwaukee, WI), acrylamide (AAm) and ammonium persulfate (APS) were obtained from Fisher Scientific (Hampton, NH). Bare gold nanorods and gold nanorods with Amine-terminated PEG chains, N-therapy amine-polymer gold nanorods, were obtained from Nanopartz (Loveland, CO). Acrylic acid was purified using vacuum distillation. All other materials were used as received.

Composite systems incorporating temperature-sensitive polymers were synthesized using two different methods. The first method involved dispersing gold nanorods in the pre-polymerization aqueous solution. Polymerization proceeded using an aqueous dispersion polymerization method and gold nanorods served as nucleation points, entrapping them inside of polymer nanoparticles.

Crosslinked PNIPAAM composite nanoparticles were synthesized along with P(NIPAAm-co-AAm), and P(NIPAAm-co-AA) at molar crosslinking ratios of 10 %. To synthesize LCST composite monomer, crosslinker, N,N'-Methylene bisacrylamide, and a stabilizer (usually SDS) are added to a 100 ml aqueous phase in a 250 ml round bottomed flask at a total monomer concentration of 5.5 g/L and a typical stabilizer concentration of 0.3 g/L. The monomers and stabilizer were first dissolved in the aqueous medium. 2 ml of gold nanorods were added to the polymerization flask at a concentration of approximately 0.2 mg/ml. Next, the aqueous reaction solution was purged with nitrogen to remove oxygen from the reaction flask. A 70 °C oil bath was prepared and the purged reaction flask was submerged in the oil bath. An aqueous solution of the free radical initiator, APS, was injected into the reaction flask to initiate reaction. The polymerization was allowed to proceed for at least two hours. After completion, the reaction flask is opened to the air and removed from the heat source.

The resulting composite nanoparticle suspension was dialyzed against DI water for 10 days using a 12-14,000 MWCO dialysis tubing. Dialysis water was changed twice daily. Particle solutions were then frozen in a -80° C freezer and lyophilized until dry. Dry particle solutions were resuspended in the appropriate medium or used dry as necessary for further analysis.

Transmission Fourier transform infrared (FT-IR) spectrometry was performed on freeze dried nanogels dispersed in potassium bromide (KBr) to verify synthesis of P(NIPAAm-co-AA). KBr was dehydrated at 125 °C prior to use to remove water. Samples

were mixed with KBr at 1-2wt% and crushed with a mortar and pestle. Approximately 200mg of this powder dispersion was pressed into clear, 13 mm pellets using a hydraulic press and evacuable potassium bromide die. IR spectra were recorded using a Nicolet Magna IR-560 FTIR Spectrophotometer. The machine was purged with nitrogen gas for at least two hours before acquiring spectra. Each spectrum was an average of 100 scans with a resolution of 4 cm-1.

The second method to synthesize PNIPAAm based gold-polymer systems consisted of grafting gold nanorods to the surface of the polymer nanoparticles. First P(NIPAAm-co-AA) with 10 mol % crosslinking feed ratio were synthesized using aqueous dispersion polymerization as previously described. Gold nanorods were received capped with a PEG chain with a primary amine on the terminal end of the PEG. The attachment of the PEG chain to the gold nanorods is achieved by reacting a heterobifunctional PEG molecule with a thiol group on one end and the primary amine on the other with the gold.

A condensation reaction was used to form a peptide bond grafting the gold nanorods to the surface of the polymer nanoparticles. Polymer nanoparticles were suspended in DI water at a concentration of 5 mg/ml. Gold nanorods were used as received at a concentration of approximately 2 mg/ml. In a typical reaction 100 µl of polymer nanoparticle stock solution was added to 2.2 ml DI water. A 0.5 mg weight of EDC was added to the solution and it was mixed on a rotary mixer for 15 minutes. A volume of 250 µl of gold nanorod solution was added to the mixture and stirred

overnight. Particles were dialyzed against DI water for 2 days with water changed twice daily.

5.2.2 UCST Composite Nanoparticle Synthesis

Acrylic acid (AA, inhibited with 200 ppm hydroquinone monomethyl ether), N,N'-methylenebisacrylamide (MBAAm), polyethylene glycol laurylether (Brij 30), cyclohexane, and sodium bis(2-ethylhexyl) sulfosuccinate (AOT) were obtained from Sigma Aldrich (Milwaukee, WI), acrylamide (AAm) and lauroyl peroxide were obtained from Fisher Scientific (Hampton, NH). Gold nanorods with Amine-terminated PEG chains, N-therapy amine-polymer gold nanorods, were obtained from Nanopartz (Loveland, CO).All materials were used as received.

First, the IPN 50/50 PAAm/PAA polymer nanoparticles were synthesized using a two-step inverse (water-in-oil) microemulsion free radical polymerization. The inverse emulsion solution consists of a cyclohexane continuous phase, surfactants, and an aqueous phase split into two separate premixes that are reacted consecutively, containing monomer, initiator, and water. The only difference in these two premixes was that one contains only AAm monomer and the other only AA monomer.

A typical polymerization medium consisted of 81% cyclohexane oil phase, 13% surfactants, and 6% total aqueous phase by weight. The surfactant mixture was a 50:50 weight percent mixture of Brij 30 and AOT. The aqueous phase typically consisted of approximately 80% water and 5% initiator by weight with the balance consisting of

monomer and crosslinker, N,N'-Methylene bisacrylamide (MBAAm), in the desired synthesis ratio.

The surfactant was dissolved first in cyclohexane. AAm monomer along with MBAAm crosslinker was dissolved in the separate water phase. The first premixed aqueous phase containing AAm monomer was added to the cyclohexane and the mixture of the two phases along with surfactant was homogenized at 24,000 RPM for 5 minutes. The reaction flask was then purged with nitrogen for 30 minutes to remove oxygen from the system.

An oil bath was prepared at 60 °C . The reaction was initiated following the purge by immersion in the oil bath to heat to 60 °C. After reaction for 2 hours, the reaction was terminated by removal from heat and exposure to the atmosphere. A second aqueous monomer phase was prepared. The second aqueous phase, consisting of AA and additional initiator and crosslinker, is added to the reaction flask and again homogenized, purged, and reacted for 2 hours at 60 °C to form a second crosslinked polymer network that is physically entangled with the first network, but not covalently attached.

After synthesis the cyclohexane solvent was removed using rotary evaporation under vacuum at 40 °C. Five successive ethanol wash cycles were used to wash polymer. One wash cycle consisted of suspension of approximately 0.5 g of nanoparticles in 25 ml of ethanol and centrifugation at 3200 rcf. Ethanol supernatant was then removed and particles resuspended in ethanol for the next wash. After

ethanol washing the particles were suspended in DI water and dialyzed for 10 days using a 12-14,000 MWCO dialysis tubing with dialysis water being changed twice daily. Particle solutions were then frozen in a -80° C freezer and lyophilized until dry. Dry particle solutions were resuspended in the appropriate medium or used dry as necessary for further analysis.

Transmission Fourier transform infrared (FT-IR) spectrometry was performed on freeze dried nanogels dispersed in KBr. KBr was dehydrated at 125 °C prior to use to remove water. Samples were mixed with KBr at 1-2wt% and crushed with a mortar and pestle. Approximately 200mg of this powder dispersion was pressed into clear, 13 mm pellets using a hydraulic press and evacuable potassium bromide die. IR spectra were recorded using a Nicolet Magna IR-560 FTIR Spectrophotometer. The machine was purged with nitrogen gas for at least two hours before acquiring spectra. Each spectrum was an average of 100 scans with a resolution of 4 cm-1.

Gold nanorods were attached to the surface of the IPN nanoparticles using a condensation reaction to form a peptide bond. Polymer nanoparticles were suspended in DI water at a concentration of 5 mg/ml. Gold nanorods were used as received at a concentration of approximately 2 mg/ml. In a typical reaction, 100 µl of polymer nanoparticle stock solution was added to 2.2 ml DI water. A 0.5 mg weight of EDC was added to the solution and it was mixed on a rotary mixer for 15 minutes. A volume of 250 µl of gold nanorod solution was added to the mixture and stirred overnight. Particles were dialyzed against DI water for 2 days with water changed twice daily.

5.2.3 Composite Nanoparticle Characterization by Transmission Electron Microscopy

Transmission electron microscopy was performed to analyze particle size, morphology, polydispersity, and confirm attachment of gold nanorods. TEM samples were prepared by placing 5 µl of aqueous particle suspension on a formvar coated copper TEM grid (Electron Microscopy Sciences, Hatfield, PA). After one minute the grid was blotted dry using filter paper. Particles were imaged using a FEI Tecnai Transmission Electron Microscope (FEI; Hillsboro, OR) operating at 80 kv equipped with a top mount AMT Advantage HR 1kX1k digital camera. Composite nanoparticles were viewed to analyze the extent of grafting of gold nanorods to the surface of LCST and UCST polymer nanoparticles.

5.3 Results and Discussion

5.3.1 LCST Composite Nanoparticle Synthesis

Gold nanorods were incorporated into LCST polymer nanoparticles during aqueous dispersion polymerization. PNIPAAm, 90/10 P(NIPAAm-co-AAm), and 90/10 P(NIPAAm-co-AA) were synthesized in the presence of bare gold nanorods and in each case a fraction of the polymer particles had entrapped gold nanorods. Typical polymerizations yielded systems in which 5-10% of polymer nanoparticles contained gold nanorods which will be discussed in further detail in Section 4.3.3. All three of the polymer nanoparticle systems were able to entrap bare gold nanorods during polymerizations.

Systems with gold nanorods grafted to the surface of LCST hydrogel nanoparticles were also synthesized. In this case 90/10 P(NIPAAm-co-AA) were used so that carboxyl pendant groups would be available for the grafting procedure. Gold nanorods were attached to the surface of the polymer nanoparticles, and surface coverage was shown to be controlled depending on the concentration of gold nanorods added during incubation with polymer nanoparticles.

The P(NIPAAm-co-AA) FT-IR spectrum is shown in Figure 5.5. Several important bands are present to identify the copolymer. A broad band between 3100 and 3400 cm^{-1} is caused by O-H stretching in the AA groups. N-H stretching in the secondary amide leads to a peak at 3300 cm^{-1}. The CO carbonyl band is a sharp beak at 1650 cm^{-1} because of intramolecular hydrogen bonding. The amide CO stretching band adds to the peak at 1650 cm^{-1} [10].

5.3.2 UCST Composite Nanoparticle Synthesis

Composites of UCST IPN nanoparticles and gold nanorods were formed by grafting gold nanorods to the surface of the polymer nanoparticles. Amine functionalized gold nanorods were attached to the acrylic acid residues present in the polymer backbone using the peptide coupling reaction activated by EDC. The surface coverage of the grafted nanorods on the polymer was a function of gold nanorod concentration incubated with the polymer nanoparticles, which will be further discussed in Section 4.3.4.

The FT-IR spectrum is displayed in Figure 5.6. The stretching of C-N, and C=O coupled with the bending of O-H groups leads to an absorption band centered at 1200 cm^{-1}. Absorption bands at 1455 and 1416 cm^{-1} are caused by scissor and bending vibrations of CH_2 and CH-CO. The band at 1680 cm^{-1} is caused by combined stretching vibrations of the C=O groups of both PAAm and PAA as well as the effects of hydrogen bonding between the two networks. An absorption band at 2950 cm^{-1} corresponds to the combined stretching of CH_2 groups in both PAAm (2945 cm^{-1}) and PAA (2960 cm^{-1}). O-H and NH_2 stretching vibrations lead to absorption bands between 3100 and 3500 cm^{-1} [11].

5.3.3 Composite Nanoparticle Characterization by Transmission Electron Microscopy

Gold-polymer composites formed during the aqueous dispersion polymerization of LCST hydrogel nanoparticles were imaged using TEM. Based on TEM micrographs, gold nanorods were entrapped in up to 10% of polymer nanoparticles during nucleation in dispersion polymerization. Representative micrographs of nanoparticles synthesized using this method are shown in Figures 5.7 through 5.9.

Transmission electron microscopy was used to examine the gold-polymer grafted nanoparticles after composite synthesis and evaluate the effectiveness of the procedures. TEM samples were prepared by depositing nanoparticles on a TEM grid directly from aqueous suspensions. TEM images confirm the attachment of gold nanorods to the surface of the temperature responsive polymer nanoparticles.

Representative TEM images of P(NIPAAm-co-AA) based polymer nanoparticles of several different magnifications are shown in Figures 5.10 through 5.12. IPN nanoparticles are shown in TEM micrographs in Figures 5.13 and 5.14.

5.4 CONCLUSIONS

In order to formulate systems that could be used to externally trigger the release of a drug using NIR light, two components were necessary in the system. First, a polymer nanoparticle capable of entrapping a drug and release it upon heating, and second a means to respond to light in a manner in which it will transmit heat to this polymer layer. Gold nanorods were identified as an appropriate heating element. In order for the system to be formulated the gold nanorods were incorporated into the polymer nanoparticle systems using two different means. Gold nanorods were entrapped in PNIPAAm, P(NIPAAm-co-AAm), and P(NIPAAm-co-AA) systems during aqueous dispersion polymerization as confirmed by transmission electron microscopy.

Gold nanorods were also grafted to the surface of temperature responsive nanoparticles following polymerization. 50/50 PAAm/PAA nanoparticles and 90/10 P(NIPAAm-co-AA) nanoparticles were synthesized using a water-in-oil microemulsion polymerization and aqueous dispersion polymerization, respectively. Amine functionalized gold nanorods were grafted to the surface of the nanoparticles using an EDC activated condensation reaction between carboxyl groups on the polymers and the amine groups on the nanorods. TEM results confirmed the formation of these gold-

polymer composite nanoparticle systems. Measurement of the absorption spectra over a 600-1000 nm wavelength range further demonstrated the attachment of gold nanorods to the surface of LCST polymer nanoparticles. A broadening and shifting of the spectrum was observed as the temperature was increased through and above the LCST transition temperature.

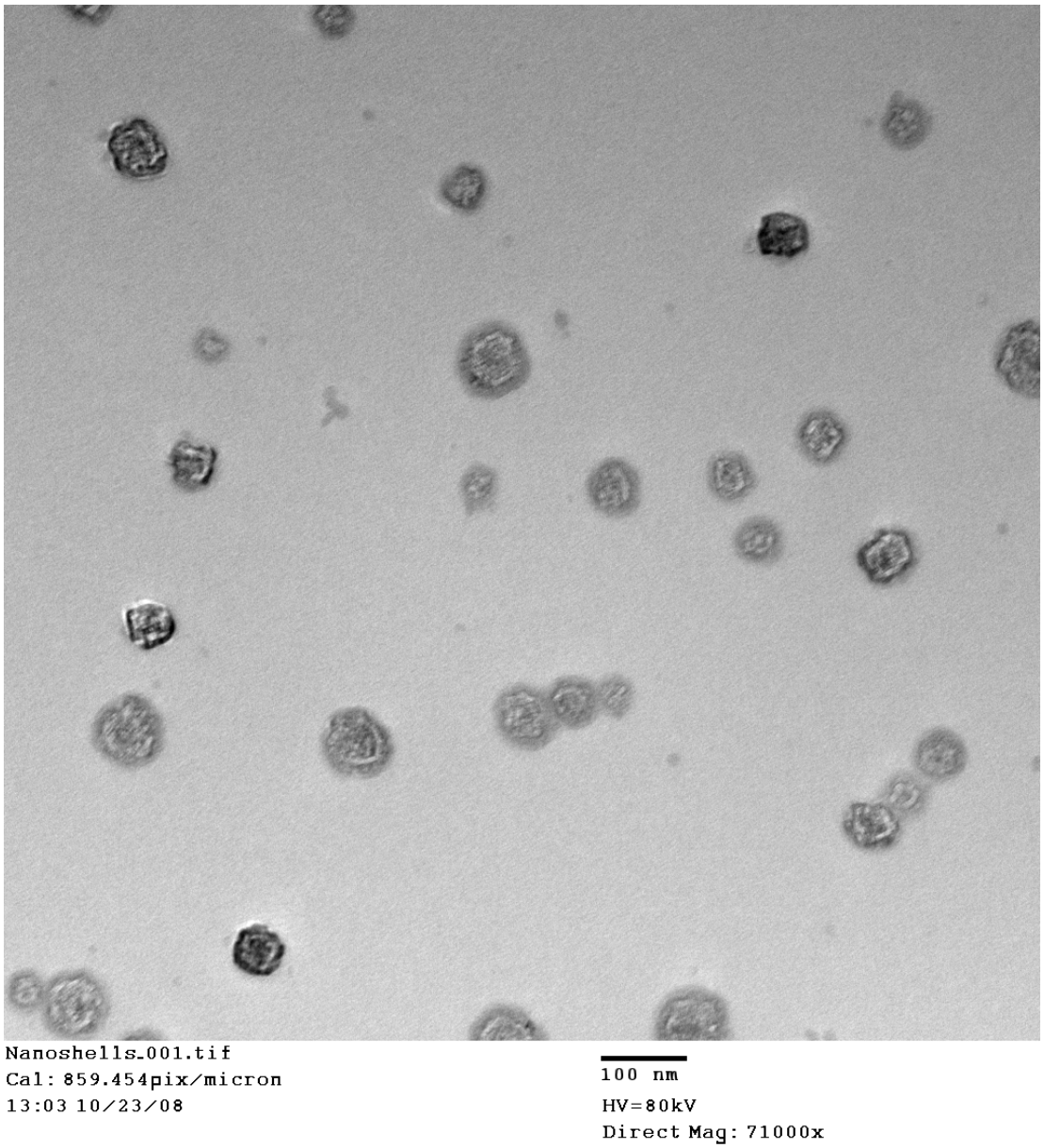

Figure 5.1 TEM micrograph of gold nanoshells formed from a gold coated silica particle with absorption centered around 800 nm.

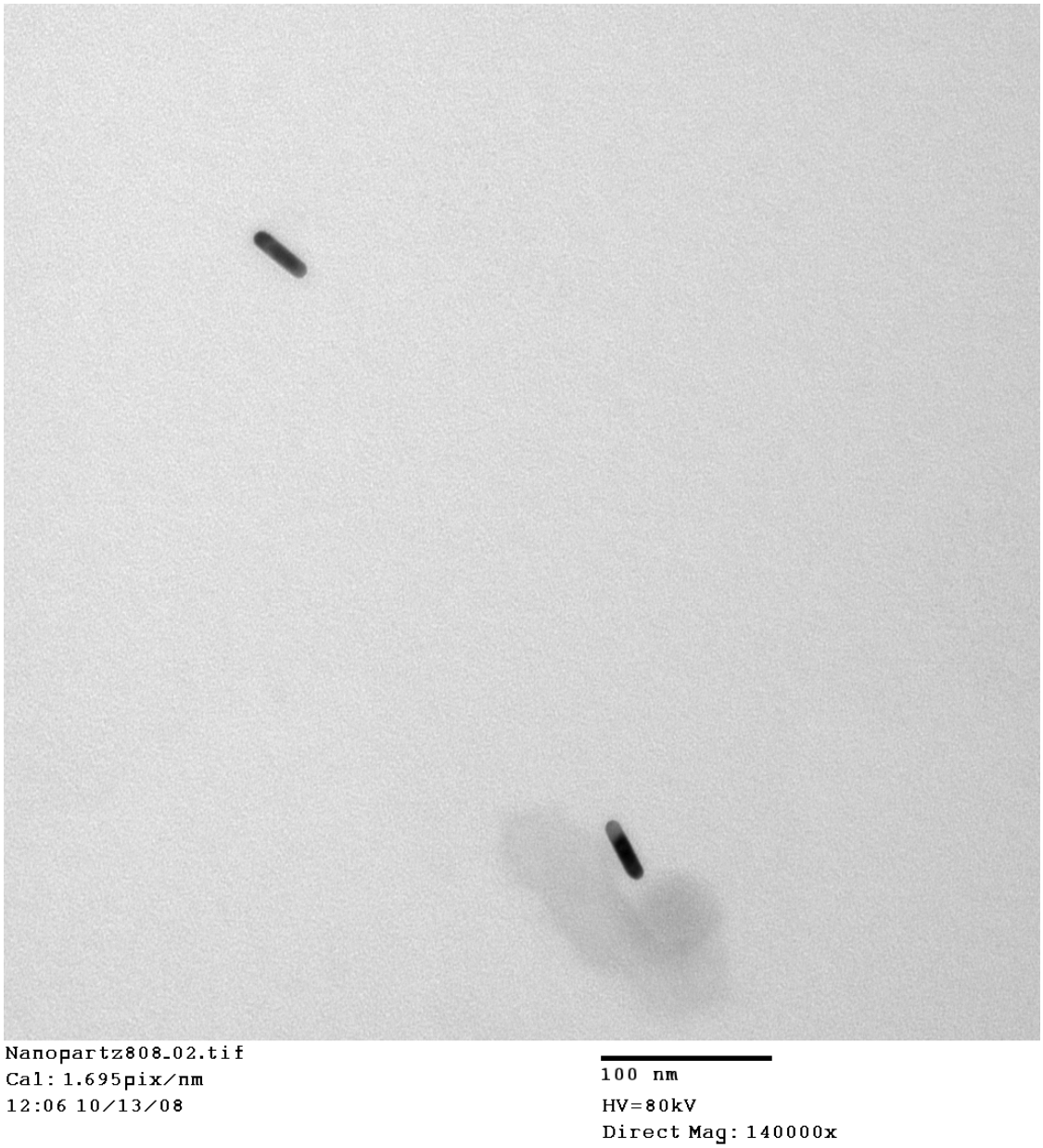

Figure 5.2 TEM micrograph of gold nanorods with 4:1 aspect ratio, 40 nm in length and 10 nm wide having absorption peak centered around 808 nm.

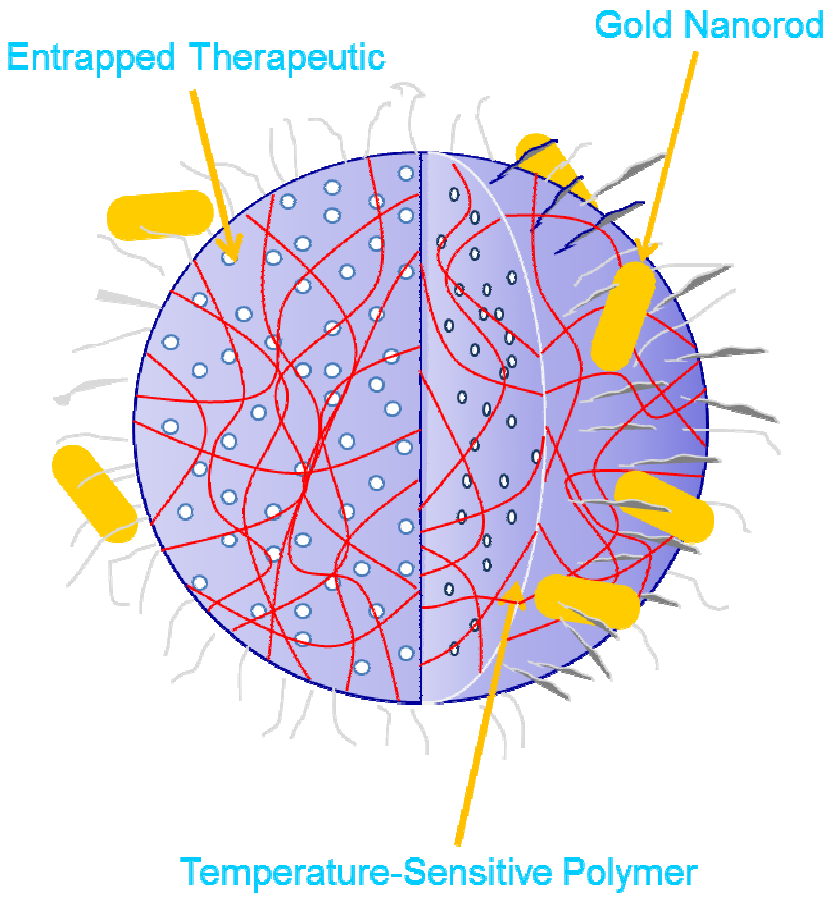

Figure 5.2 Schematic of the proposed externally-controlled therapeutic system consisting of gold-nanorods grafted to a temperature sensitive polymer nanoparticle.

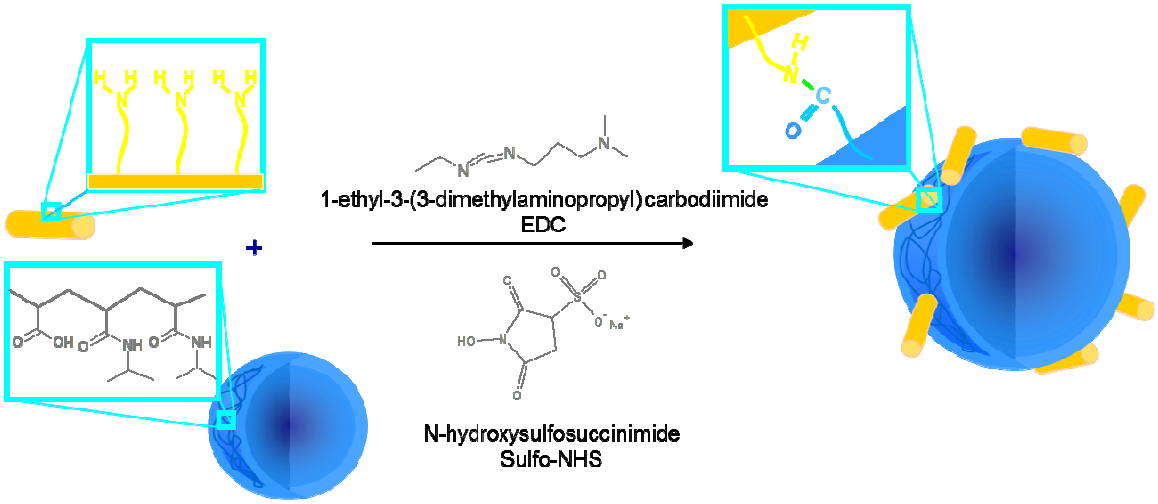

Figure 5.3 Schematic of the procedure for grafting of gold nanorods to polymer nanoparticles to form gold-polymer composites for externally-triggered systems.

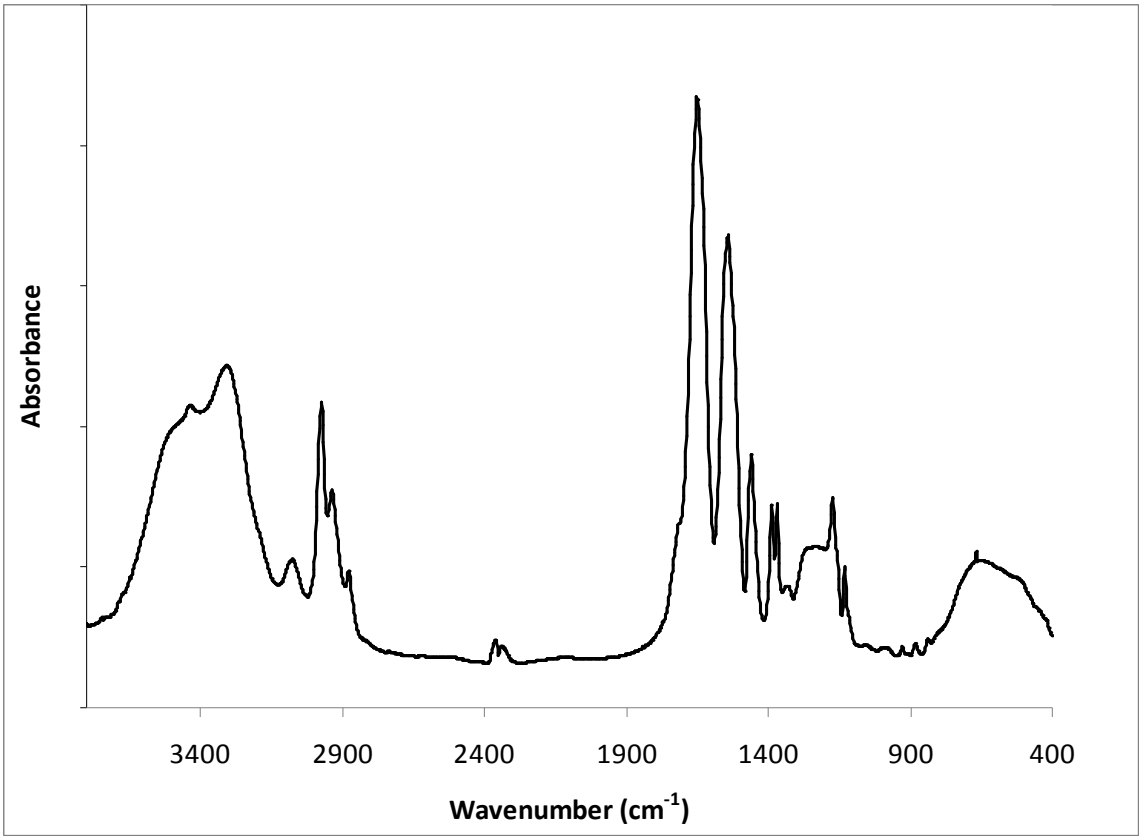

Figure 5.5 FT-IR absorption spectrum of P(NIPAAm-co-AA) nanoparticles.

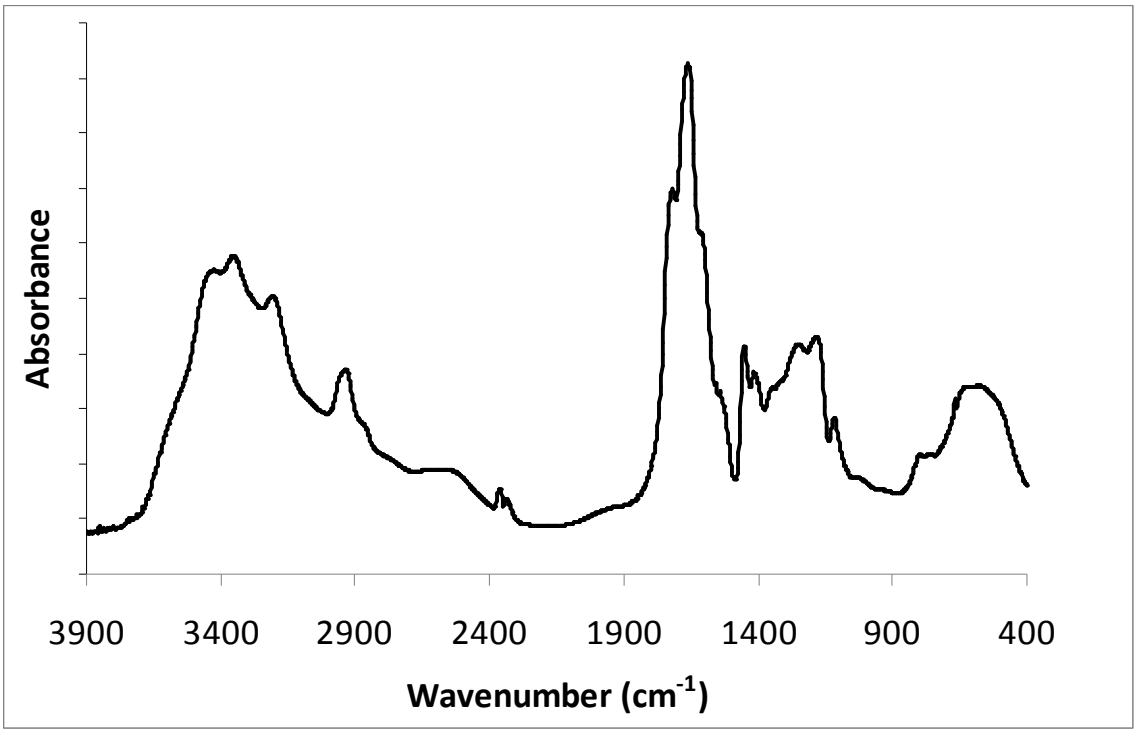

Figure 5.6 FT-IR absorption spectrum of 50/50 PAAm/PAA IPN nanoparticles.

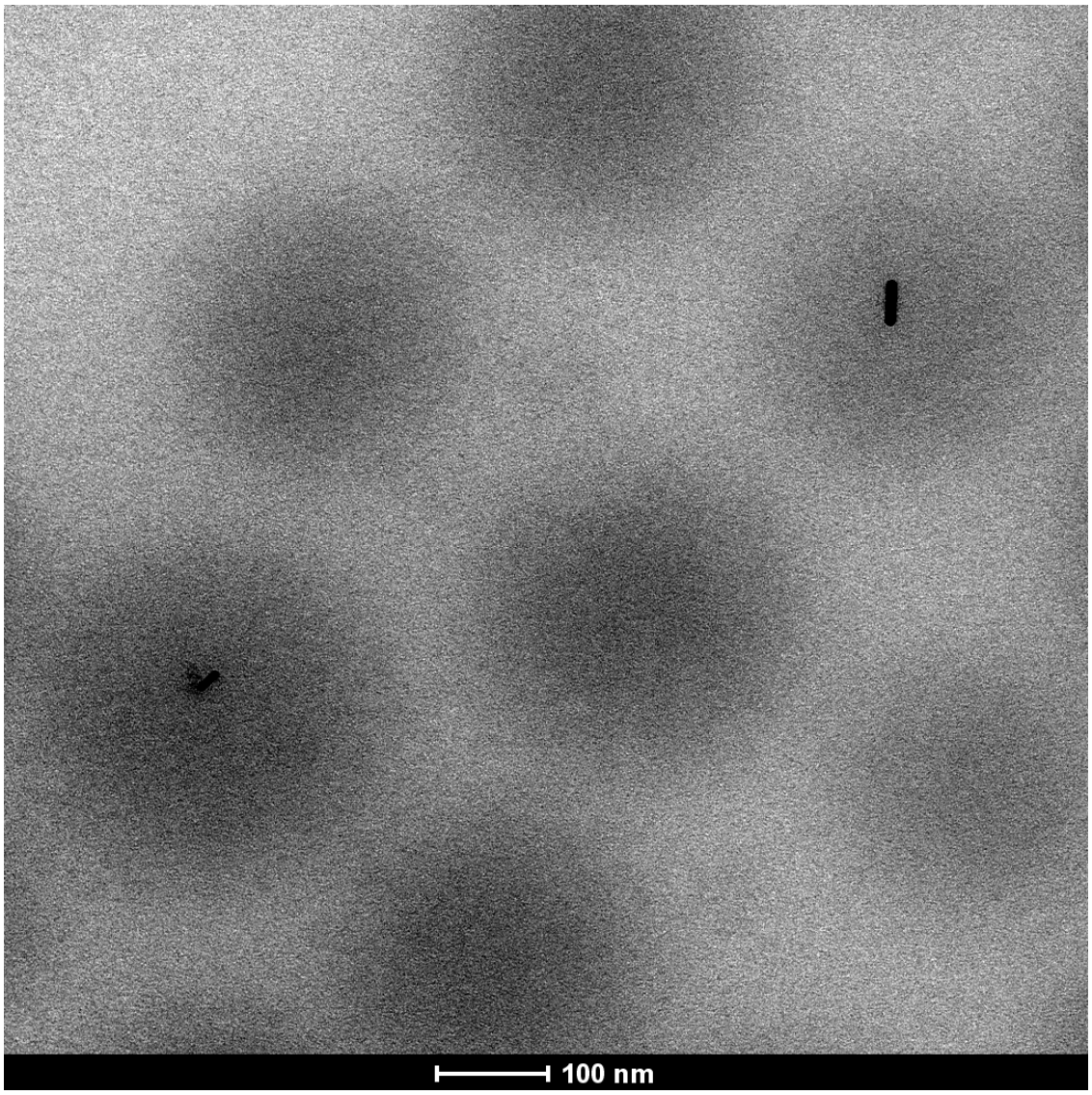

Figure 5.7 TEM micrograph of gold-polymer composites formed during nucleation of LCST polymers in aqueous dispersion polymerization.

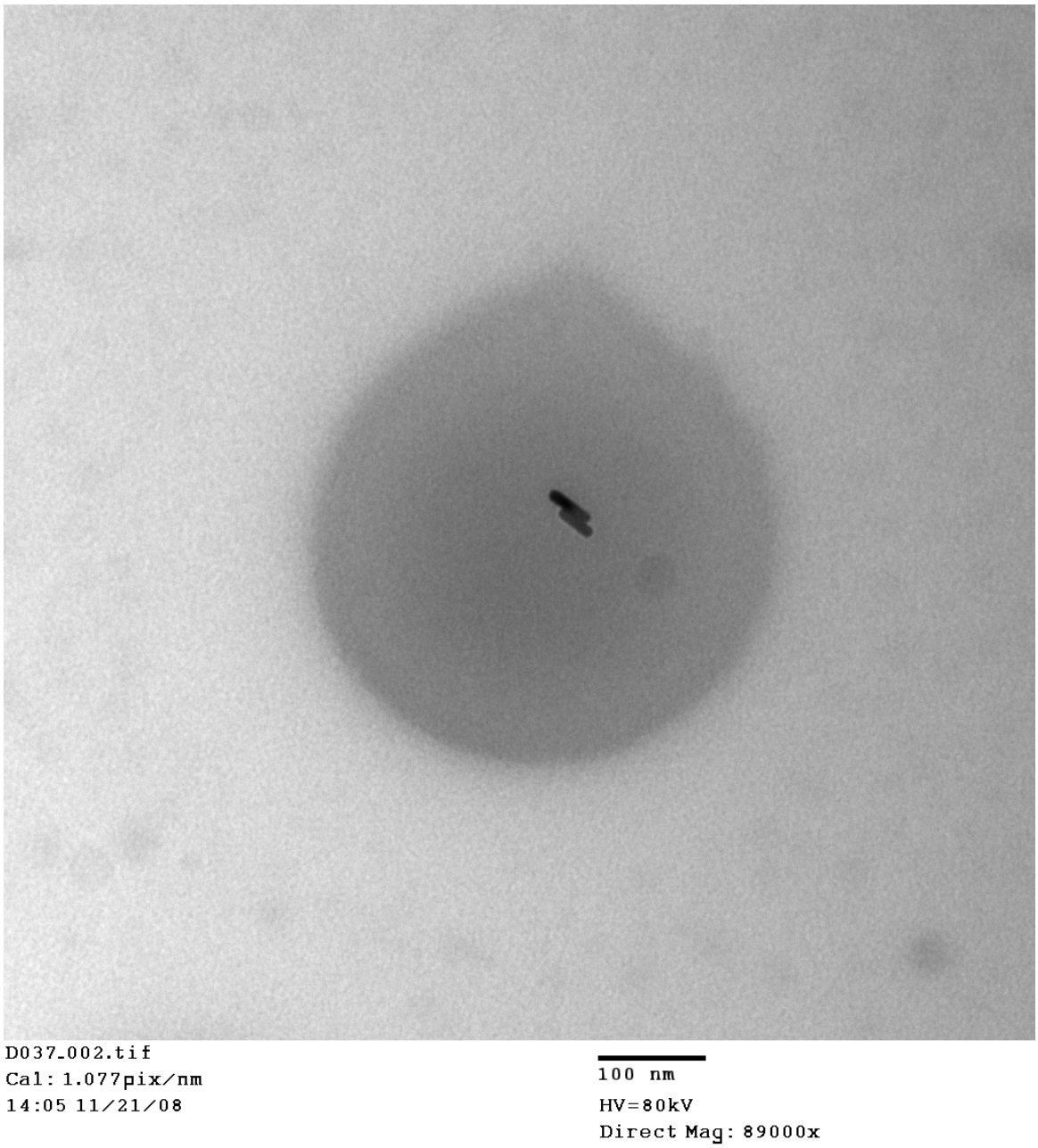

Figure 5.8 TEM micrograph of a single gold-polymer composite formed during nucleation of LCST polymer via dispersion polymerization.

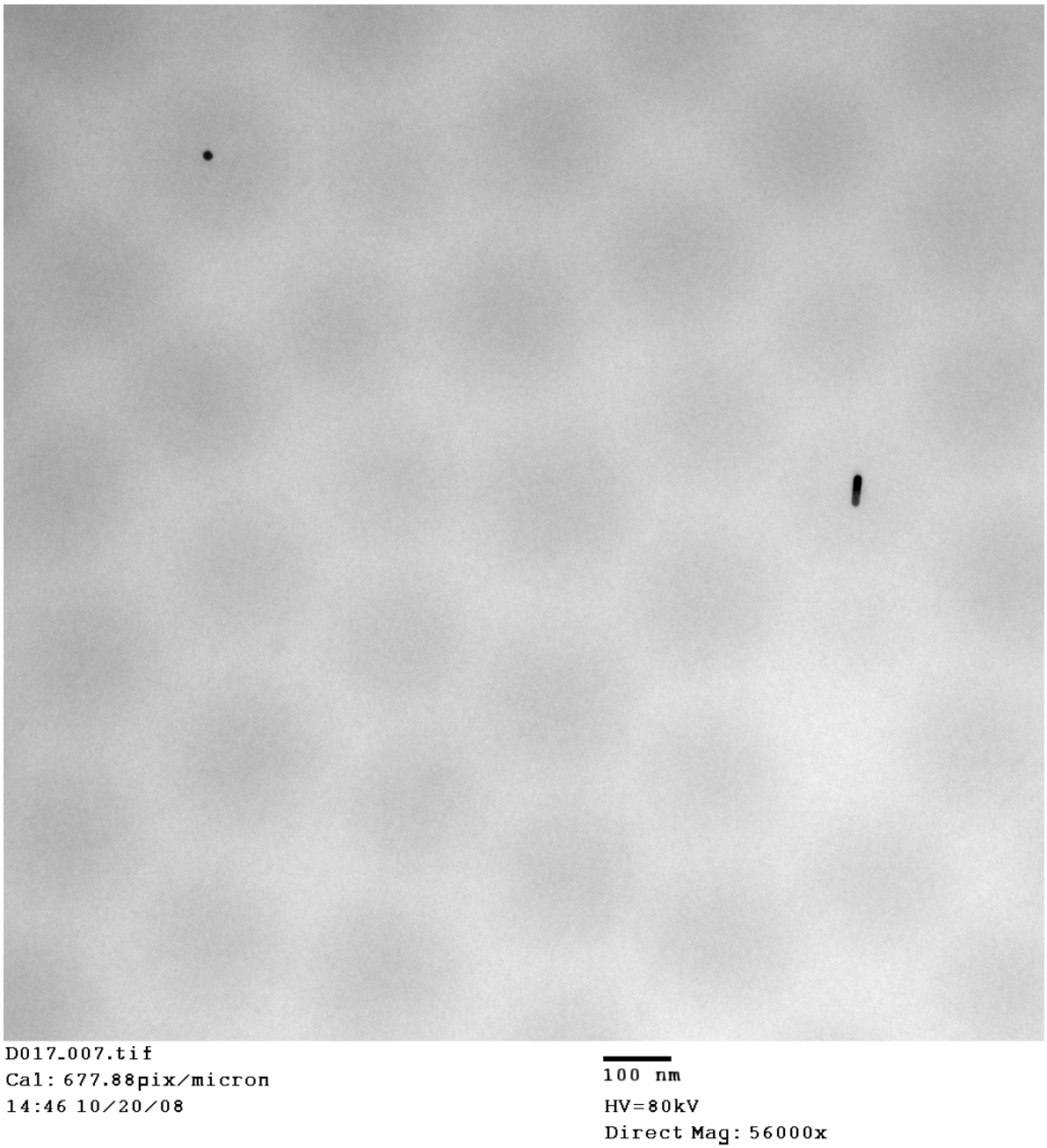

Figure 5.9 TEM image of gold-polymer composites formed during nucleation process in aqueous dispersion polymerization.

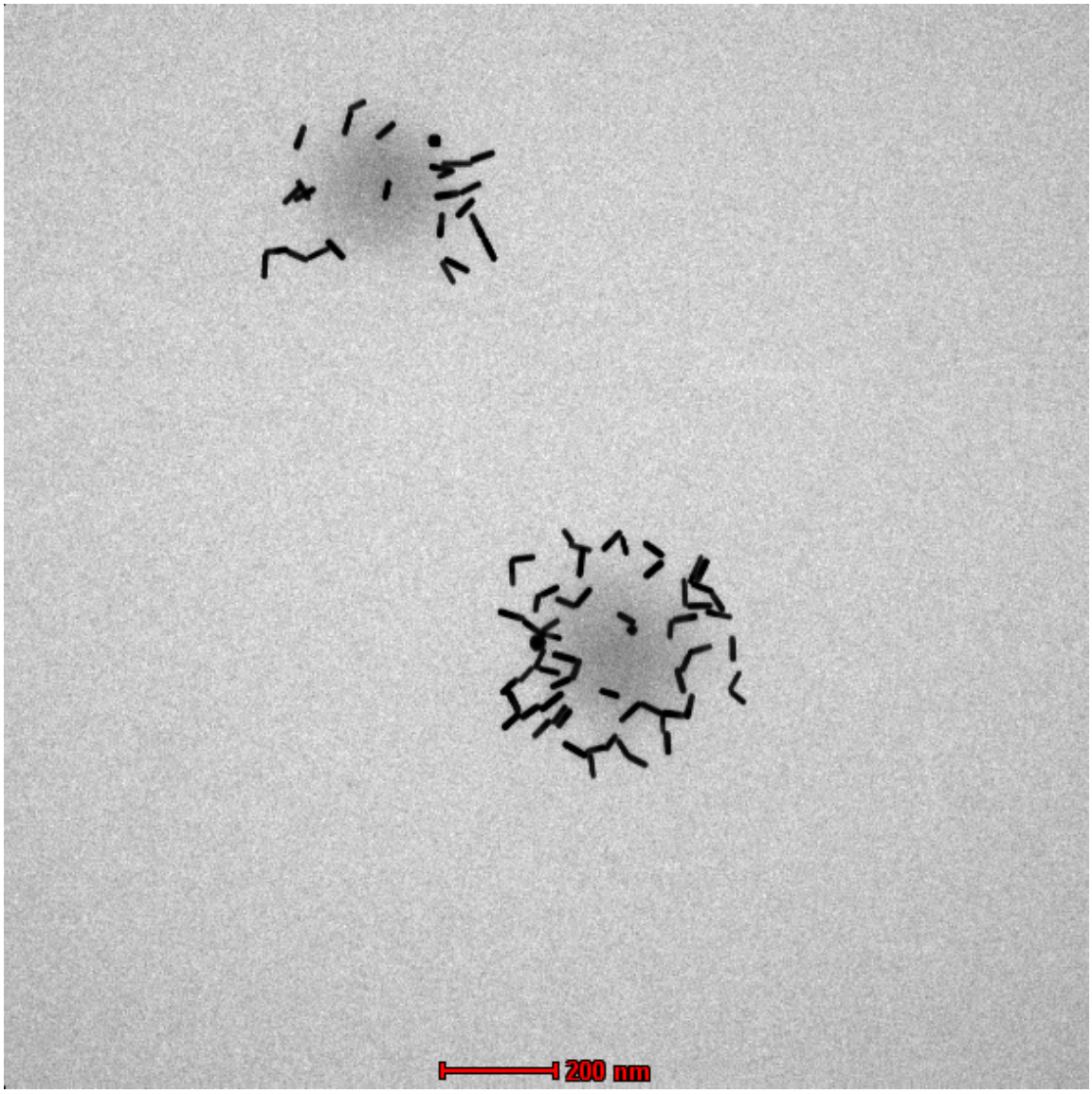

Figure 5.10 TEM micrograph of P(NIPAAm-co-AA) grafted with gold nanorods for externally-controlled systems.

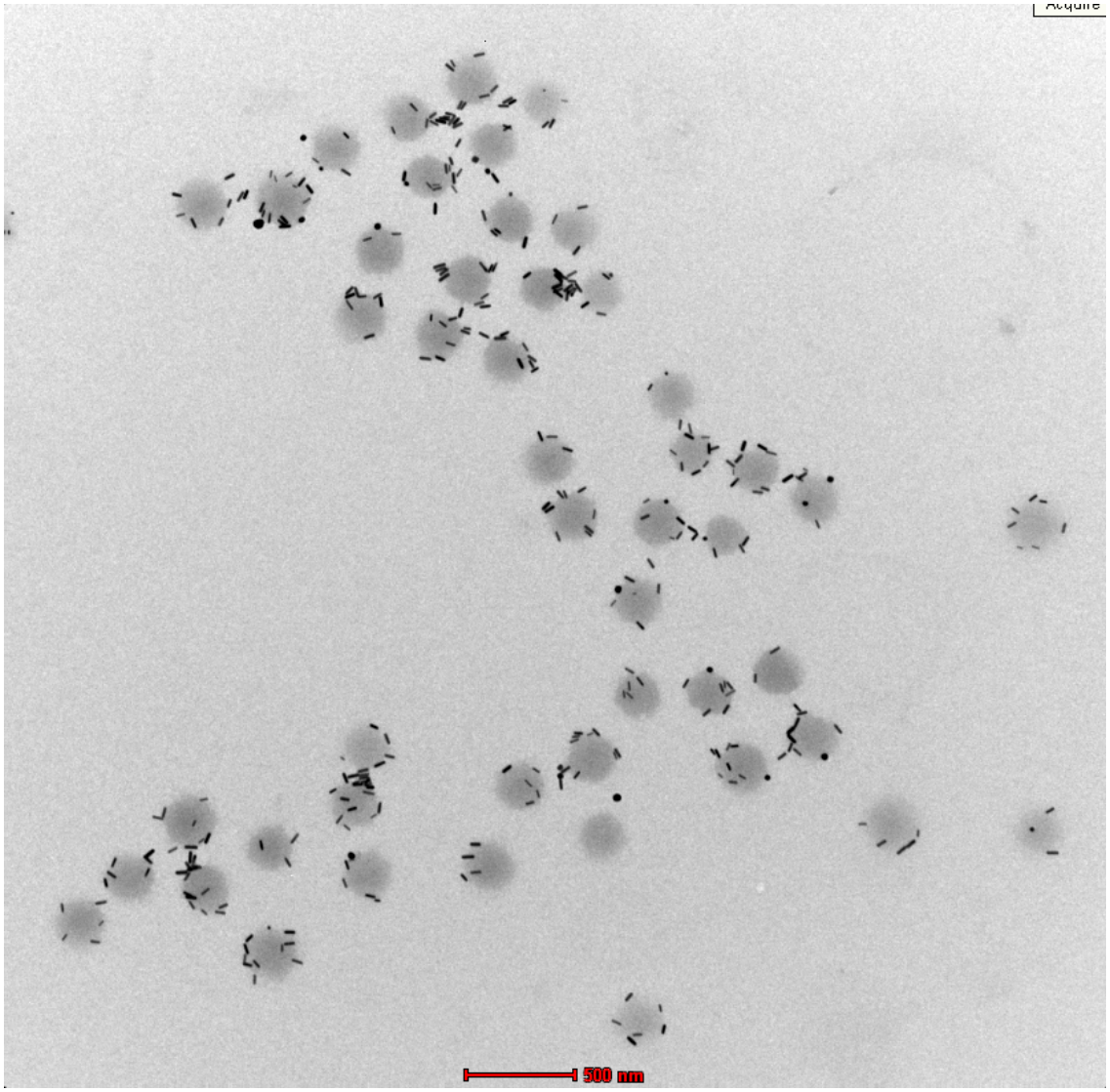

Figure 5.11 TEM micrograph of gold-polymer composite with P(NIPAAm-co-AA) nanoparticles grafted with gold nanorods.

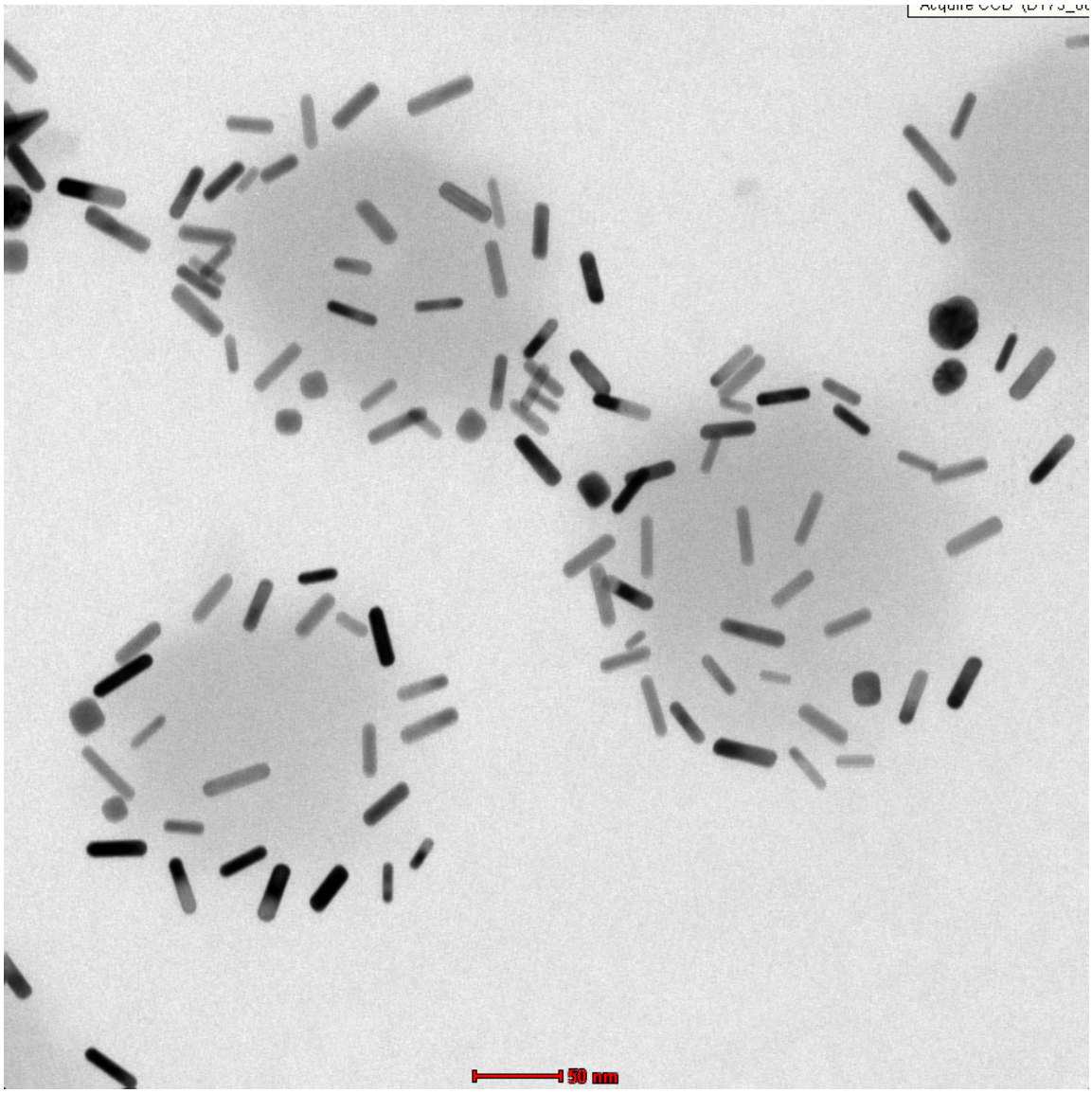

Figure 5.12 Gold-polymer composite TEM micrograph og P(NIPAAm-co-AA) nanoparticles grafted with gold nanorods at high magnification.

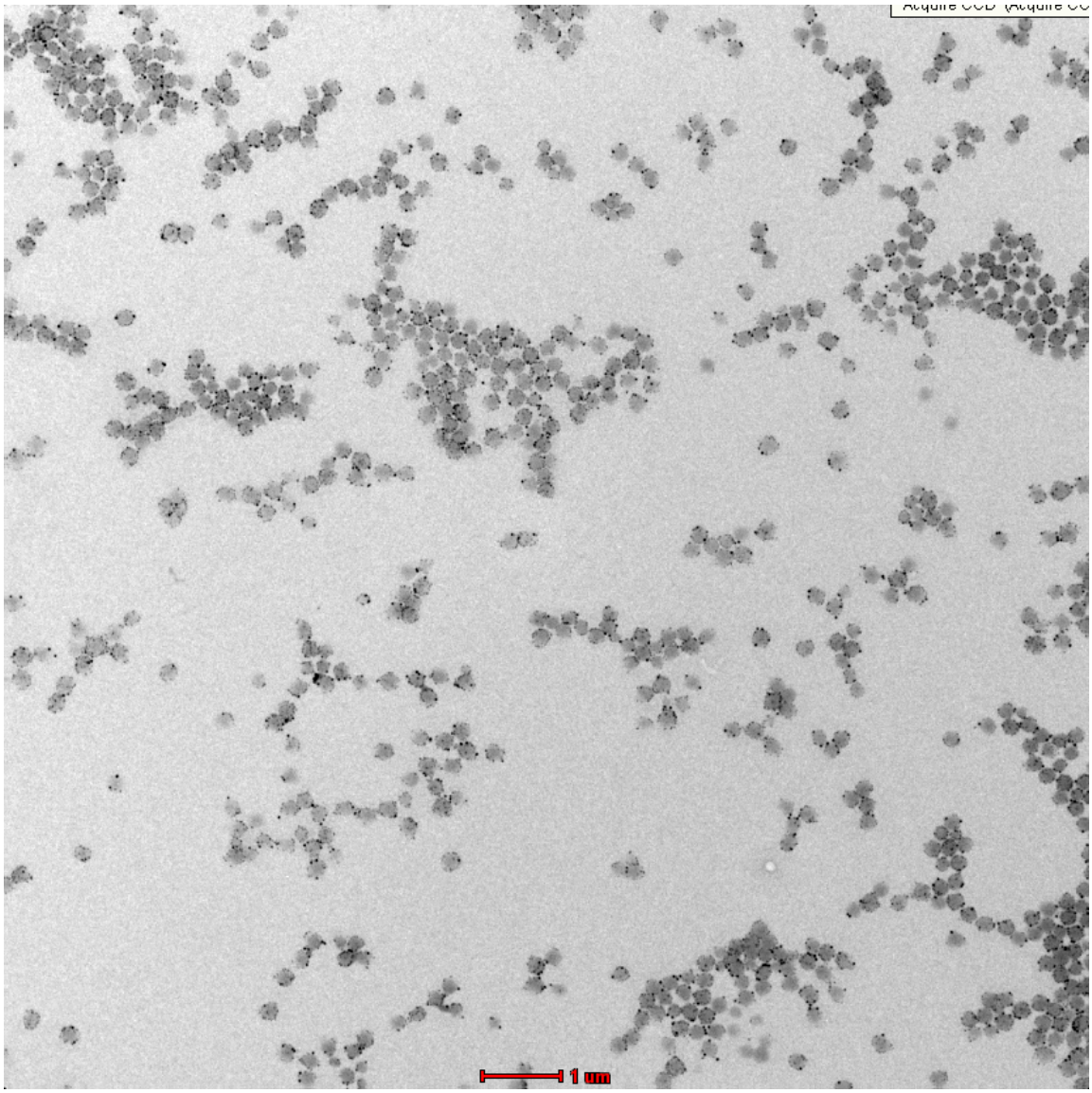

Figure 5.13 TEM micrograph of IPN based gold-polymer composite formed by grafting gold nanorods to polymer nanoparticles.

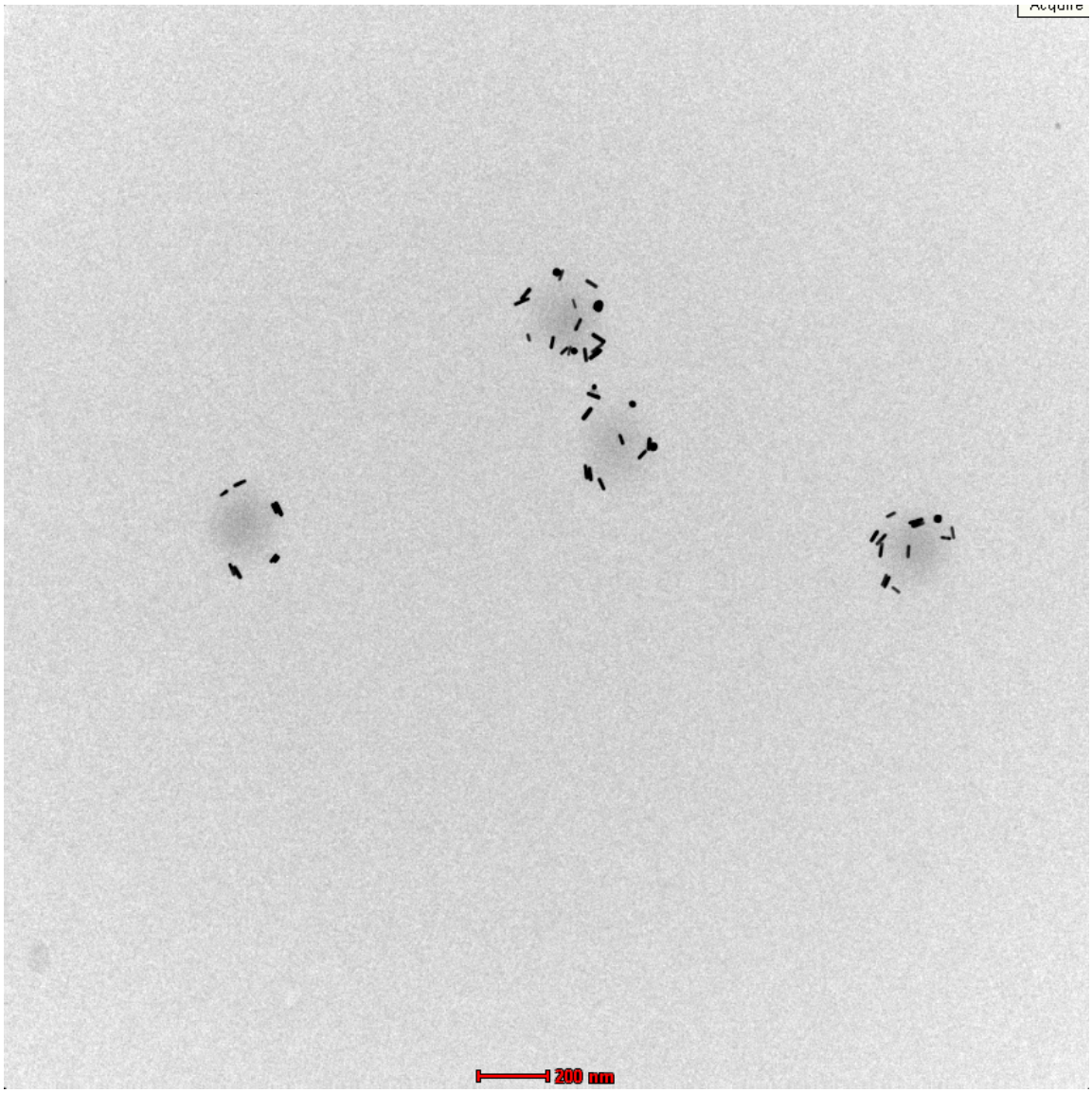

Figure 5.4 TEM image of IPN nanoparticle grafted with gold nanorods for externally-controlled systems.

REFERENCES

1. West, J.L. and Halas, N.J., *Engineered nanomaterials for biophotonics applications: Improving sensing, imaging, and therapeutics.* Annu. Rev. Biomed. Eng., 2003. **5**: p. 285-292.

2. Loo, C., Lin, A., Hirsch, L., Lee, M.H., et al., *Nanoshell-enabled photonics-based imaging and therapy of cancer.* Technol. Cancer Res. T., 2004. **3**(1): p. 33-40.

3. Vorobyova, S.A., Lesnikovich, A.I., and Sobal, N.S., *Preparation of silver nanoparticles by interphase reduction.* Colloid. Surface. A, 1999. **152**(3): p. 375-379.

4. Zhang, J.Z. and Noguez, C., *Plasmonic Optical Properties and Applications of Metal Nanostructures.* Plasmonics, 2008. **3**(4): p. 127-150.

5. Pérez-Juste, J., Pastoriza-Santos, I., Liz-Marzán, L.M., and Mulvaney, P., *Gold nanorods: Synthesis, characterization and applications.* Coordin. Chem. Rev., 2005. **249**(17-18): p. 1870-1901.

6. Grubbs, R.B., *Hybrid metal–polymer composites from functional block copolymers.* J. Polym. Sci. Part A, 2005. **43**(19): p. 4323-4336.

7. Sershen, S.R., Mensing, G.A., Ng, M., Halas, N.J., et al., *Independent optical control of microfluidic valves formed from optomechanically responsive nanocomposite hydrogels.* Adv. Mater., 2005. **17**(11): p. 1366-+.

8. Sershen, S.R., Halas, N.J., and West, J.L. *Pulsatile release of insulin via photothermally modulated drug delivery*. in *[Engineering in Medicine and Biology, 2002. 24th Annual Conference and the Annual Fall Meeting of the Biomedical Engineering Society] EMBS/BMES Conference, 2002. Proceedings of the Second Joint*. 2002.

9. Funston, A.M., Novo, C., Davis, T.J., and Mulvaney, P., *Plasmon Coupling of Gold Nanorods at Short Distances and in Different Geometries.* Nano Lett., 2009. **9**(4): p. 1651-1658.

10. Petrovic, S.C., Zhang, W., and Ciszkowska, M., *Preparation and Characterization of Thermoresponsive Poly(N-isopropylacrylamide-co-acrylic acid) Hydrogels: Studies with Electroactive Probes.* Ana. Chem., 2000. **72**(15): p. 3449-3454.

11. Moharram, M.A., Balloomal, L.S., and El-Gendy, H.M., *Infrared study of the complexation of poly(acrylic acid) with poly(acrylamide).* J. Appl. Polym. Sci., 1996. **59**(6): p. 987-990.

Chapter 6: Loading and Release Characteristics of a Model Therapeutic from Hydrogel Nanoparticles

6.1 Introduction

In order to evaluate the potential use of a nanoparticle delivery system for therapeutic use, laboratory tests can be conducted to measure the effectiveness of the system to entrap and release a compound under relevant conditions. Small scale loading tests can be conducted to measure the amount of a therapeutic or model that can be carried by the system. Prior to testing a therapeutic system in live animal or human subjects, the release characteristics can be measured at the lab bench under conditions to best mimic the physiological environment.

A variety of different polymer nanoparticle systems have been developed to load and release therapeutics. Biodegradable, self-assembled, and hydrogel nanoparticles have been used to quantify loading and release of drugs. The loading of a therapeutic refers to entrapment, encapsulation, attachment, or otherwise incorporation of a compound of interest into the carrier system. When discussing the loading of a molecule of interest in a delivery system there are two common numbers cited to quantify the extent of loading. Encapsulation or entrapment efficiency (EE) which is the fraction of a compound that was successfully loaded in a carrier based on the amount of that compound that was initially used in the loading procedure as shown in the following equation:

$$EE = \frac{Entrapped\ Weight}{Total\ Weight\ of\ Drug}$$

Loading capacity provides a measure of how much of a compound is incorporated into a carrier with respect to the amount of carrier. Typically described as a weight fraction, loading capacity is simply the weight of the compound loaded into the system divided by the total weight of the carrier system itself prior to the loading procedure. Loading capacity is quantified using the following equation:

$$Loading\ Capacity = \frac{Entrapped\ Drug\ Weight}{Total\ Polymer\ Weight}$$

Self-assembled nanoparticles, including liposomes, micelles, and polymersomes, can be formed using various amphiphiles such as natural lipids or block copolymers. Liposomal encapsulation is a versatile method to load therapeutics, because hydrophilic drugs and biomolecules can be loaded in the inner aqueous void, while hydrophobic molecules can be entrapped in the lipid bilayer. Liposomal delivery of chemotherapeutics has been established as an effective method to increase efficacy and decrease toxicity over free drug, evidenced by the success of liposomal doxorubicin, Doxil®, which has been approved for human use in cancer treatment [1].

In addition to the lipid structures, synthetic block copolymers built with one hydrophilic block and one hydrophobic block have been shown to exhibit a variety of self-assembled structures including spherical or cylindrical micelles and vesicles with architectures that resemble liposomes known as polymersomes [2]. Micelles,

nanoparticles with a hydrophobic core and hydrophilic outer layer, self-assembled from amphiphilic block copolymers in aqueous media, are frequently used to entrap hydrophobic drugs during micelle formation. During spontaneous micelle formation in an aqueous environment, hydrophobic drugs such as anticancer agents are localized in and around the hydrophobic core [3-6].

While traditional micelle systems have been used primarily to incorporate hydrophobic drugs, adapted systems have been used to entrap more hydrophilic species such as biomolecules. For example, drug carrier systems called polyion complex (PIC) micelles have been synthesized from PEG block copolymers. The PIC micelles are formed using block copolymers consisting of a hydrophilic block and a polyionic block. In this case, electrostatic interactions between the ionic polymer and an oppositely charged species are a driving force for the formation of the micelles. Poly(ethylene glycol-grafted-chitosan), PEG-g-chitosan, block copolymers were used to entrap diammonium glycyrrhizinate (DG) in micelles assembled in acetate buffer after addition of TPP to induce chitosan aggregation [7].

Polymer vesicles called polymersomes or polymerosomes have been used to entrap a variety of therapeutics and model drugs. [8, 9]. Recently, there has been interest in creating systems that are hybrid particles combining properties of liposomes and synthetic polymer systems for nanodelivery applications. Several of these systems have been used to entrap hydrophobic cancer drugs while incorporating synthetic

polymers such as PEG to add stealth characteristics to the system or include targeting ligands in the system [10, 11].

Biodegradable polymers such as poly(lactic acid-co-glycolic acid) (PLGA) are also of interest for nanoparticle based drug delivery systems. A number of hydrophobic compounds have been loaded into PLGA degradable particles using double emulsion methods. These oil-in-water emulsions have been used to load anti-cancer therapeutics [12-14]. In addition to hydrophobic drugs, encapsulation of water-soluble drugs and biomolecules, including proteins and certain chemotherapeutics, has been achieved with water-in-oil-in-water double emulsion techniques [15-17]. Alternatively a few other techniques have been used to load drugs into PLGA particles including nanoprecipitation, spray drying, and spray freezing into liquid [18-22]. There has also been some work incorporating drugs into biodegradable polyanhydride carriers on the nanoscale during particle formation or using double emulsion techniques such as water-in-oil-in-water [23, 24].

Naturally occurring biodegradable polymers have also been investigated for their loading and release characteristics. For example, chitosan carriers have received considerable attention for delivery of nucleic acids and a number of techniques have been developed to synthesize chitosan nanoparticles including ionic gelation, precipitation, reverse micelle formation, self-assembly, and spray drying [25, 26]. In one study, bovine serum albumin (BSA), was loaded into chitosan nanoparticles prepared by two different methods using tripolyphosphate (TPP) as an ionic crosslinker either during

particle formation or using an incubation method where BSA was adsorbed to the surface of nanoparticles [27]. In another study, chitosan nanoparticles crosslinked with TPP were loaded with methotrexate disodium (MTX) using a post-polymerization incubation method. [28]. Chitosan nanoparticles have also been formulated to deliver anticancer drugs using emulsion methods. For example, a water-in-oil microemulsion method was used to entrap a doxorubicin-dextran conjugate in chitosan nanoparticles having a hydrodynamic diameter of 100 nm [29].

The anionic biopolymer alginate has also been explored for its drug loading and release character. Most often calcium chloride is added to a solution of alginate to induce ionic crosslinking, resulting in micro- and nanoparticle polymer networks. In one case, alginate gelation with calcium ions followed by coating with chitosan produced nanoparticles intended for oral insulin delivery applicationsIsoniazid, rifampicin, and pyrazinamide were encapsulated in alginate particles using a cation gelation method in an effort to design aerosolized nanoparticles for treatment of tuberculosis. Calcium chloride was added to sodium alginate solution containing varying amounts of the three drugs to induce the gelation and encapsulation of the drug [30].

While most biodegradable or self-assembled nanoparticle systems are formed from previously synthesized polymers, hydrogel nanoparticles are most commonly synthesized using heterogeneous polymerization techniques. Because the hydrogel nanoparticles are formed during polymerization, incorporating a therapeutic at this stage requires exposing the drug to polymerization conditions that could potentially

damage or modify the drug. However, the porous characteristics of nanogel matrices allows for drug loading following polymerization by partitioning methods, which eliminates the need to subject the drug to harsh polymerization conditions. In most situations, the drug is loaded into the nanogel by incubating the nanoparticles with the drug in aqueous conditions such that the particles are in their most swollen state. After a period of time to allow the therapeutic to diffuse into the polymer matrix, a condition (most commonly pH or temperature) is altered, leading to a particle size transition to a more collapsed state with a smaller mesh size, physically entrapping the therapeutic in the polymer matrix.

The hydrophilic nature of hydrogel systems makes them an ideal candidate for the loading and delivery of water soluble therapeutics, of particular interest biomacromolecules such as proteins or nucleic acids. Several nanogel systems have been investigated for the delivery of insulin to the small intestine. In addition to their ability to entrap the water soluble insulin, some of these systems have advantageous pH-sensitive properties allowing them to protect insulin in the acidic environment of the stomach and release it in the more neutral pH of the small intestine [31, 32]. Polybasic nanoparticles are cationic pH responsive hydrogels. Insulin as a model drug was added to a solution of the nanogels and the pH was adjusted to 6.5 to swell the nanoparticles. After a loading period the pH was raised quickly to 7.4 to collapse the particles and entrap the loaded protein. Encapsulation efficiencies were measured up to 92% for

insulin in PDGP particles with low crosslinking densities when equal weights of particles and protein were added to the loading solution [33].

While most hydrogel nanodelivery systems have been used to entrap hydrophilic molecules, recent work on modified hydrogels has demonstrated the potential to load hydrophobic drugs as well. In order to do so, the hydrophobicity of the nanogels has been increased through the incorporation of amphiphiles into the hydrogel matrix. An acrylated PEG-PPG-PEG triblock copolymer with both hydrophobic and hydrophilic groups was used to synthesize crosslinked nanoparticles via an inverse microemulsion using a PEG crosslinker. These nanogels were then loaded with doxorubicin [34]. Temperature responsive nanoparticles have also been used to entrap hydrophobic drugs. PNIPAAm and P(NIPAAm-co-AA) nanoparticles were loaded with 5-fluorouracil and release was shown to be a function of pH and temperature [35].

The nanogel systems that have been developed for this thesis were analyzed to investigate their loading and release characteristics. The systems are of interest for their ability to load and release anticancer therapeutics. Because of the intended application for breast cancer treatment chemotherapeutics that are highly used in breast cancer treatment, but have significant adverse health effects are of interest for loading into these externally controlled release systems. Doxorubicin was identified as a specific compound of interest because of its frequent treatment usage but significant number of adverse effects such as cardiotoxixity, nausea, vomiting, hair loss, and immunosuppression [36].

Loading of a model therapeutic, fluorescein, was quantified. Fluorescein was chosen as the molecule of interest because it is similar in size, structure, and hydrophobicity to the chemotherapeutic doxorubicin. Fluorescein is much less expensive to work with, is easily quantified using fluorescence spectroscopy and is safer to work with than chemotherapeutics such as doxorubicin. The model therapeutic was loaded into nanoparticles using equilibrium partitioning methods following polymerization. Loading capacity and entrapment efficiency were quantified for nanoparticles synthesized using several different crosslinking ratios. Release from the nanoparticles was quantified in phosphate buffered saline (PBS) buffer to simulate conditions in the bloodstream.

6.2 Materials and Methods

6.2.1 Hydrogel Nanoparticle Synthesis

Acrylic acid (AA, inhibited with 200 ppm hydroquinone monomethyl ether), N-Isopropylacrylamide (NIPAAm), and sodium dodecyl sulfate (SDS) were obtained from Sigma Aldrich (Milwaukee, WI), acrylamide (AAm) and ammonium persulfate (APS) were obtained from Fisher Scientific (Hampton, NH). Acrylic acid was purified using vacuum distillation. All other materials were used as received.

In order to quantify loading and release of the carrier systems nanogels were first synthesized using an aqueous dispersion polymerization. Crosslinked 90/10 P(NIPAAm-co-AA) nanoparticles were used because of the shown efficacy in forming

gold-polymer composites as described in Chapter 3. Crosslinking molar feed ratios were also varied from 1-10 % and polymer nanoparticles were synthesized containing feed ratios of 1, 5, and 10 mol %.

To synthesize LCST polymers monomer, crosslinker, N,N'-Methylene bisacrylamide, and a stabilizer, SDS, were added to a 100 ml aqueous phase in a 250 ml round bottomed flask at a total monomer concentration of 5.5 g/L and a typical stabilizer concentration of 0.3 g/L. The monomers and stabilizer were first dissolved in the aqueous medium. Next, the aqueous reaction solution was purged with nitrogen to remove oxygen from the reaction flask. A 70 °C oil bath was prepared and the purged reaction flask was submerged in the oil bath. An aqueous solution of the free radical initiator, APS, was injected into the reaction flask to initiate reaction. Reaction was allowed to proceed for at least two hours. After completion, the reaction flask is opened to the air and removed from the heat source.

The resulting nanoparticle suspension was dialyzed against DI water for 10 days using a 12-14,000 MWCO dialysis tubing. Dialysis water was changed twice daily. Particle solutions were then frozen in a -80° C freezer and lyophilized until dry. Dry particle solutions were resuspended in distilled and deionized water (ddH2O) for use in model compound loading studies or in the appropriate medium for other analysis and characterization.

Several techniques were used to confirm synthesis of the polymer nanoparticles before using them for loading and release studies. Dynamic light scattering (DLS) was

used to measure the overall size distributions of the hydrogel nanoparticles solution and to quantify polydispersity. Transmission electron microscopy (TEM) was used to examine the particle size distribution and to confirm the average size and spherical nature of the nanoparticles.

6.2.2 Loading of Fluorescein into Hydrogel Nanoparticles

A model therapeutic was selected in order to measure the potential ability of the LCST nanocarriers to load an anticancer therapeutic such as doxorubicin. Fluorescein was chosen for use as a model therapeutic because it is similar in size, structure, and hydrophobicity to the chemotherapeutic doxorubicin. Fluorescein was purchased from Sigma-Aldrich (Milwaukee, WI) and used as received. Using fluorescein as a model therapeutic has several advantages over using doxorubicin in the loading studies. Doxorubicin and other anticancer agents are expensive to work with in comparison to fluorescein. Fluorescein is also easily quantified using fluorescence spectroscopy and is safer to work with than chemotherapeutics such as doxorubicin.

The model compound was loaded into the polymer nanoparticles using equilibrium partitioning methods with considerations made for the hydrophobic model and the temperature responsive polymer nanoparticles. Fluorescein was loaded into swollen P(NIPAAm-co-AA) nanoparticles at several crosslinking densities in a water/acetone mixture with loading proceeding with the vessel open to air over a period of time where the acetone was allowed to evaporate.

In each study, a polymer nanoparticle suspension was first prepared by adding 100 mg of dried P(NIPAAm-co-AA) particles. The particles were added to each of three separate 40 ml centrifuge tubes containing 10 ml of ddH_2O. Separately, 15 mg of fluorescein was dissolved into three different 5 ml aliquots of acetone. The three fluorescein solutions were added to the centrifuge tubes containing the aqueous nanoparticle dispersions. The drug-polymer mixtures were stirred in the dark uncovered for 36 h as the acetone was allowed to evaporate.

Following the 36 h loading period, samples were centrifuged at 2000 rcf and the supernatant containing the loaded nanoparticles was removed from the fluorescein pellet. The pelleted fluorescein samples were dried in a vacuum oven at 40 °C and then resuspended in enough PBS to solubilize the fluorescein for quantification. A 350 µl sample was collected from the supernatant solution and polymer nanoparticles were filtered out to quantify the amount of fluorescein remaining in solution. Anotop anodisc aluminum oxide based syringe filters with a 100 nm pore size (Whatman, Piscataway, NJ) were used to filter out the polymer nanoparticles.

Fluorescence spectroscopy was used at an excitation wavelength of 485 nm and emission of 528 nm to quantify the samples (Bio-Tek, Synergy HT, Winooski, VT). 100 µl samples in triplicate were used to measure the amount of fluorescein in the resuspended dry particles and the free solution. A fluorescein standard curve was prepared in PBS and samples were read in a 96 well plate for fluorescence. Based on

the total amount of fluorescein in the pellet and in the free supernatant solution the amount of fluorescein loaded into polymer nanoparticles was calculated.

Loaded P(NIPAAm-co-AA) nanoparticles were dialyzed against ddH_2O for 24 hours to remove free fluorescein in the solution. The particle solution was then removed from the dialysis bag, placed in a 40 ml centrifuge tube and then frozen in liquid nitrogen. Nanoparticles were stored in a -80 °C freezer and then lyophilized just prior to use in fluorescein release studies.

6.2.3 Release of Fluorescein from Hydrogel Nanoparticles

After loading of polymer nanoparticles with the model therapeutic fluorescein, release was characterized over a period of 48 hours. The studies were performed at physiological conditions in PBS, 37 °C and 7.4 pH. All experiments were done using freeze-dried P(NIPAAm-co-AA) nanoparticles of either 1, 5, 10 mol % crosslinking that had previously been loaded with the model therapeutic. Particles were taken directly from the lyophilizer, weighed out as necessary, and taken directly to the release medium for the study to ensure maximum dryness. All release studies were performed in triplicate using three separate release vessels.

After removing loaded nanoparticles from the lyophilizer three 30 mg dry samples were prepared from the 100 mg of loaded nanoparticles that had been prepared during the corresponding loading study. Three release vessels were prepared with 400 ml of PBS solution at a pH of 7.4 in each. Each release vessel was brought to

temperature equilibrium in a water bath at 37 °C while continuously stirred. Next, 30 mg of the dried, fluorescein loaded nanoparticles was added to each of the release volumes. Samples of 350 µl were withdrawn from the solution at set time points over a 48 h time period and replaced with fresh buffer. After withdrawal of each sample it was immediately filtered using an Anotop syringe filter made of an aluminum oxide membrane with a pore size of 100 nm. Filtration collected the polymer particles while allowing free fluorescein to pass through the filter.

Fluorescence spectroscopy was used at an excitation wavelength of 485 nm and emission of 528 nm to quantify the samples. Volumes of 100 µl in triplicate were used to measure the amount of free fluorescein in the release media. A fluorescein standard curve was prepared in PBS and samples were read in a 96 well plate for fluorescence. The total amount of release of fluorescein into free solution was calculated based on the measured fluorescein concentration.

6.3 Results and Discussion

6.3.1 Hydrogel Nanoparticle Synthesis

Dispersion polymerization was used to successfully synthesize P(NIPAAm-co-AA) nanoparticles with molar extents of crosslinking of 1%, 5%, 10%. A TEM micrograph of P(NIPAAm-co-AA) particles is shown in Figure 6.1.

Crosslinking ratio is an important parameter when considering a LCST hydrogel delivery system. The crosslinking ratio affects the mesh size of the polymer which must

be small enough to entrap and protect the therapeutic at 37 °C, but such that there is release when the polymer shrinks and squeezes out the drug. Crosslinking also affects the size of the nanoparticle and swelling behavior which is discussed in detail in section 6.3.3. More highly crosslinked polymers have more tightly bound networks and a smaller relative mesh size. Typically lightly crosslinked polymers are necessary to entrap larger therapeutics such as proteins while highly crosslinked materials more effectively entrap small molecular weight drugs, with medium sized drugs such as small proteins or peptides entrapped best at intermediate crosslinking ratios.

In this case polymer nanoparticles were synthesized at several crosslinking ratios including the relatively high 5 and 10 % molar crosslinking in an effort to most effectively entrap the small molecular weight fluorescein, which is a good model for the anticancer drug doxorubicin. Polymers that are more highly crosslinked than 10 % show minimum amounts of temperature-sensitive swelling behavior as shown in Chapter 4 that would render them ineffective in temperature triggered delivery systems.

The polymer nanoparticles that were synthesized include a 10 % molar ratio of acrylic acid for two reasons. First, the addition of the more hydrophilic monomer to the polymer shifts the transition swelling region into a relevant temperature range centered at approximately 40 °C. The presence of the acrylic acid also allows for the grafting of gold nanorods to the surface of the particles as described in Chapter 5. The crosslinking ratios that were studied were high enough to entrap a therapeutic, but also low enough such that the temperature responsive swelling is significant. In short, these systems

were successfully synthesized to best model systems for analysis as effective externally-controlled delivery systems.

6.3.2 Loading of Fluorescein into Hydrogel Nanoparticles

Many hydrogel systems have been used to load hydrophilic molecules such as proteins, while results for loading small molecular weight hydrophobic drugs in hydrogel carriers are far less prevalent. The PNIPAAm based systems have shown potential as nanogel systems for loading of hydrophobic drugs because the structure of the polymer includes hydrophobic domains due to the isopropyl groups present in the pendant groups of P(NIPAAm-co-AA).

The trend of entrapment efficiency as a function of nanoparticle crosslinking ratio is shown in Figure 6.2. Loading capacity in relation to the crosslinking ratio of the nanoparticle carriers is shown in Figure 6.3. Based on the data it is clear that the ability of the polymer carriers to entrap fluorescein increases at higher crosslinking ratios as expected due to the small molecular weight and size of the model therapeutic compound. The highly crosslinked (10 mol %) polymer was able to entrap the maximum amount of fluorescein with an overall entrapment efficiency of 80.0% and a loading capacity of 12.0%. Table 6.1 summarizes the overall loading characteristics for all of the P(NIPAAm-co-AA) hydrogel nanoparticle systems including their respective entrapment efficiencies and loading capacities.

6.3.3 Release of Fluorescein from Hydrogel Nanoparticles

Release of fluorescein from the polymer nanoparticles was characterized over a period of 48 hours. The studies were performed in PBS at physiological pH and temperature to mimic conditions present in the body. The purpose of these studies was to show that release at physiological conditions would occur over a long period (on the order of hours or days) so that an externally controlled release could be triggered in the first hour or two of administration.

The release of fluorescein from the materials was successfully measured using fluorescence spectroscopy on a UV-VIS-NIR plate spectrophotometer. Release studies performed in triplicate for each polymer show sustained release of the drug from the nanoparticles. Release measurements shown as a fraction of the total amount of fluorescein loaded into the polymers are shown in Figure 6.4 for each of the three differently crosslinked polymers.

All of the polymer systems showed that total release occurred over a time period in excess of 12 h which makes them potential candidates for the desired types of drug release systems. The more highly crosslinked systems protected the drug inside the particle for longer periods of time. The entire amount of fluorescein was released from the 1 % crosslinked materials within 24 hours, while the 10 % crosslinked polymer showed that full release of the entrapped fluorescein was not achieved until over 48 hours had elapsed. The 5 % crosslinked system released all of the entrapped model therapeutic over a 24 hour period.

Overall 10 % crosslinked 90/10 P(NIPAAm-co-AA) demonstrated the best ability to entrap a high amount of fluorescein and protect it from release for the longest period of time. Additionally, these particles still demonstrate an overall temperature-sensitive volume swelling ratio over 5. Because of the combination of an ability to load a high level of drug, protect it for significant amount of time, and exhibit temperature-responsive swelling this material is a strong candidate for development of a nanoscale externally-controlled release system.

6.4 Conclusions

The capability of temperature-responsive nanoparticle systems to entrap and release a compound of interest was investigated. LCST nanocarriers were first synthesized using aqueous dispersion polymerization methods. The hydrogel nanoparticles were synthesized at varying crosslinking ratios including 1, 5, and 10 mol %. A model therapeutic, fluorescein, was selected to mimic anticancer therapeutics, specifically doxorubicin. Fluorescein has a similar molecular weight, structural character, and hydrophobicity to doxorubicin.

Experiments were performed in the laboratory to measure the entrapment efficiency and loading capacity of the polymer nanocarriers. These parameters that quantify loading increased in polymer systems as the amount of crosslinker present in the polymer system increased. Because fluorescein is a small molecule, maximum

loading was achieved in very highly crosslinked systems where the polymer hydrogel network is tightly structured and mesh size is at a minimum.

In order to mimic physiological conditions, release studies were performed in PBS buffer at 37 °C. Samples were collected to measure release of fluorescein into the PBS medium using fluorescence spectroscopy after filtration of particles out of the sample. Results displayed a release curve that occurred over a period of hours or days. The results demonstrated that at constant temperature release from the systems is slow enough that release could be triggered in the nanocarriers using laser light over shorter time periods before the entire payload naturally diffused out of the system. The systems show potential for use as externally controlled polymer nanoparticle therapeutic carriers.

Polymer nanoparticles formed using 10 % crosslinked 90/10 P(NIPAAm-co-AA) showed the highest potential for carrying and releasing a hydrophobic anticancer drug for the described externally triggered application. These materials entrapped the highest amount of the model therapeutic and best protected the compound from release at constant physiological temperature and pH. Because of the positive results from the loading and release studies along with their ability to exhibit temperature-responsive swelling behavior this material is a strong candidate for development of nanoscale externally-controlled release systems.

Percent Crosslinker	Encapsulation Efficiency	Loading Capacity
10%	80.0 ± 5.77	12.0 ± 0.86
5%	70.4 ± 4.85	10.6 ± 0.73
1%	52.2 ± 6.22	7.83 ± 0.93

Table 6.1 Encapsulation efficiencies and loading capacities for fluorescein loaded into P(NIPAAm-co-AA) polymer nanoparticles of varying extents of crosslinking.

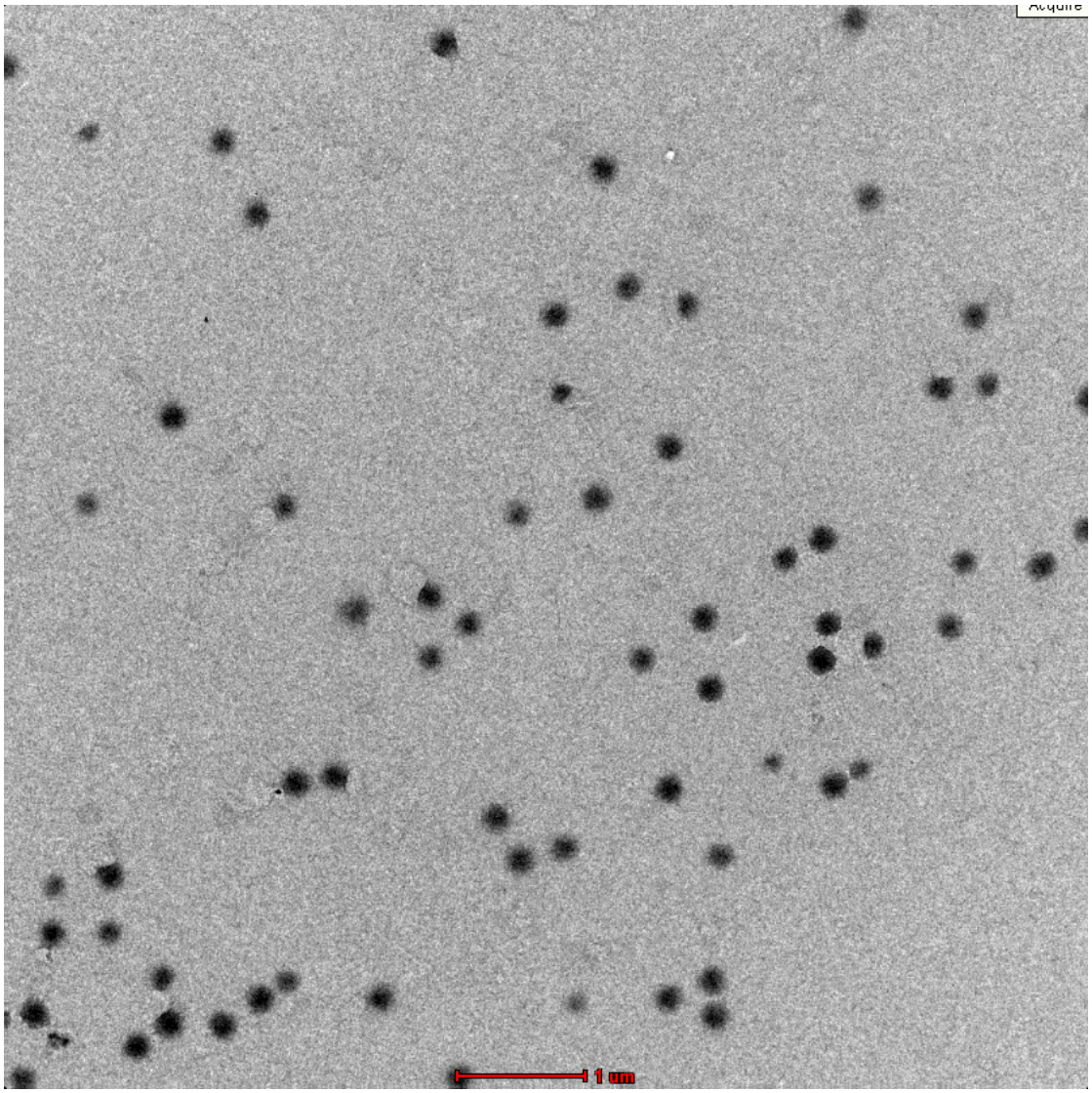

Figure 6.1 TEM micrograph of P(NIPAAm-co-AA) nanoparticles for use in fluorescein loading studies.

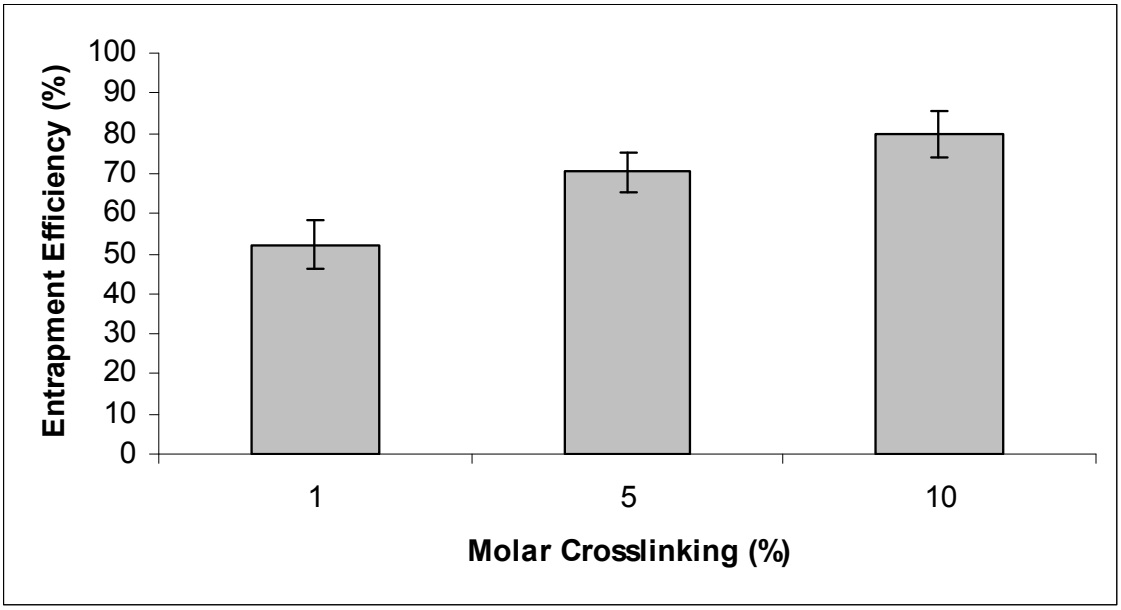

Figure 6.2 Entrapment efficiency of fluorescein loaded in P(NIPAAm-co-AA) hydrogel nanoparticles with varied extents of crosslinking.

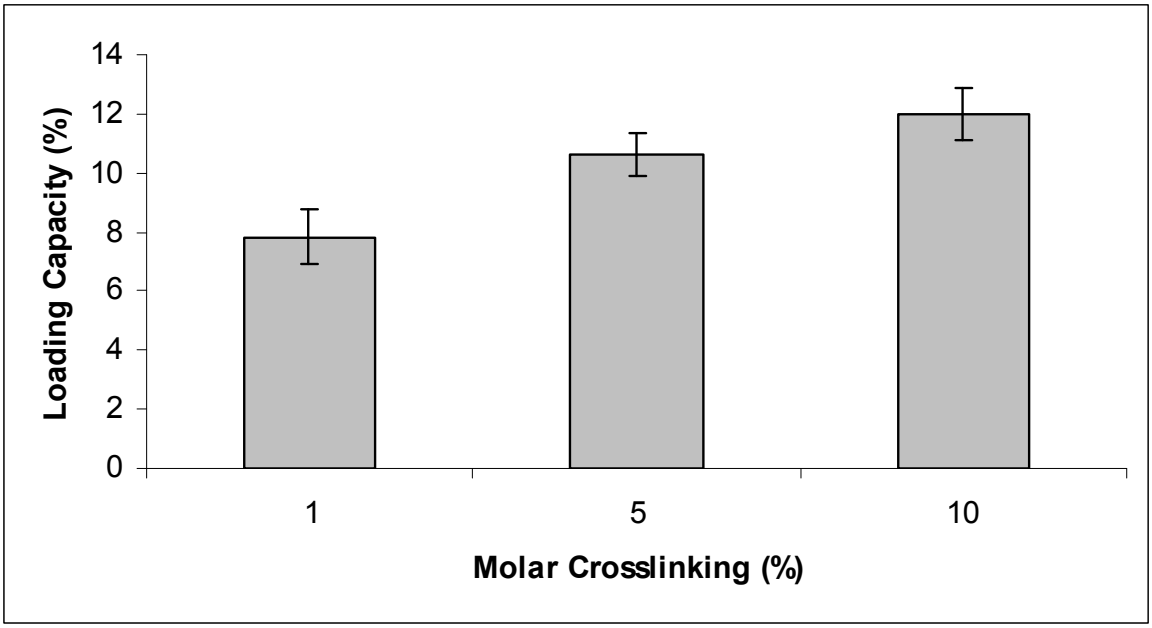

Figure 6.3 Loading Capacity of fluorescein in P(NIPAAm-co-AA) hydrogel nanoparticles with varied extents of crosslinking.

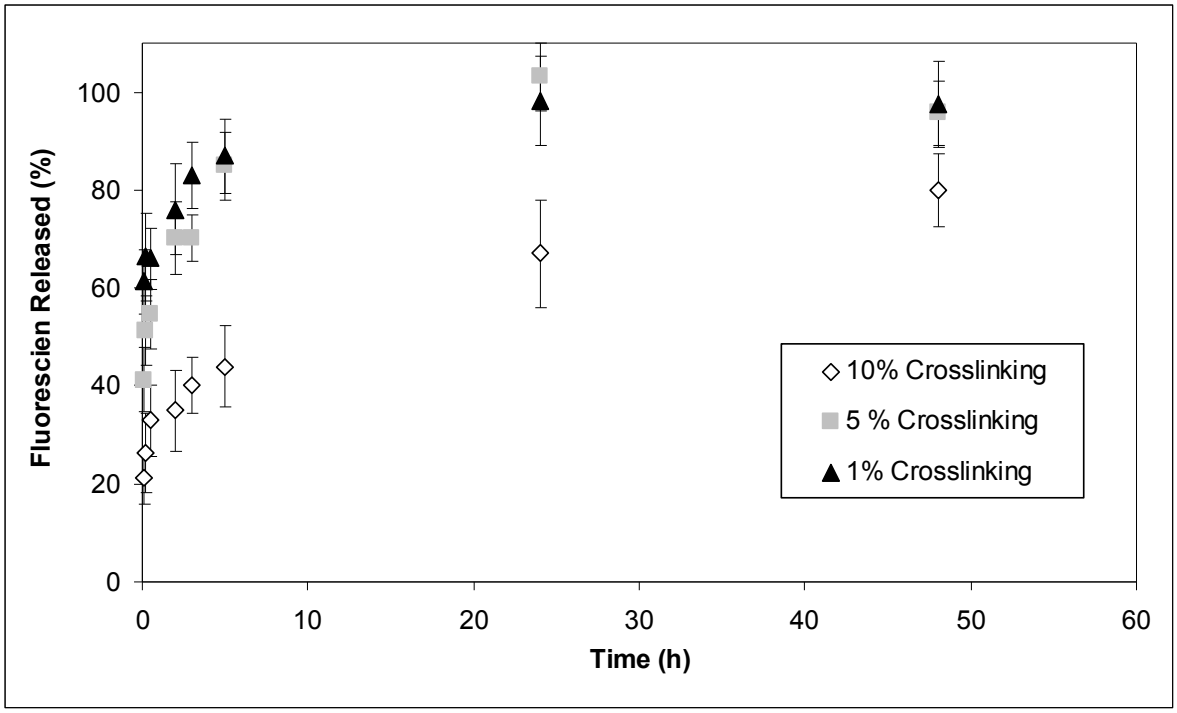

Figure 6.4 Measurement of release of a model therapeutic, fluorescein, from nanogels at 37 °C over a 48 h period. Release is quantified as a percentage of total amount of fluorescein loaded in the particles.

REFERENCES

1. Malam, Y., Loizidou, M., and Seifalian, A.M., *Liposomes and nanoparticles: nanosized vehicles for drug delivery in cancer.* Trends in Pharmacol. Sci., 2009. **30**(11): p. 592-599.

2. Discher, D.E., Ortiz, V., Srinivas, G., Klein, M.L., et al., *Emerging applications of polymersomes in delivery: From molecular dynamics to shrinkage of tumors.* Prog. Polym. Sci., 2007. **32**(8-9): p. 838-857.

3. Torchilin, V.P., *Micellar Nanocarriers: Pharmaceutical Perspectives.* Pharm. Res., 2007. **24**(1): p. 1-16.

4. Kabanov, A.V., Batrakova, E.V., and Alakhov, V.Y., *Pluronic® block copolymers as novel polymer therapeutics for drug and gene delivery.* J. Control. Release, 2002. **82**(2-3): p. 189-212.

5. Hamaguchi, T., Matsumura, Y., Suzuki, M., Shimizu, K., et al., *NK105, a paclitaxel-incorporating micellar nanoparticle formulation, can extend in vivo antitumour activity and reduce the neurotoxicity of paclitaxel.* Brit. J. Cancer, 2005. **92**(7): p. 1240-1246.

6. Kataoka, K., Harada, A., and Nagasaki, Y., *Block copolymer micelles for drug delivery: design, characterization and biological significance.* Adv. Drug Deliver. Rev., 2001. **47**(1): p. 113-131.

7. Yang, K.W., Li, X.R., Yang, Z.L., Li, P.Z., et al., *Novel polyion complex micelles for liver-targeted delivery of diammonium glycyrrhizinate: in vitro and in vivo characterization.* J. Biomed. Mater. Res. Part A, 2009. **88**(1): p. 140-148.

8. Rastogi, R., Anand, S., and Koul, V., *Flexible polymerosomes-An alternative vehicle for topical delivery.* Colloid Surf. B, 2009. **72**(1): p. 161-166.

9. Xu, H., Meng, F., and Zhong, Z., *Reversibly crosslinked temperature-responsive nano-sized polymersomes: synthesis and triggered drug release.* J. Mater. Chem., 2009. **19**(24): p. 4183-4190.

10. Wang, M., Lowik, D.W., Miller, A.D., and Thanou, M., *Targeting the Urokinase Plasminogen Activator Receptor with Synthetic Self-Assembly Nanoparticles.* Bioconjugate Chem., 2009. **20**(1): p. 32-40.

11. Chan, J.M., Zhang, L., Yuet, K.P., Liao, G., et al., *PLGA-lecithin-PEG core-shell nanoparticles for controlled drug delivery.* Biomaterials, 2009. **30**(8): p. 1627-1634.

12. Govender, T., Stolnik, S., Garnett, M.C., Illum, L., and Davis, S.S., *PLGA nanoparticles prepared by nanoprecipitation: drug loading and release studies of a water soluble drug.* J. Control. Release, 1999. **57**(2): p. 171-185.

13. Mu, L. and Feng, S.S., *A novel controlled release formulation for the anticancer drug paclitaxel (Taxol®): PLGA nanoparticles containing vitamin E TPGS.* J. Control. Release, 2003. **86**(1): p. 33-48.

14. Fonseca, C., Simões, S., and Gaspar, R., *Paclitaxel-loaded PLGA nanoparticles: preparation, physicochemical characterization and in vitro anti-tumoral activity.* J. Control. Release, 2002. **83**(2): p. 273-286.

15. Bilati, U., Allemann, E., and Doelker, E., *Poly(D,L-lactide-co-glycolide) protein-loaded nanoparticles prepared by the double emulsion method-processing and formulation issues for enhanced entrapment efficiency.* J. Microencapsul., 2005. **22**(2): p. 205-214.

16. Li, Y.P., Pei, Y.Y., Zhang, X.Y., Gu, Z.H., et al., *PEGylated PLGA nanoparticles as protein carriers: synthesis, preparation and biodistribution in rats.* J. Control. Release, 2001. **71**(2): p. 203-211.

17. Avgoustakis, K., Beletsi, A., Panagi, Z., Klepetsanis, P., et al., *PLGA-mPEG nanoparticles of cisplatin: in vitro nanoparticle degradation, in vitro drug release and in vivo drug residence in blood properties.* J. Control. Release, 2002. **79**(1-3): p. 123-135.

18. Astete, C.E. and Sabliov, C.M., *Synthesis and characterization of PLGA nanoparticles.* J. Biomater. Sci.-Polym. Ed., 2006. **17**(3): p. 247-289.

19. Raffin Pohlmann, A., Weiss, V., Mertins, O., Pesce da Silveira, N., and Stanisçuaski Guterres, S., *Spray-dried indomethacin-loaded polyester nanocapsules and nanospheres: development, stability evaluation and nanostructure models.* Eur. J. of Pharm. Sci., 2002. **16**(4-5): p. 305-312.

20. Rogers, T.L., Hu, J., Yu, Z., Johnston, K.P., and Williams, R.O., *A novel particle engineering technology: spray-freezing into liquid.* Int. J. of Pharm., 2002. **242**(1-2): p. 93-100.

21. Hu, J., Johnston, K.P., and Williams, R.O., *Spray freezing into liquid (SFL) particle engineering technology to enhance dissolution of poorly water soluble drugs: organic solvent versus organic/aqueous co-solvent systems.* Eur. J. Pharm. Sci., 2003. **20**(3): p. 295-303.

22. Rogers, T.L., Overhoff, K.A., Shah, P., Santiago, P., et al., *Micronized powders of a poorly water soluble drug produced by a spray-freezing into liquid-emulsion process.* Euro. J. Pharm. and Biopharm., 2003. **55**(2): p. 161-172.

23. Determan, A.S., Graham, J.R., Pfeiffer, K.A., and Narasimhan, B., *The role of microsphere fabrication methods on the stability and release kinetics of ovalbumin encapsulated in polyanhydride microspheres.* J. Microencapsul., 2006. **23**(8): p. 832-843.

24. Agüeros, M., Ruiz-Gatón, L., Vauthier, C., Bouchemal, K., et al., *Combined hydroxypropyl-[beta]-cyclodextrin and poly(anhydride) nanoparticles improve the oral permeability of paclitaxel.* Eur. J. Pharm. Sci., 2009. **38**(4): p. 405-413.

25. Agnihotri, S.A., Mallikarjuna, N.N., and Aminabhavi, T.M., *Recent advances on chitosan-based micro- and nanoparticles in drug delivery.* J. Control. Release, 2004. **100**(1): p. 5-28.

26. Berger, J., Reist, M., Mayer, J.M., Felt, O., et al., *Structure and interactions in covalently and ionically crosslinked chitosan hydrogels for biomedical applications.* Euro. J. Pharm. Biopharm., 2004. **57**(1): p. 19-34.

27. Gan, Q. and Wang, T., *Chitosan nanoparticle as protein delivery carrier--Systematic examination of fabrication conditions for efficient loading and release.* Colloids Surface. B, 2007. **59**(1): p. 24-34.

28. Zhang, H., Mardyani, S., Chan, W.C., and Kumacheva, E., *Design of biocompatible chitosan microgels for targeted pH-mediated intracellular release of cancer therapeutics.* Biomacromolecules, 2006. **7**(5): p. 1568-1572.

29. Mitra, S., Gaur, U., Ghosh, P.C., and Maitra, A.N., *Tumour targeted delivery of encapsulated dextran-doxorubicin conjugate using chitosan nanoparticles as carrier.* J. Control. Release, 2001. **74**(1-3): p. 317-323.

30. Zahoor, A., Sharma, S., and Khuller, G.K., *Inhalable alginate nanoparticles as antitubercular drug carriers against experimental tuberculosis.* Int. J. of Antimicrob. Ag., 2005. **26**(4): p. 298-303.

31. Yamagata, T., Morishita, M., Kavimandan, N.J., Nakamura, K., et al., *Characterization of insulin protection properties of complexation hydrogels in gastric and intestinal enzyme fluids.* J. Control. Release, 2006. **112**(3): p. 343-349.

32. Morishita, M., Goto, T., Nakamura, K., Lowman, A.M., et al., *Novel oral insulin delivery systems based on complexation polymer hydrogels: Single and multiple administration studies in type 1 and 2 diabetic rats.* J. Control. Release, 2006. **110**(3): p. 587-594.

33. Fisher, O.Z. and Peppas, N.A., *Polybasic Nanomatrices Prepared by UV-Initiated Photopolymerization.* Macromolecules, 2009. **42**(9): p. 3391-3398.

34. Missirlis, D., Kawamura, R., Tirelli, N., and Hubbell, J.A., *Doxorubicin encapsulation and diffusional release from stable, polymeric, hydrogel nanoparticles.* Eur. J. Pharm. Sci., 2006. **29**(2): p. 120-129.

35. Chen, H., Gu, Y., Hu, Y., and Qian, Z., *Characterization of pH- and Temperature-sensitive Hydrogel Nanoparticles for Controlled Drug Release.* PDA J. Pharm. Sci. Tech., 2007. **61**(4): p. 303-313.

36. Eifel, P., Axelson, J.A., Costa, J., Crowley, J., et al., *National Institutes of Health Consensus Development Conference statement: Adjuvant therapy for breast cancer, November 1-3, 2000.* J. Natl. Cancer I., 2001. **93**(13): p. 979-989.

Chapter 7: Characterization of Externally Triggered Systems, Light Responsive Behavior, Cytocompatibility, and Medical Imaging

7.1 Introduction

Light in the near-infrared region (NIR) is of particular interest for use in various in vivo applications because it can penetrate through tissue. The region of light from approximately 650-900 nm has a maximum penetration depth because components of tissue that absorb in the visible-IR range such as water and hemoglobin have minimum absorptions at these wavelengths. NIR light has been shown to penetrate at least 10 cm through breast tissue and about 4 cm through muscle tissue using an FDA Class 1, microwatt laser and while light has been shown to travel up to 7 cm through muscle using a higher Class 3 laser source [1-2]. Because of these properties the use of NIR light has been investigated for use in a number of biomedical applications.

Externally-triggered systems such as those described in this thesis have been developed that use light in the NIR region as a trigger for drug release or other functions. Past systems have been developed to control the release of a therapeteutic using light. In one case, gold nanoshells have been incorporated into poly(N-isoproplyacrylamide-co-acrylamide), P(NIPAAm-co-AAm), films or disks. Upon exposure to certain wavelengths of light, gold nanoshells heat the polymer and trigger a negative swelling transition. This behavior has been used to externally control the opening and

closing of a microvalve and to trigger pulsatile release of insulin from a polymer loaded film [3, 4].

A number of medical imaging techniques have also been developed to take advantage of the penetration depths of NIR light. Reflectance imaging, multi-spectral imaging and fluorescence-mediated molecular tomography (FMT) have been used to image tissues using NIR emitting fluorochromes [5]. Several types of cyanine dyes such as indocyanine green have been used as contrast agent for fluorescent imaging techniques because they have excitation and emission maxima in the NIR range [6]. These molecules can be coupled to targeting ligands to image tissues of interest.

Gold nanorods are a versatile contast agent that have been used in a number of medical imaging techniques and have certain advantages over other contrast agents used in NIR based imaging modalities. Gold nanorods have much larger cross-sections of absorption than molecules such as dyes and fluorophores, and the occurrence of optical fatigue is much lower in nanorods than other contrast agents. Gold nanorods have been investigated for use in two-photon luminescence, optical coherence tomography, photacoustic imaging and darkfield microscopy.

In photoacoustic imaging contrast agent that absorbs nanopulsed light undergoes thermoelastic expansion in response to the pulsed laser light. A temperature rise associated with the excitation from the nanopulsed light leads to thermal expansion. This pulsed expansion produces ultrasonic waves that are detected by the transducer. The detected pattern can be used to reconstruct an image of the area of

interest. A number of materials have been used as contrast agents for photoacoustic imaging.

Single-walled carbon nanotubes have been used as a contrast agent to image tumors [7]. The targeted carbon nanotubes were administered intravenously to mice with tumors and a photoacoustic signal was observed at the tumor that was 8 times stronger than the signal from nontargeted carbon nanotubes.

Gold nanoparticles, nanoshells, nanocages, and nanorods have all been used as contrast agents to create a photoacoustic signal when irradiated with short pulses of light [8-12]. Silver nanosystems have also been used as a contrast agent for photoacoustic imaging [13]. In another system gold coated ferromagnetic cobalt nanoparticles were shown to be an effective contrast agent [14].

In vitro tests have been performed to evaluate the cytocompatibility of the polymer nanoparticle and composite nanoparticle systems. These studies were performed using NIH/3T3 mouse fibroblasts as a cell model to measure the cytocompatibility of the nanoparticle systems with normal cell tissue. Cellular proliferation in the presence of various nanoparticle was quantified using a standard MTS assay which measures dehydrogenase enzyme activity of metabolically active cells.

The inclusion of gold nanorods in this system allows for the possibility to externally trigger drug delivery using NIR laser light. Additionally, because the gold nanorods can act as contrast agents for several types of non-invasive medical imaging the systems have future potential for use as both diagnostic and therapeutic systems.

Demonstration of light-triggered swelling behavior of the nanoparticle systems demonstrates the potential for triggering of drug release. Basic photoacoustic imaging trials show the potential of the system for use in medical imaging, and cell viability in the presence of the particles demonstrates potential for safe, in vivo use. Overall the studies described in this chapter give evidence for the potential use of these systems for in vivo externally controlled drug delivery systems with imaging capabilities.

7.2 Materials and Methods

7.2.1 Gold-Polymer Composite Synthesis

Acrylic acid (AA, inhibited with 200 ppm hydroquinone monomethyl ether), N-Isopropylacrylamide (NIPAAm), and sodium dodecyl sulfate (SDS) were obtained from Sigma Aldrich (Milwaukee, WI), acrylamide (AAm) and ammonium persulfate (APS) were obtained from Fisher Scientific (Hampton, NH). Bare gold nanorods and gold nanorods with amine-terminated PEG chains, N-therapy amine-polymer gold nanorods, were obtained from Nanopartz (Loveland, CO). All materials were used as received.

Composite systems incorporating temperature-sensitive polymers were synthesized using two different methods. The first method involved dispersing gold nanorods in the pre-polymerization aqueous solution. Polymerization proceeded using an aqueous dispersion polymerization method and gold nanorods served as nucleation points, entrapping them inside of polymer nanoparticles.

Crosslinked PNIPAAM composite nanoparticles were synthesized along with P(NIPAAm-co-AAm), and P(NIPAAm-co-AA) at molar crosslinking ratios of 10 %. To synthesize LCST composite monomer, crosslinker, N,N'-Methylene bisacrylamide, and a stabilizer (usually SDS) are added to a 100 ml aqueous phase in a 250 ml round bottomed flask at a total monomer concentration of 5.5 g/L and a typical stabilizer concentration of 0.3 g/L. The monomers and stabilizer were first dissolved in the aqueous medium. 2 ml of gold nanorods at a concentration of were added to the polymerization flask at a concentration of approximately 0.2 mg/ml. Next, the aqueous reaction solution was purged with nitrogen to remove oxygen from the reaction flask. A 70 °C oil bath was prepared and the purged reaction flask was submerged in the oil bath. An aqueous solution of the free radical initiator, APS, was injected into the reaction flask to initiate reaction. Reaction was allowed to proceed for at least two hours. After completion, the reaction flask is opened to the air and removed from the heat source.

The resulting composite nanoparticle suspension was dialyzed against DI water for 10 days using a 12-14,000 MWCO dialysis tubing. Dialysis water was changed twice daily. Particle solutions were then frozen in a -80° C freezer and lyophilized until dry. Dry particle solutions were resuspended in the appropriate medium or used dry as necessary for further analysis.

The second method to synthesize PNIPAAm based gold-polymer systems consisted of grafting gold nanorods to the surface of the polymer nanoparticles. First

P(NIPAAm-co-AA) with 10 mol % crosslinking were synthesized using aqueous dispersion polymerization as previously described. Gold nanorods were received functionalized with a PEG chain with a primary amine termination. The attachment of the PEG chain to the gold nanorods is achieved by reacting a heterobifunctional PEG molecule with a thiol group on one end the amine on the other with the gold.

A condensation reaction was used to form a peptide bond grafting the gold nanorods to the surface of the polymer nanoparticles. Polymer nanoparticles were suspended in DI water at a concentration of 5 mg/ml. Gold nanorods were used as received at a concentration of approximately 2 mg/ml. In a typical reaction 100 µl of polymer nanoparticle stock solution was added to 2.2 ml DI water. A 0.5 mg weight of EDC was added to the solution and it was mixed on a rotary mixer for 15 minutes. 250 µl of gold nanorod solution was added to the mixture and stirred overnight. Particles were dialyzed against DI water for 2 days with water changed twice daily.

7.2.2 Light-responsive Swelling Behavior

Gold-polymer composite nanoparticles were characterized for their swelling behavior in response to exposure to NIR light using dynamic light scattering (DLS, ZetaPlus, Brookhaven, Holtsville, NY). The hydrodynamic diameter of the particles was measured in solution using the DLS operating at 90˚ scattering angle with a 635 nm 35 mW diode laser source.

Composite nanoparticle samples were suspended in PBS buffer at a pH of 7.4. Concentration of the particle solution was adjusted as necessary to achieve a photon count rate of approximately 300,000 counts per second. A continuous wavelength laser with wavelength centered around 808 nm was used to illuminate the particles in buffer. The laser was set up at a 90˚ angle above the detector pointing down into the cuvette holding the particles.

Measurement of the hydrodynamic diameter was collected with the laser light alternately turned on and off. Each measurement was collected over a 2 minute time period. The light was cycled on or off after every 2 measurement periods for a total of 10 measurement runs. The diameter was measured with no laser exposure for the first 4 minutes (2 measurement runs) then turned on for the next 4 minutes, and repeatedly cycled in that manner for the duration of the 10 run sequence.

7.2.3 Cytocompatibility

In vitro tests have been performed to evaluate the cytocompatibility of the polymer nanoparticle and composite nanoparticle systems. These studies were performed using NIH/3T3 mouse fibroblasts as a cell model to measure the cytocompatibility of the nanoparticle systems with normal cell tissue. Cellular proliferation in the presence of various nanoparticle was quantified using a standard MTS assay which measures dehydrogenase enzyme activity of metabolically active cells.

The NIH/3T3 cells were maintained in DMEM with 4 mM glutamine, 4.5 g/L glucose, and 10% bovine calf serum. The cells were incubated in a humidified environment with 5% carbon dioxide until ready for use. In preparation for cytocompatibility studies, cells were seeded in 96-well plates at a density of 3000 cells/cm^2. Cells were grown in the wells until they reached at least 95% confluence.

When the cells were ready for the viability studies, 200 µl of fresh media was placed in each well and the plate was incubated for 1 h. Several concentrations were prepared using dry P(NIPAAm-co-AA) polymer nanoparticles and gold polymer composites in PBS buffer solution. A 50 µl volume of each particle solution was added to each well in the 96-well plate. The plate was incubated for a 2 h period in a 5% CO_2 environment.

After the 2 h incubation period, the media was removed from each well and replaced with MTS assay solution (CellTiter 96 AQueous, Promega) in PBS. A 90 minute incubation period in the assay solution followed. The absorbance was then measured using using a microplate reader (Synergy HT, BioTek Instruments, Inc., Winooski, VT) at 490 nm.

7.2.4 Photoacoustic Imaging

Studies were performed to demonstrate the potential for these systems to be used as contrast agents for photoacoustic imaging. P(NIPAAm-co-AA) nanoparticles

were first grafted with gold nanorods as previously described. Next samples of the gold-polymer composites were prepared in PBS solution.

A nanopulsed laser operating at 775 nm and 5 mJ/cm^2 was used to trigger the thermoelastic expansion in the gold nanorods that leads to the photoacoustic signal. After exposure to a nanopulsed laser a signal was detected from an ultrasound transducer. Nanoparticles were loaded into a capillary that was exposed to the nanopulsed laser source and an ultrasound transducer was situated above the capillary which was temperature controlled. Measurements were collected over a temperature range between 30 and 50 °C.

7.3 Results and Discussion

7.3.1 Gold-Polymer Composite Synthesis

Gold nanorods were incorporated into LCST polymer nanoparticles during aqueous dispersion polymerization. PNIPAAm, 90/10 P(NIPAAm-co-AAm), and 90/10 P(NIPAAm-co-AA) were synthesized in the presence of bare gold nanorods and in each case a fraction of the polymer particles entrapped gold nanorods. Typical polymerizations yielded systems in which 5-10% of polymer nanoparticles contained gold nanorods which will be discussed in further detail in section 4.3.3. All three of the polymer nanoparticle systems were able to entrap bare gold nanorods during polymerizations.

Systems with gold nanorods grafted to the surface of LCST hydrogel nanoparticles were also synthesized. In this case 90/10 P(NIPAAm-co-AA) were used so that carboxyl pendant groups would be available for the grafting procedure. Gold nanorods were attached to the surface of the polymer nanoparticles and surface coverage was shown to be controlled depending on the concentration of gold nanorods added during incubation with polymer nanoparticles.

7.3.2 Light-responsive Swelling Behavior

Dynamic light scattering was used to measure the hydrodynamic diameter of the particles before, during, and after exposure to a NIR light source. Hydrodynamic diameter of the particle solution was measured at 37 °C prior to exposure to light source and shown to be consistent with previous swelling results. A reversible swelling behavior was observed in response to light exposure as shown in Figure 7.1.

During periods of time where the light was off the particles were in the normal swollen state expected at 37 °C, but during periods of time where the laser was turned on the particles collapsed into a less swollen state demonstrating the potential to squeeze out an entrapped drug. This change was reversible. When the laser was turned off the particles swelled back to their initial state. All of the swelling events occurred rapidly, but because each measurement is taken over a period of 2 minutes it is not possible to conclude how quickly swelling took place other than to say it occurred in less than 2 minutes.

7.3.3 Cytocompatibility

An NIH/3T3 mouse fibroblast model was used to demonstrate cell viability in the presence of nanoparticle systems. The MTS assays were used to quantify viability in 96-well plates. Figure 7.2 displays the results of cell viability for P(NIPAAm-co-AA) polymer systems at several concentrations. Proliferation measurements are shown as a percentage of the control systems. At all concentrations there was not significant cell death caused by the presence of the polymer nanoparticles. All of the measurements showed that at least 80% of the cells remained viable. Concentrations all the way up to 4 mg/ml were studied and shown to have minimal impact on cell survival.

All systems showed high cellular compatibility. Cell proliferation in the studies does decrease slightly as the concentration of the gold-polymer nanoparticles is increased. Results as quantified using the MTS assay are shown for gold-polymer systems in Figure 7.3. All of the samples had cell viabilities above 80%. The lower concentrations that were tested, up to 250 μg/ml did not show statistically significant cell death compared to control. At a concentration of 500 μg/ml there was slightly lower cell viability, but still over 80% cell viability.

7.3.4 Photoacoustic Imaging

Gold-polymer composite systems were shown to have potential for use as contrast agents in medical imaging such as photoacoustic imaging. After exposure to a nanopulsed laser a signal was detected from an ultrasound transducer. Nanoparticles

were loaded into a capillary that was exposed to the nanopulsed laser source and an ultrasound transducer was situated above the capillary which was temperature controlled.

The results in Figure 7.4 demonstrate the magnitude of the photoacoustic signal detected by the ultrasound transducer at a range of temperatures. A photoacoustic signal was dectected over a range of temperatures from 35 to 50 °C using 0.5 mg/ml and 2 mg/ml concentrations of particles. Based on this data there is potential for photoacoustic imaging to be used in conjuction with therapeutic delivery from these systems and an ultrasound transducer may be used to correlate the temperature of the systems in vivo.

7.4 Conclusions

Gold-polymer composites were synthesized in the lab for use as externally triggered delivery systems. In order to demonstrate the potential of these systems for diagnostic and therapeutic use several proof of concept studies were performed. The results of these studies can be used to conclude that the systems show potential for biocompatibility and safe use. The composite systems also may be triggered to collapse and subsequently release a therapeutic. Lastly, an experiment to test the photoacoustic signal produced by the particles demonstrates that the gold nanorods present in the system can be used as a contrast agent for potentially non-invasive medical imaging using NIR light.

Cell proliferation studies demonstrated that the particles cause limited cell death in a 3T3 mouse fibroblast cell model. Both polymer nanoparticles and gold-polymer systems showed high cellular compatibility that was a function of particle concentration. Light was used to induce a swelling response in gold-polymer composites. Particles were shown to quickly collapse in response to the light and reversibly swell after the light was switched off. After previous results demonstrated that the particle systems have the ability to entrap a model therapeutic it is clear that these systems may be used to trigger a drug delivery response with light. A photoacoustic signal was detected in response to a nanopulsed laser with NIR wavelength. The signal from these nanoparticle systems was shown to be a function of temperature over a relevant therapeutic range showing the potential for the use of in vivo medical imaging techniques.

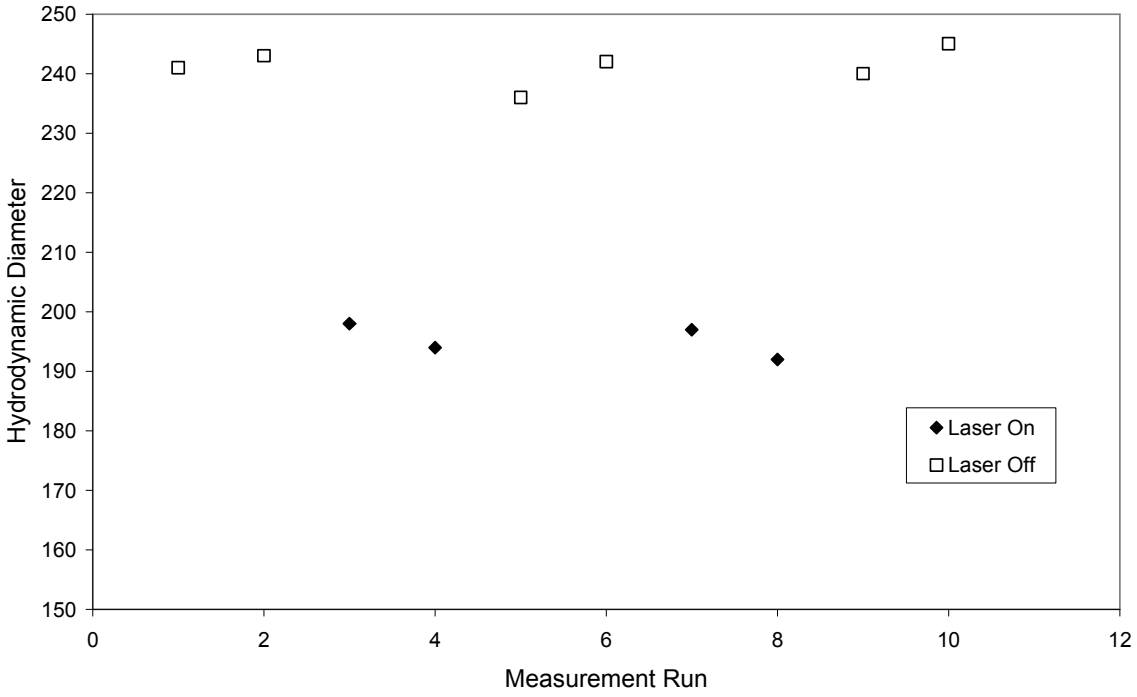

Figure 7.5 Swelling behavior of gold-polymer composites with alternating laser exposure. P(NIPAAm-co-AA) polymer nanoparticles grafted with gold nanorods were intermittently exposed to 808 nm CW laser.

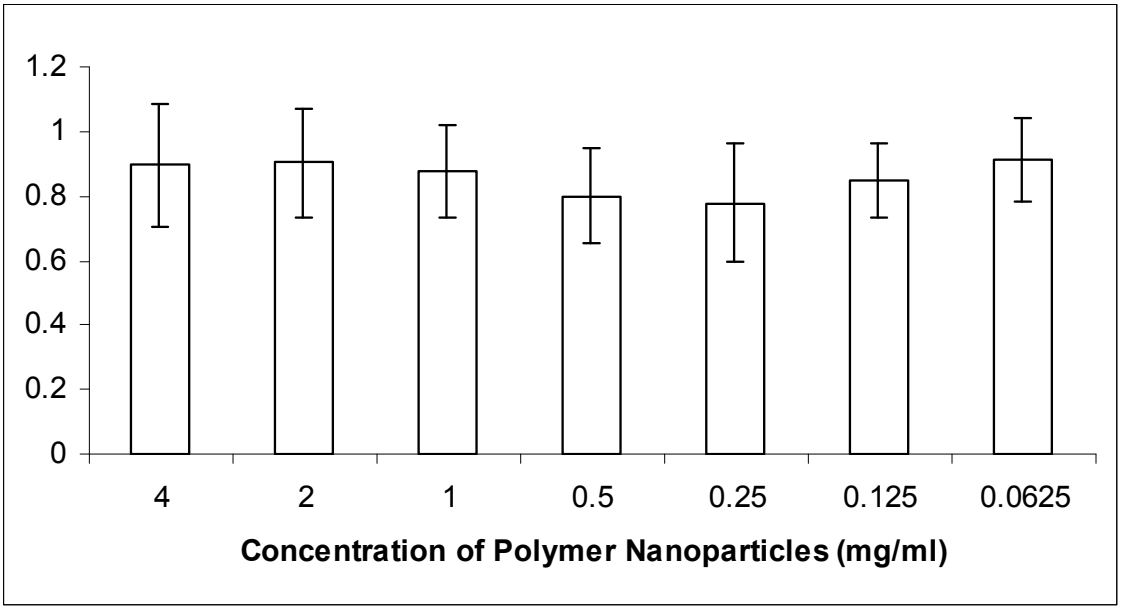

Figure 7.2 Cell viability of 3T3 mouse fibroblasts as a percentage of control when incubated with varying concentrations of P(NIPAAm-co-AA) nanoparticles.

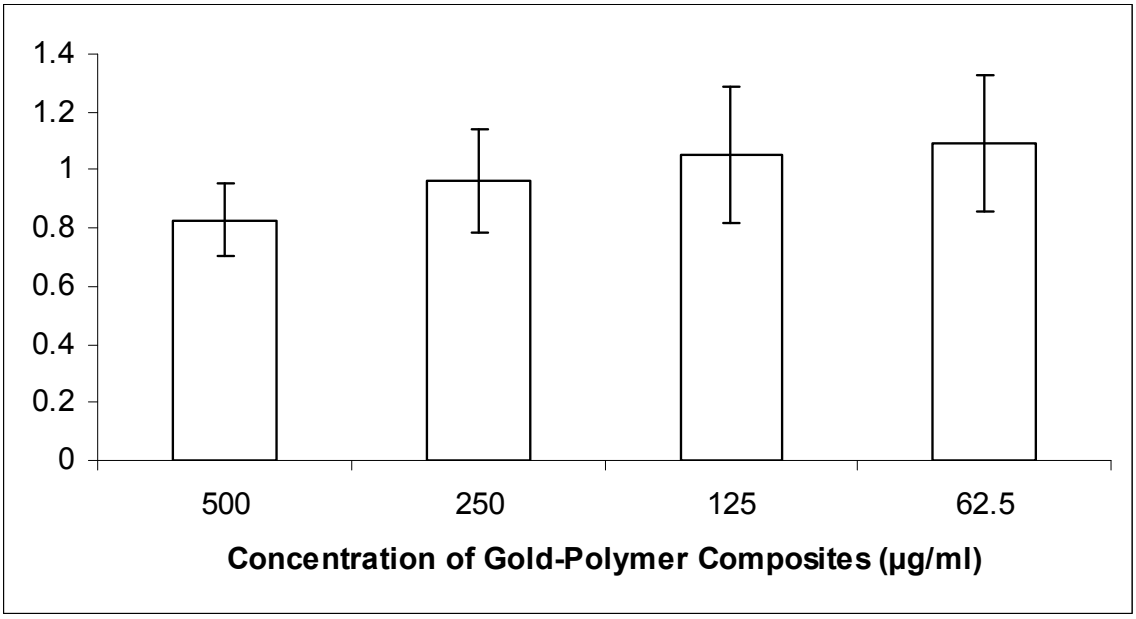

Figure 7.3 Cell viability of 3T3 mouse fibroblasts as a percentage of control when incubated with varying concentrations of gold-polymer composite nanoparticles.

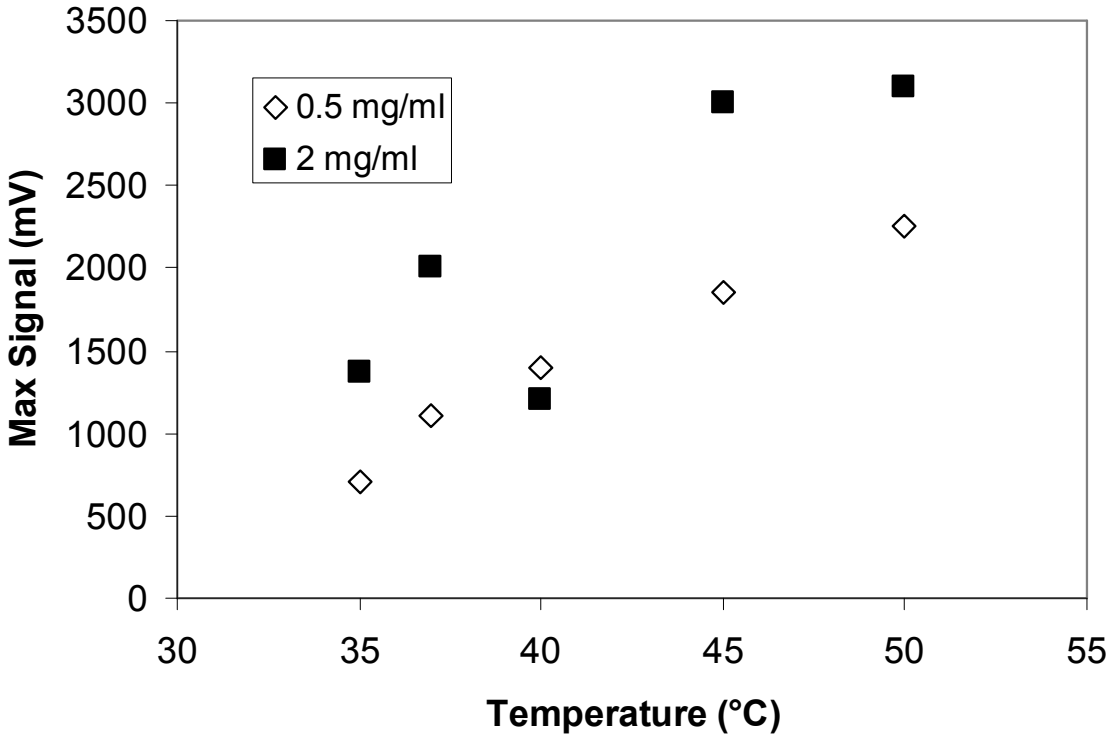

Figure 7.4 Photoacoustic signal measured from gold-polymer composites. Signal measured from P(NIPAAm-co-AA) nanoparticles grafted with gold nanorods when exposed to 775 nm nanopulsed laser at 5 mJ/cm.

REFERENCES

1. Franceschini, M.A., Moesta, K.T., Fantini, S., Gaida, G., et al., *Frequency-domain techniques enhance optical mammography: Initial clinical results.* P. Natl. Acad. Sci. USA, 1997. **94**(12): p. 6468-6473.

2. Weissleder, R., *A clearer vision for in vivo imaging.* Nat. Biotech., 2001. **19**(4): p. 316-317.

3. Sershen, S.R., Mensing, G.A., Ng, M., Halas, N.J., et al., *Independent optical control of microfluidic valves formed from optomechanically responsive nanocomposite hydrogels.* Adv. Mater., 2005. **17**(11): p. 1366-+.

4. Sershen, S.R., Halas, N.J., and West, J.L. *Pulsatile release of insulin via photothermally modulated drug delivery*. in *[Engineering in Medicine and Biology, 2002. 24th Annual Conference and the Annual Fall Meeting of the Biomedical Engineering Society] EMBS/BMES Conference, 2002. Proceedings of the Second Joint*. 2002.

5. Ntziachristos, V., Bremer, C., and Weissleder, R., *Fluorescence imaging with near-infrared light: new technological advances that enable in vivo molecular imaging.* Eur. Radiol., 2003. **13**(1): p. 195-208.

6. Bremer, C., Ntziachristos, V., and Weissleder, R., *Optical-based molecular imaging: contrast agents and potential medical applications.* Eur. Radiol., 2003. **13**(2): p. 231-243.

7. De La Zerda, A., Zavaleta, C., Keren, S., Vaithilingam, S., et al., *Carbon nanotubes as photoacoustic molecular imaging agents in living mice.* Nat. Nano., 2008. **3**(9): p. 557-562.

8. Li, P.-C., Wei, C.-W., Liao, C.-K., Chen, C.-D., et al. *Multiple targeting in photoacoustic imaging using bioconjugated gold nanorods*. 2006: SPIE.

9. Eghtedari, M., Oraevsky, A., Copland, J.A., Kotov, N.A., et al., *High Sensitivity of In Vivo Detection of Gold Nanorods Using a Laser Optoacoustic Imaging System.* Nano Lett., 2007. **7**(7): p. 1914-1918.

10. Mallidi, S., Larson, T., Tam, J., Joshi, P.P., et al., *Multiwavelength Photoacoustic Imaging and Plasmon Resonance Coupling of Gold Nanoparticles for Selective Detection of Cancer.* Nano Lett., 2009. **9**(8): p. 2825-2831.

11. Joshi, P.P., Yun-Sheng, C., Seungsoo, K., Shah, J., et al. *Molecular therapeutic agents for noninvasive photoacoustic image-guided photothermal therapy*. in *Engineering in Medicine and Biology Society, 2009. EMBC 2009. Annual International Conference of the IEEE*. 2009.

12. Yang, X., Skrabalak, S.E., Li, Z.-Y., Xia, Y., and Wang, L.V., *Photoacoustic Tomography of a Rat Cerebral Cortex in vivo with Au Nanocages as an Optical Contrast Agent.* Nano Lett., 2007. **7**(12): p. 3798-3802.

13. Homan, K., Shah, J., Gomez, S., Gensler, H., et al., *Silver nanosystems for photoacoustic imaging and image-guided therapy.* J. Biomed. Opt., **15**(2): p. 021316-9.

14. Bouchard, L.-S., Anwar, M.S., Liu, G.L., Hann, B., et al., *Picomolar sensitivity MRI and photoacoustic imaging of cobalt nanoparticles.* P. Natl. Acad. Sci. USA, **106**(11): p. 4085-4089.

Chapter 8: Conclusions

Externally-triggered therapeutic systems are those that allow a therapeutic to be released from a carrier in response to some external stimulus. In this thesis nanoscale externally-triggered systems were developed for use in chemotherapy for breast cancer treatment and medical imaging techniques. Nanoscale systems are of interest because they could be administered intravenously, extend half-lives of circulation, and localize at a disease site because of the enhanced permeability and retention (EPR) effect.

The proposed system uses a NIR light source as the external stimulus to trigger drug release. NIR light has the ability to penetrate through tissue and is therefore an attractive external trigger for drug deliver. Gold nanorods can absorb light in this region of interest and convert it to heat. A temperature responsive polymer hydrogel nanoparticle can entrap a drug and release it in response to heating through a swelling transition temperature. In this work gold nanorods were grafted to the surface of temperature responsive nanoparticles so that light absorbed by the gold is converted to heat which induces a swelling transition and associated therapeutic release from the polymer. Additionally, the gold nanorods can act as a contrast agent for certain non-invasive medical imaging techniques such as photoacoustic imaging.

Several types of temperature responsive nanogels were synthesized for use in these drug delivery systems. Particles exhibiting LCST behavior including PNIPAAm, P(NIPAAm-co-AAm), and P(NIPAAm-co-AA) were synthesized using an aqueous

dispersion polymerization. Copolymers with varying monomer ratios were examined for their ability to tune the LCST of the systems, and the ability to increase the temperature of this transition by addition of a more hydrophilic monomer was confirmed. IPN nanoparticles exhibiting UCST behavior composed of equimolar networks of PAA and PAAm were formulated with a water-in-oil microemulsion polymerization. The effect of surfactant concentration and crosslinking ratio on size and swelling behavior of the nanoparticles was analyzed. Polymer size, shape, and morphology were verified using microscopy techniques including SEM and TEM. The characterizations can be used to gain insight into the potential of these systems as nanoscale drug carriers, where the determination of size and swelling behavior can be used to select the appropriate particles for delivery of a specified therapeutic.

In order to formulate systems that could be used to externally trigger the release of a drug using NIR light an additional component other than the temperature-responsive polymer was necessary in the system. The component must respond to light in a manner in which it will transmit heat to this polymer layer and trigger release of an entrapped therapeutic agent. Gold nanorods were identified as an appropriate heating element. In order for the system to be realized the gold nanorods were incorporated into the polymer nanoparticle systems using two different means. Gold nanorods were entrapped in PNIPAAm, P(NIPAAM-co-AAm), and P(NIPAAm-co-AA) systems during aqueous dispersion polymerization as confirmed by transmission electron microscopy.

Gold nanorods were also grafted to the surface of temperature responsive nanoparticles following polymerization. 50/50 PAAm/PAA nanoparticles and 90/10 P(NIPAAm-co-AA) nanoparticles were synthesized using water in oil microemulsion polymerization and aqueous dispersion polymerization respectively. Amine functionalized gold nanorods were grafted to the surface of the nanoparticles using an EDC activated condensation reaction between carboxyl groups on the polymers and the amine groups on the nanorods. TEM results confirmed the formation of these gold-polymer composite nanoparticle systems. Measurement of the absorption spectra over a 600-1000 nm wavelength range further demonstrated the attachment of gold nanorods to the surface of LCST polymer nanoparticles. A broadening and shifting of the spectrum was observed as the temperature was increased through and above the LCST transition temperature.

The capability of temperature responsive nanoparticle systems to entrap and release a compound of interest was investigated. LCST nanocarriers were first synthesized using aqueous dispersion polymerization methods. The hydrogel nanoparticles were synthesized at varying crosslinking ratios including 1, 5, and 10 mol %. A model therapeutic, fluorescein, was selected to mimic anticancer therapeutics, specifically doxorubicin. Fluorescein has a similar molecular weight, structural character, and hydrophobicity to doxorubicin.

The entrapment efficiency and loading capacity of the polymer nanocarriers were measured for fluorescein, a model for chemotherapeutics. These parameters that

quantify loading increased in polymer systems as the amount of crosslinker present in the polymer system increased. Because fluorescein is a small molecule, maximum loading was achieved in very highly crosslinked systems where the polymer hydrogel network is tightly structured and mesh size is at a minimum.

In order to mimic physiological conditions, release studies were performed in PBS buffer at 37 °C. Samples were collected to measure release of fluorescein into the PBS medium using fluorescence spectroscopy after filtration of particles out of the sample. Results showed a release curve that occurred over a period of hours or days depending on the hydrogel formulation. The results demonstrated that release from the systems is slow enough at constant temperature that release could be triggered in the nanocarriers using laser light over shorter time periods before the entire payload naturally diffused out of the system. The systems show potential for use as externally controlled polymer nanoparticle therapeutic carriers.

Polymer nanoparticles formed using 10 % crosslinked 90/10 P(NIPAAm-co-AA) showed the highest potential for carrying and releasing a hydrophobic anticancer drug for the described externally triggered application. These materials entrapped the highest amount of the model therapeutic and best protected the compound from release at constant physiological temperature and pH. Because of the positive results from the loading and release studies along with their ability to exhibit temperature-responsive swelling behavior this material is a strong candidate for development of nanoscale externally-controlled release systems

In order to demonstrate the potential of these systems for diagnostic and therapeutic use, several proof of concept studies were performed. The results of these studies can be used to conclude that the systems show potential for biocompatibility and safe use. The composite systems also may be triggered to collapse and subsequently release a therapeutic. Lastly, an experiment to test the photoacoustic signal produced by the particles demonstrates that the gold nanorods present in the system can be used as a contrast agent for potentially non-invasive medical imaging using NIR light.

Cell proliferation studies demonstrated that the particles cause limited cell death in a 3T3 mouse fibroblast cell model. Both polymer nanoparticles and gold-polymer systems showed high cellular compatibility that was a function of particle concentration. Light was used to induce a swelling response in gold-polymer composites. Particles were shown to quickly collapse in response to NIR light and reversibly swell after the light was switched off. After previous results demonstrated that the particle systems have the ability to entrap a model therapeutic it is clear that these systems may be used to trigger a drug delivery response with light. A photoacoustic signal was detected in response to a nanopulsed laser with NIR wavelength. The signal from these nanoparticle systems was shown to be a function of temperature over a relevant therapeutic range showing the potential for the use of in vivo medical imaging techniques.

Overall, the materials developed in this thesis show potential for use as externally-triggered nanoscale systems for delivery of chemotherapeutics. Future work

needs to be done to optimize the systems for light-triggered delivery of a therapeutic agent. Additional studies to validate the efficacy of the systems as a contrast agent for photoacoustic imaging could show that the systems could be effectively used to simultaneously image a disease site and deliver a drug. There is also a great need for detailed studies on the biocompatibility and toxicity of nanoscale materials such as these developed for applications in drug delivery.

References

Abe, O., R. Abe, et al. *Effects of chemotherapy and hormonal therapy for early breast cancer on recurrence and 15-year survival: an overview of the randomised trials*. Lancet 2005. **365**(9472): 1687-1717.

Abe, O., R. Abe, et al. *Polychemotherapy for early breast cancer: an overview of the randomised trials*. Lancet 1998. **352**(9132): 930-942.

Agnihotri, S. A., N. N. Mallikarjuna, et al. *Recent advances on chitosan-based micro- and nanoparticles in drug delivery*. J. Control. Release 2004. **100**(1): 5-28.

Agueros, M., L. Ruiz-Gaton, et al. *Combined hydroxypropyl-beta-cyclodextrin and poly(anhydride) nanoparticles improve the oral permeability of paclitaxel*. Eur. J. Pharm. Sci. 2009. **38**(4): 405-413.

Andersson, M. and S. L. Maunu. *Structural studies of Poly(N-isopropylacrylamide) microgels: Effect of SDS surfactant concentration in the microgel synthesis*. J. Polym. Sci. Pt. B-Polym. Phys. 2006. **44**(23): 3305-3314.

Astete, C. E. and C. M. Sabliov. *Synthesis and characterization of PLGA nanoparticles*. J. Biomater. Sci.-Polym. Ed. 2006. **17**(3): 247-289.

Avgoustakis, K., A. Beletsi, et al. *PLGA-mPEG nanoparticles of cisplatin: in vitro nanoparticle degradation, in vitro drug release and in Vivo drug residence in blood properties*. J. Control. Release 2002. **79**(1-3): 123-135.

Bartlett, D. W., H. Su, et al. *Impact of tumor-specific targeting on the biodistribution and efficacy of siRNA nanoparticles measured by multimodality in vivo imaging*. P. Natl. Acad. Sci. U.S.A. 2007. **104**(39): 15549-15554.

Berger, J., M. Reist, et al. *Structure and interactions in covalently and ionically crosslinked chitosan hydrogels for biomedical applications*. Eur. J. Pharm. Biopharm. 2004. **57**(1): 19-34.

Bilati, U., E. Allemann, et al. *Poly(D,L-lactide-co-glycolide) protein-loaded nanoparticles prepared by the double emulsion method-processing and formulation issues for enhanced entrapment efficiency*. J. Microencapsul. 2005. **22**(2): 205-214.

Bouchard, L.-S., M. S. Anwar, et al. *Picomolar sensitivity MRI and photoacoustic imaging of cobalt nanoparticles*. P. Natl. Acad. Sci. U.S.A. 2009. **106**(11): 4085-4089.

Bouillot, P. and B. Vincent. *A comparison of the swelling behaviour of copolymer and interpenetrating network microgel particles*. Colloid Polym. Sci. 2000. **278**(1): 74-79.

Brannon-Peppas, L. and J. O. Blanchette. *Nanoparticle and targeted systems for cancer therapy*. Adv. Drug Deliv. Rev. 2004. **56**(11): 1649-1659.

Bremer, C., V. Ntziachristos, et al. *Optical-based molecular imaging: contrast agents and potential medical applications*. Eur. Radiol. 2003. **13**(2): 231-243.

Brigger, I., C. Dubernet, et al. *Nanoparticles in cancer therapy and diagnosis*. Adv. Drug Deliv. Rev. 2002. **54**(5): 631-651.

Buzdar, A. U. *Preoperative chemotherapy treatment of breast cancer—A review*. Cancer 2007. **110**(11): 2394-2407.

Byrne, J. D., T. Betancourt, et al. *Active targeting schemes for nanoparticle systems in cancer therapeutics*. Adv. Drug Deliv. Rev. 2008. **60**(15): 1615-1626.

Cattel, L., M. Ceruti, et al. *From conventional to stealth liposomes a new frontier in cancer chemotherapy*. Tumori 2003. **89**(3): 237-249.

Chan, J. M., L. F. Zhang, et al. *PLGA-lecithin-PEG core-shell nanoparticles for controlled drug delivery*. Biomaterials 2009. **30**(8): 1627-1634.

Chen, H., Y. Gu, et al. *Characterization of pH- and Temperature-sensitive Hydrogel Nanoparticles for Controlled Drug Release*. PDA J. Pharm. Sci. Tech. 2007. **61**(4): 303-313.

Daniels, T. R., T. Delgado, et al. *The transferrin receptor part I: Biology and targeting with cytotoxic antibodies for the treatment of cancer*. Clin. Immunol. 2006. **121**(2): 144-158.

Dawes, G. J. S., L. E. Fratila-Apachitei, et al. *Size effect of PLGA spheres on drug loading efficiency and release profiles*. J. Mater. Sci.-Mater. Med. 2009. **20**(5): 1089-1094.

De La Zerda, A., C. Zavaleta, et al. *Carbon nanotubes as photoacoustic molecular imaging agents in living mice*. Nat. Nanotechnol. 2008. **3**(9): 557-562.

Determan, A. S., J. R. Graham, et al. *The role of microsphere fabrication methods on the stability and release kinetics of ovalbumin encapsulated in polyanhydride microspheres*. J. Microencapsul. 2006. **23**(8): 832-843.

Discher, D. E., V. Ortiz, et al. *Emerging applications of polymersomes in delivery: From molecular dynamics to shrinkage of tumors*. Prog. Polym. Sci. 2007. **32**(8-9): 838-857.

Doiron, A. L., K. Chu, et al. *Preparation and initial characterization of biodegradable particles containing gadolinium-DTPA contrast agent for enhanced MRI*. P. Natl. Acad. Sci. U.S.A. 2008. **105**(45): 17232-17237.

Edwards, B. K., M. L. Brown, et al. *Annual report to the Nation on the status of cancer, 1975-2002, featuring population-based trends in cancer treatment*. J. Natl. Cancer Inst. 2005. **97**(19): 1407-1427.

Eghtedari, M., A. Oraevsky, et al. *High Sensitivity of In Vivo Detection of Gold Nanorods Using a Laser Optoacoustic Imaging System*. Nano Lett. 2007. **7**(7): 1914-1918.

Eifel, P., J. A. Axelson, et al. *National Institutes of Health Consensus Development Conference statement: Adjuvant therapy for breast cancer, November 1-3, 2000*. J. Natl. Cancer Inst. 2001. **93**(13): 979-989.

El Bayoumil, T. and V. P. Torchilin. *Tumor-Targeted Nanomedicines: Enhanced Antitumor Efficacy In vivo of Doxorubicin-Loaded, Long-Circulating Liposomes Modified with Cancer-Specific Monoclonal Antibody*. Clin. Cancer Res. 2009. **15**(6): 1973-1980.

Fang, J., H. Nakamura, et al. *The EPR effect: Unique features of tumor blood vessels for drug delivery, factors involved, and limitations and augmentation of the effect*. Adv. Drug Deliv. Rev. 2010.

Ferrara, K., R. Pollard, et al. *Ultrasound microbubble contrast agents: fundamentals and application to gene and drug delivery*. Annu. Rev. Biomed. Eng. 2007. **9**: 415-47.

Ferrara, K. W. *Driving delivery vehicles with ultrasound*. Adv. Drug Deliv. Rev. 2008. **60**(10): 1097-1102.

Ferrari, M., T. Desai, et al. 2007. Diagnostic and Therapeutic Applications of Metal Nanoshells. BioMEMS and Biomedical Nanotechnology, Springer US**:** 157-169.

Fisher, O. Z. and N. A. Peppas. *Polybasic Nanomatrices Prepared by UV-Initiated Photopolymerization*. Macromolecules 2009. **42**(9): 3391-3398.

Fonseca, C., S. Simoes, et al. *Paclitaxel-loaded PLGA nanoparticles: preparation, physicochemical characterization and in vitro anti-tumoral activity*. J. Control. Release 2002. **83**(2): 273-286.

Fowble, B. 1991. Breast cancer treatment: a comprehensive guide to management, Mosby-Year Book.

Franceschini, M. A., K. T. Moesta, et al. *Frequency-domain techniques enhance optical mammography: Initial clinical results*. Proceedings of the National Academy of Sciences of the United States of America 1997. **94**(12): 6468-6473.

Funston, A. M., C. Novo, et al. *Plasmon Coupling of Gold Nanorods at Short Distances and in Different Geometries*. Nano Lett. 2009. **9**(4): 1651-1658.

Gabizon, A., H. Shmeeda, et al. *Pharmacokinetics of pegylated liposomal doxorubicin - Review of animal and human studies*. Clin. Pharmacokinet. 2003. **42**(5): 419-436.

Gan, Q. and T. Wang. *Chitosan nanoparticle as protein delivery carrier - Systematic examination of fabrication conditions for efficient loading and release*. Colloid Surf. B-Biointerfaces 2007. **59**(1): 24-34.

Ganta, S., H. Devalapally, et al. *A review of stimuli-responsive nanocarriers for drug and gene delivery*. J. Control. Release 2008. **126**(3): 187-204.

Glangchai, L. C., M. Caldorera-Moore, et al. *Nanoimprint lithography based fabrication of shape-specific, enzymatically-triggered smart nanoparticles*. J. Control. Release 2008. **125**(3): 263-272.

Govender, T., S. Stolnik, et al. *PLGA nanoparticles prepared by nanoprecipitation: drug loading and release studies of a water soluble drug*. J. Control. Release 1999. **57**(2): 171-185.

Grubbs, R. B. *Hybrid metal–polymer composites from functional block copolymers*. J. Polym. Sci. Pol. Chem. 2005. **43**(19): 4323-4336.

Guowei, D., K. Adriane, et al. *PVP magnetic nanospheres: Biocompatibility, in vitro and in vivo bleomycin release*. Int. J. Pharm. 2007. **328**(1): 78-85.

Haag, R. and F. Kratz. *Polymer Therapeutics: Concepts and Applications*. Angew. Chem. Int. Edit. 2006. **45**(8): 1198-1215.

Hamaguchi, T., Y. Matsumura, et al. *NK105, a paclitaxel-incorporating micellar nanoparticle formulation, can extend in vivo antitumour activity and reduce the neurotoxicity of paclitaxel*. Brit. J. Cancer 2005. **92**(7): 1240-1246.

Hans, M. L. and A. M. Lowman. *Biodegradable nanoparticles for drug delivery and targeting*. Curr. Opin. Solid St. M. 2002. **6**(4): 319-327.

Harris, L., G. Batist, et al. *Liposome-encapsulated doxorubicin compared with conventional doxorubicin in a randomized multicenter trial as first-line therapy of metastatic breast carcinoma*. Cancer 2002. **94**(1): 25-36.

Homan, K., J. Shah, et al. *Silver nanosystems for photoacoustic imaging and image-guided therapy*. J. Biomed. Opt. **15**(2): 021316-9.

Hu, J. H., K. P. Johnston, et al. *Spray freezing into liquid (SFL) particle engineering technology to enhance dissolution of poorly water soluble drugs: organic solvent versus organic/aqueous co-solvent systems*. Eur. J. Pharm. Sci. 2003. **20**(3): 295-303.

Iglesias, J. *nab-Paclitaxel (Abraxane(R)): an albumin-bound cytotoxic exploiting natural delivery mechanisms into tumors*. Breast Cancer Res. 2009. **11**(Suppl 1): S21.

Jemal, A., R. Siegel, et al. *Cancer statistics, 2008*. CA-Cancer J. Clin. 2008. **58**(2): 71-96.

Joshi, P. P., C. Yun-Sheng, et al. 2009. Molecular therapeutic agents for noninvasive photoacoustic image-guided photothermal therapy. Engineering in Medicine and Biology Society, 2009. EMBC 2009. Annual International Conference of the IEEE.

Kabanov, A. V., E. V. Batrakova, et al. *Pluronic (R) block copolymers as novel polymer therapeutics for drug and gene delivery*. J. Control. Release 2002. **82**(2-3): 189-212.

Kataoka, K., A. Harada, et al. *Block copolymer micelles for drug delivery: design, characterization and biological significance*. Adv. Drug Deliv. Rev. 2001. **47**(1): 113-131.

Kim, H. S. and I. W. Wainer. *Simultaneous analysis of liposomal doxorubicin and doxorubicin using capillary electrophoresis and laser induced fluorescence*. J. Pharm. Biomed. Anal. 2010. **52**(3): 372-376.

Lammers, T., V. Subr, et al. *Polymeric nanomedicines for image-guided drug delivery and tumor-targeted combination therapy*. Nano Today **5**(3): 197-212.

Langer, R. *New methods of drug delivery*. Science 1990. **249**(4976): 1527-1533.

Langer, R. *Polymer Implants for Drug Delivery in the Brain.*. J. Control. Release 1991. **16**(1-2): 53-59.

Lee, A. L. Z., Y. Wang, et al. *The co-delivery of paclitaxel and Herceptin using cationic micellar nanoparticles*. Biomaterials 2009. **30**(5): 919-927.

Lee, C. F., C. C. Lin, et al. *Thermosensitive and control release behavior of poly (N-isopropylacrylamide-co-acrylic acid) latex particles*. Journal of Polymer Science Part a-Polymer Chemistry 2008. **46**(17): 5734-5741.

Lee, K. S. and M. A. El-Sayed. *Gold and silver nanoparticles in sensing and imaging: Sensitivity of plasmon response to size, shape, and metal composition*. J. Phys. Chem. B 2006. **110**(39): 19220-19225.

Lentacker, I., B. Geers, et al. *Design and Evaluation of Doxorubicin-containing Microbubbles for Ultrasound-triggered Doxorubicin Delivery: Cytotoxicity and Mechanisms Involved*. Mol. Ther. 2010. **18**(1): 101-108.

Li, C. and S. Wallace. *Polymer-drug conjugates: Recent development in clinical oncology*. Adv. Drug Deliv. Rev. 2008. **60**(8): 886-898.

Li, P.-C., C.-W. Wei, et al. 2006. Multiple targeting in photoacoustic imaging using bioconjugated gold nanorods, SPIE.

Li, Y. P., Y. Y. Pei, et al. *PEGylated PLGA nanoparticles as protein carriers: synthesis, preparation and biodistribution in rats*. J. Control. Release 2001. **71**(2): 203-211.

Longley, D. B., D. P. Harkin, et al. *5-Fluorouracil: mechanisms of action and clinical strategies*. Nat. Rev. Cancer 2003. **3**(5): 330-338.

Loo, C., A. Lin, et al. *Nanoshell-enabled photonics-based imaging and therapy of cancer*. Technol. Cancer Res. T. 2004. **3**(1): 33-40.

Lopac, S. K., M. P. Torres, et al. *Effect of Polymer Chemistry and Fabrication Method on Protein Release and Stability From Polyanhydride Microspheres*. J. Biomed. Mater. Res. Part B 2009. **91B**(2): 938-947.

Maeda, H., J. Wu, et al. *Tumor vascular permeability and the EPR effect in macromolecular therapeutics: a review*. J. Control. Release 2000. **65**(1-2): 271-284.

Malam, Y., M. Loizidou, et al. *Liposomes and nanoparticles: nanosized vehicles for drug delivery in cancer*. Trends Pharmacol. Sci. 2009. **30**(11): 592-599.

Mallidi, S., T. Larson, et al. *Multiwavelength Photoacoustic Imaging and Plasmon Resonance Coupling of Gold Nanoparticles for Selective Detection of Cancer*. Nano Lett. 2009. **9**(8): 2825-2831.

McPhee, S., L. Tierney, et al. 2006. Current medical diagnosis & treatment 2007, McGraw-Hill Medical.

Missirlis, D., R. Kawamura, et al. *Doxorubicin encapsulation and diffusional release from stable, polymeric, hydrogel nanoparticles*. Eur. J. Pharm. Sci. 2006. **29**(2): 120-129.

Mitra, S., U. Gaur, et al. *Tumour targeted delivery of encapsulated dextran-doxorubicin conjugate using chitosan nanoparticles as carrier*. J. Control. Release 2001. **74**(1-3): 317-323.

Moharram, M. A., L. S. Balloomal, et al. *Infrared study of the complexation of poly(acrylic acid) with poly(acrylamide)*. J. Appl. Polym. Sci. 1996. **59**(6): 987-990.

Morishita, M., T. Goto, et al. *Novel oral insulin delivery systems based on complexation polymer hydrogels: Single and multiple administration studies in type 1 and 2 diabetic rats*. J. Control. Release 2006. **110**(3): 587-594.

Moulder, S. and G. N. Hortobagyi. *Advances in the Treatment of Breast Cancer*. Clin. Pharmacol. Ther. 2007. **83**(1): 26-36.

Mu, L. and S. S. Feng. *A novel controlled release formulation for the anticancer drug paclitaxel (Taxol (R)): PLGA nanoparticles containing vitamin E TPGS*. J. Control. Release 2003. **86**(1): 33-48.

Murray, M. J. and M. J. Snowden. *The preparation, characterisation and applications of colloidal microgels*. Adv. Colloid Interfac. 1995. **54**: 73-91.

Ntziachristos, V., C. Bremer, et al. *Fluorescence imaging with near-infrared light: new*

technological advances that enable in vivo molecular imaging. Eur. Radiol. 2003. **13**(1): 195-208.

Okano, T. *Molecular Design of Temperature-Responsive Polymers as Intelligent Materials*. Adv. Polym. Sci. 1993. **110**: 179-197.

O'Neal, D. P., L. R. Hirsch, et al. *Photo-thermal tumor ablation in mice using near infrared-absorbing nanoparticles*. Cancer Lett. 2004. **209**(2): 171-176.

Owens, D. E., Y. Jian, et al. *Thermally Responsive Swelling Properties of Polyacrylamide/Poly(acrylic acid) Interpenetrating Polymer Network Nanoparticles*. Macromolecules 2007. **40**(20): 7306-7310.

Owens III, D. E., J. K. Eby, et al. *Temperature-responsive polymer-gold nanocomposites as intelligent therapeutic systems*. J. Biomed. Mater. Res. A. 2007. **83A**(3): 692-695.

Owens III, D. E. and N. A. Peppas. *Opsonization, biodistribution, and pharmacokinetics of polymeric nanoparticles*. Int. J. Pharm. 2006. **307**(1): 93-102.

Parkin, D. M., F. Bray, et al. *Global cancer statistics, 2002*. CA-Cancer J. Clin. 2005. **55**(2): 74-108.

Peer, D., J. M. Karp, et al. *Nanocarriers as an emerging platform for cancer therapy*. Nat. Nanotechnol. 2007. **2**(12): 751-760.

Pelton, R. *Temperature-sensitive aqueous microgels*. Adv. Colloid Interfac. 2000. **85**(1): 1-33.

Peppas, N. A., P. Bures, et al. *Hydrogels in pharmaceutical formulations*. Eur. J. Pharm. Biopharm. 2000. **50**(1): 27-46.

Peppas, N. A. and J. Klier. *Controlled release by using poly(methacrylic acid-g-ethylene glycol) hydrogels*. J. Control. Release 1991. **16**(1-2): 203-214.

Pérez-Juste, J., I. Pastoriza-Santos, et al. *Gold nanorods: Synthesis, characterization and applications*. Coordin. Chem. Rev. 2005. **249**(17-18): 1870-1901.

Petrovic, S. C., W. Zhang, et al. *Preparation and Characterization of Thermoresponsive Poly(N-isopropylacrylamide-co-acrylic acid) HydrogelsStudies with Electroactive Probes*. Anal. Chem. 2000. **72**(15): 3449-3454.

Pohlmann, A. R., V. Weiss, et al. *Spray-dried indomethacin-loaded polyester nanocapsules and nanospheres: development, stability evaluation and nanostructure models*. Eur. J. Pharm. Sci. 2002. **16**(4-5): 305-312.

Qiu, Y. and K. Park. *Environment-sensitive hydrogels for drug delivery*. Adv. Drug Deliv. Rev. 2001. **53**(3): 321-339.

Raemdonck, K., J. Demeester, et al. *Advanced nanogel engineering for drug delivery*. Soft Matter 2009. **5**(4): 707-715.

Rastogi, R., S. Anand, et al. *Flexible polymerosomes-An alternative vehicle for topical delivery*. Colloid Surf. B-Biointerfaces 2009. **72**(1): 161-166.

Ren, L. and G. M. Chow. *Synthesis of NIR-sensitive Au-Au2S nanocolloids for drug delivery*. Mat. Sci. Eng. C. 2003. **23**: 113-116.

Rogers, T. L., J. H. Hu, et al. *A novel particle engineering technology: spray-freezing into liquid*. Int. J. Pharm. 2002. **242**(1-2): 93-100.

Rogers, T. L., K. A. Overhoff, et al. *Micronized powders of a poorly water soluble drug produced by a spray-freezing into liquid-emulsion process*. Eur. J. Pharm. Biopharm. 2003. **55**(2): 161-172.

Romond, E. H., E. A. Perez, et al. *Trastuzumab plus adjuvant chemotherapy for operable HER2-positive breast cancer*. N. Engl. J. Med. 2005. **353**(16): 1673-1684.

Sahoo, S. K. and V. Labhasetwar. *Enhanced Antiproliferative Activity of Transferrin-Conjugated Paclitaxel-Loaded Nanoparticles Is Mediated via Sustained Intracellular Drug Retention*. Mol. Pharm. 2005. **2**(5): 373-383.

Sarmento, B., A. J. Ribeiro, et al. *Insulin-loaded nanoparticles are prepared by alginate ionotropic pre-gelation followed by chitosan polyelectrolyte complexation*. J. Nanosci. Nanotechnol. 2007. **7**(8): 2833-2841.

Satarkar, N. S. and J. Z. Hilt. *Magnetic hydrogel nanocomposites for remote controlled pulsatile drug release*. J. Control. Release 2008. **130**(3): 246-251.

Sershen, S. R., N. J. Halas, et al. 2002. Pulsatile release of insulin via photothermally modulated drug delivery. [Engineering in Medicine and Biology, 2002. 24th

Annual Conference and the Annual Fall Meeting of the Biomedical Engineering Society] EMBS/BMES Conference, 2002. Proceedings of the Second Joint.

Sershen, S. R., G. A. Mensing, et al. *Independent optical control of microfluidic valves formed from optomechanically responsive nanocomposite hydrogels*. Adv. Mater. 2005. **17**(11): 1366-+.

Sershen, S. R., S. L. Westcott, et al. *Temperature-sensitive polymer-nanoshell composites for photothermally modulated drug delivery*. J. Biomed. Mater. Res. 2000. **51**(3): 293-298.

Services, C. D. o. H., C. S. C. A. Council, et al. 1991. Breast cancer treatment: summary of effective methods, risks, advantages, disadvantages, Printed and distributed by the Medical Board of California.

Shmeeda, H., D. Tzernach, et al. *Her2-targeted pegylated liposomal doxorubicin: Retention of target-specific binding and cytotoxicity after in vivo passage*. J. Control. Release 2009. **136**(2): 155-160.

Singh, R. and J. W. Lillard. *Nanoparticle-based targeted drug delivery*. Exp. Mol. Pathol. 2009. **86**(3): 215-223.

Strangman, G., D. A. Boas, et al. *Non-invasive neuroimaging using near-infrared light*. Biol. Psychiat. 2002. **52**(7): 679-693.

Sudimack, J. and R. J. Lee. *Targeted drug delivery via the folate receptor*. Adv. Drug Deliv. Rev. 2000. **41**(2): 147-162.

Sun, Y. and Y. Xia. *Shape-Controlled Synthesis of Gold and Silver Nanoparticles*. Science 2002. **298**(5601): 2176-2179.

Tabata, Y., S. Gutta, et al. *Controlled Delivery Systems for Proteins Using Polyanhydride Microspheres.*. Pharm. Res. 1993. **10**(4): 487-496.

Torchilin, V. P. *Micellar nanocarriers: Pharmaceutical perspectives*. Pharm. Res. 2007. **24**(1): 1-16.

Vauthier, C. and K. Bouchemal. *Methods for the Preparation and Manufacture of Polymeric Nanoparticles*. Pharm. Res. 2009. **26**(5): 1025-1058.

Vicent, M. J. and R. Duncan. *Polymer conjugates: nanosized medicines for treating cancer*. Trends Biotechnol. 2006. **24**(1): 39-47.

Vorobyova, S. A., A. I. Lesnikovich, et al. *Preparation of silver nanoparticles by interphase reduction*. Colloid Surface A 1999. **152**(3): 375-379.

Wang, M., D. Lowik, et al. *Targeting the Urokinase Plasminogen Activator Receptor with Synthetic Self-Assembly Nanoparticles*. Bioconjugate Chem. 2009. **20**(1): 32-40.

Wang, X., J. Li, et al. *HFT-T, a Targeting Nanoparticle, Enhances Specific Delivery of Paclitaxel to Folate Receptor-Positive Tumors*. ACS Nano 2009. **3**(10): 3165-3174.

Wang, Y., X. Wei, et al. *Nanoparticle delivery strategies to target doxorubicin to tumor cells and reduce side effects*. Therapeutic Delivery 2010. **1**(2): 273-287.

Weissleder, R. *A clearer vision for in vivo imaging*. Nat Biotechnol. 2001. **19**(4): 316-317.

West, J. L. and N. J. Halas. *Engineered nanomaterials for biophotonics applications: Improving sensing, imaging, and therapeutics*. Annu. Rev. Biomed. Eng. 2003. **5**: 285-292.

Xu, H., F. Meng, et al. *Reversibly crosslinked temperature-responsive nano-sized polymersomes: synthesis and triggered drug release*. J. Mater. Chem. 2009. **19**(24): 4183-4190.

Yamagata, T., M. Morishita, et al. *Characterization of insulin protection properties of complexation hydrogels in gastric and intestinal enzyme fluids*. J. Control. Release 2006. **112**(3): 343-349.

Yang, D. P. and D. X. Cui. *Advances and Prospects of Gold Nanorods*. Chem.-Asian J. 2008. **3**(12): 2010-2022.

Yang, X., S. E. Skrabalak, et al. *Photoacoustic Tomography of a Rat Cerebral Cortex in vivo with Au Nanocages as an Optical Contrast Agent*. Nano Lett. 2007. **7**(12): 3798-3802.

Zahoor, A., S. Sharma, et al. *Inhalable alginate nanoparticles as antitubercular drug carriers against experimental tuberculosis*. Int. J. Antimicrob. Agents 2005. **26**(4): 298-303.

Zhang, H., S. Mardyani, et al. *Design of biocompatible chitosan microgels for targeted pH-mediated intracellular release of cancer therapeutics*. Biomacromolecules 2006. **7**(5): 1568-1572.

Zhang, J. L., R. S. Srivastava, et al. *Core-shell magnetite nanoparticles surface encapsulated with smart stimuli-responsive polymer: Synthesis, characterization, and LCST of viable drug-targeting delivery system*. Langmuir 2007. **23**(11): 6342-6351.

Zhang, J. Z. and C. Noguez. *Plasmonic Optical Properties and Applications of Metal Nanostructures*. Plasmonics 2008. **3**(4): 127-150.

Zhu, S. L., C. L. Du, et al. *Fabrication and characterization of rhombic silver nanoparticles for biosensing*. Opt. Mater. 2009. **31**(6): 769-774.

Vita

Martin Gran graduated from Millard South High School in Omaha, NE. Following high school he attended Iowa State University to pursue a Bachelor of Science Degree in Chemical Engineering. He received his B.S. in 2006. After finishing his undergraduate studies Martin Gran chose to pursue a Ph.D. in Chemical Engineering at the Univesity of Texas at Austin. Martin performed the work for his thesis research under the guidance of Dr. Nicholas Peppas.

Email address : mlgran@mail.utexas.edu

This dissertation was typed by the author.